University of Sussex

HEARING AND ACOUSTIC INTERACTION IN MOSQUITOES

Ben Warren

Submitted for the degree of Doctor of Philosophy
July 2010

Declaration

I declare that the present thesis has not been previously submitted, in the same or different form, to this or any other University for a degree

Ben Warren

Acknowledgements

First and foremost I would like to thank Professor Ian J. Russell for welcoming me into the world of research as an undergraduate. It has been an inspiration to be guided by such a passionate and knowledgeable Professor. I would especially like to thank Dr. Gabriella Gibson for her knowledge and enthusiasm in mosquito behaviour. I would also like to thank Dr. Andrei Lukashkin for his expertise and his great ability to explain complex concepts in an understandable manner. I would like to thank James Hartley for building most of the equipment used in my experiments and for his technical expertise in electronics. I would like to thank Dr. Victoria Lukashkina for helping to maintain mosquito colonies. I would like to thank Dr. Cedric Pennetier for collecting data in Africa. I would like to thank Dr. Jörg Albert for his collaborative work with me at UCL.

I would like to thank Professor Martin Göpfert for allowing me to visit his laboratory during the early stages of my research to acquire techniques necessary for this research. I would like to thank Gareth Jones for writing programmes for data analysis and taking photos of mosquitoes.

I greatly thank the Biotechnology and Biological Sciences Research Council (BBSRC) for funding my DPhil.

I would like to thank my parents for providing me with the education needed to embark on a DPhil. I am grateful for further help and support from my Brother and older Sister. I deeply thank Lyndsay Poore for supporting me through my research career this far.

Preface

The thesis is composed of a General Introduction, Materials and methods for chapter's (II-VI), six Results chapters (II-VI) each containing an abstract and three sections: Introduction, Results and Discussion, and finally a General Discussion.

The research topic of this thesis was inspired by my 3rd year undergraduate project on the novel finding of frequency matching of wing beats between opposite sex pairs of tethered, flying predatory mosquitoes of the species *Toxorhynchites brevipalpis.* The outcome of the project was that frequency matching could provide the basis of sexual recognition between mosquitoes, as revealed in Gibson and Russell (2006). This outcome of my project, which I have outlined in the General Introduction, inspired me to investigate the audio-motor behaviour of the economically and socially important blood feeding vector mosquitoes to see if they also displayed frequency matching behaviour. At the start of my DPhil research, I therefore recorded the audio-motor behaviour of *Culex quinquefasciatus* and discovered that flying, tethered, pairs of mosquitoes of opposite sex also frequency matched. This behaviour is described in Chapter II and published in Warren *et al.* (2009). Frequency matching in *Cx. quinquefasciatus* challenged the previously known limits of auditory transduction by mosquitoes (Belton, 1974; Wishart *et al*., 1962). I therefore became interested in the physiological mechanism underpinning auditory interactions. I used a laser interferometer to measure displacements of the sound receiving flagellum and made electrical recordings from the mosquito's auditory organ in response to sound. On the basis of these measurements I postulated a physiological mechanism by which *Cx. quinquefasciatus* could frequency match. Data supporting this postulation is presented in Chapter IV and in Warren *et al*. (2009). I then embarked on collaboration with Dr. Cedric Pennetier who had contacts in Burkina Faso, which made possible the measurement of audio-motor recordings from field-caught, tethered *Anopheles Gambiae* of different molecular strains. Dr. Pennetier conducted the sound recordings whilst I performed the physiological recordings on *An. gambiae*.

Sound recordings on *An. gambiae* were jointly analysed and published in Pennetier *et al.* (2010) and presented in chapter III. The physiological studies I conducted on *An. gambiae* are presented in chapter IV. During my physiological observations of *Cx. quinquefasciatus* I noticed spontaneous mechanical oscillations of the flagellum and electrical oscillations of the JO in the majority of mosquitoes. This was the first time that repeatable and consistent spontaneous oscillations had been recorded from mosquitoes in excellent physiological condition, rather that from mosquitoes whose physiological state had been deliberately impaired. This finding allowed me to embark on a series of experiments to determine the active force producing process underlying the oscillations which are presented in chapter VI and published in Warren *et al.* (2010) and in the book Concepts and Challenges in The Biophysics of Hearing (Cooper *et al*., 2008). Central to the physiological mechanism of frequency matching was that distortion was generated through the antennae's response to sound. I was intrigued about the origin and characteristics of this distortion. I therefore performed experiments on *Cx. quinquefasciatus* and *An. Gambiae*, the outcome of which are presented in Chapter V.

UNIVERSITY OF SUSSEX

BEN WARREN - Submitted for the degree of DPhil

HEARING AND ACOUSTIC INTERACTION IN MOSQUITOES

SUMMARY

Johnston, who discovered the mosquito auditory organ at the base of the antennae 150 years ago, speculated that audition was involved in mating behaviour. Indeed, the Johnston's organ (JO) is now known to detect the whine of flying mosquitoes. Analysis of sound recordings of flight tones from tethered, flying, mosquitoes revealed that opposite-sex pairs, when within their acoustic near-fields, attempt to frequency-match the harmonic components of their flight-tones. Same-sex pairs actively avoid frequency-matching. Mosquitoes of the species *Toxorhynchites brevipalpis*, where the flight-tone frequencies of males and females are similar, attempt to match the fundamental frequency of their flight-tones. Haemophilic, vector-carrying mosquitoes *Culex quinquefasciatus* and *Anopheles gambiae ss*, where the fundamental frequency of the male flight tone is about 1.5 times that of the female, frequency-match harmonic components of their flight tones. Usually the male's 1^{st} harmonic with the 2^{nd} harmonic of the female flight-tone. In Burkina Faso, where two morphologically similar molecular forms aggregate in the same swarms but rarely hybridise, frequency-matching of flight-tones may perform a pre-mating barrier and a form of subspecies recognition. We discovered that frequency-matching occurred significantly more frequently between same-form male-female pairs of flying, tethered mosquitoes, than when each member of the pair was of a different molecular form. The bandwidth and tuning of sound-evoked flagellum vibrations and the JO's electrical responses to this mechanical input were measured using laser interferometry and extracellular electrodes, respectively. For the first time we showed that distortion products, recorded from the flagellum and JO, could provide the neural basis for frequency-matching at frequencies beyond the range of the JO's electrical responses. We also discovered that spontaneous oscillations of the antennae are produced by physiologically-sensitive mosquitoes. Through temperature-control and injection of pharmacological agents into the JO, evidence is presented advocating dynein as the molecular motor responsible for powering these oscillations.

Contents

Declaration **2**

Acknowledgements **3**

Preface **4**

Summary **6**

Abbreviations **12**

General Introduction **13**

Johnston's organ **13**

Antenna **16**

flagellum **16**

pedicel and scape **19**

Scolopidia **20**

Electrical recordings of the JO **23**

Mechanotransduction **26**

Candidate mechanotransduction channels **29**

Spontaneous motility in the Johnston's organ **33**

Behaviour **35**

Swarming behaviour **35**

Behaviour in response to acoustic cues **37**

Aims **40**

Chapter I Materials and Methods **42**

Mosquito care and preparation **42**

Electrophysiological recordings **43**

Solutions **44**

Laser interferometer measurements **44**

Acoustic recording, stimulation and sound system **47**

Temperature controlled system **49**

Data analysis **51**

Chapter II Acoustic interaction in *Cx. quinquefasciatus* **56**

Abstract **56**

Introduction **57**

Results **59**

Individual responses to acoustic stimulation **59**

Paired recordings **61**

Discussion **66**

Chapter III Acoustic interaction in *An. gambiae* **68**

Abstract **68**

Introduction **69**

Results **70**

Paired recordings **70**

Frequency matching **71**

Discussion **73**

Chapter IV Mechanical and electrical tuning of the flagellum and Johnston's organ **75**

Abstract **75**

Introduction **76**

Results **77**

Mechanical tuning of the flagellum of the antenna **77**

Electrical tuning of the JO of the antenna **81**

Motor tuning curves **87**

Discussion **90**

Mechanical properties of the flagellum of the antenna **90**

Electrical properties of the JO of the antenna **95**

Behavioural properties determined from motor neuron recordings **96**

Chapter V The generation of mechanical and electrical distortion products in the flagellum and JO **98**

Abstract **98**

Introduction **99**

Results **101**

The generation of electrical distortion products in the JO of the antenna **101**

The generation of mechanical distortion products in the flagellum of the antenna **105**

Temperature dependence of mechanical distortion products in the flagellum of the antenna **106**

Discussion **110**

Chapter VI Spontaneous oscillations of the antenna **115**

Abstract **115**

Introduction **116**

Results **118**

Spontaneous oscillations of the flagellum **118**

Temperature dependence of the oscillation frequency **119**

Temperature dependence of the oscillation amplitude **121**

Temperature dependence of the JO neural responses **125**

Colchicine blocks the SOs **127**

Dihydrostreptomycin blocks electrical transduction in the JO **130**

Discussion **132**

The dynein-tubulin system powers the SOs **133**

Independence of SOs and transduction **133**

Molecular mechanisms of SOs **133**

Physiological significance of SO **134**

Conclusion **135**

General discussion **136**

Frequency matching **136**

Mechanotransduction in mosquitoes **139**

A model of the transduction apparatus in the sensory cilia of the mosquito JO **141**

Invovlement of SOs in mechanotransduction **143**

Further experiments **146**

References **148**

Abbreviations

JO: Johnston's Organ

WBF: Wing Beat Frequency

MET: Mechanotransduction

SO: Spontaneous Oscillation

SPL: Sound Pressure Level

TTX: Tetrodotoxin

DSM: Dihydrostreptomycin

INTRODUCTION

It is estimated that 1-3 million people each year are killed by diseases such as malaria, dengue and yellow fever transmitted through mosquitoes. Therefore the behaviour of mosquitoes is of vast social and economical interest due to the ability of mosquitoes as vectors of disease. Mosquitoes are equipped with a highly developed sense of olfaction that allows them to locate breeding sites and their hosts. Considerable effort has been directed at the study and application of olfactory repellents, but with limited and only short term success. In addition to its highly sensitive olfactory reception, the exquisite sensitivity of the auditory apparatus of the mosquito surpasses that of all other arthropods (Göpfert *et al*., 1999). The acoustic behaviour of mosquitoes, and tools aimed at manipulating this behaviour, provide an attractive area for research. It has been shown, for example, that mosquito flight behaviour can be controlled by acoustic cues (Gibson *et al*., 2006). The aim of the research contributing to this thesis is to understand the role of the acoustic system in mating and sexual choice of mosquitoes. The motor system underpinning mosquito wing beating serves a dual role; flight and communication. Thus mosquitoes “sing” as they fly. This unique behaviour provides the opportunity for continuous auditory dialogue between flying mosquitoes, which is unique in caller-receiver interactions, which are often antiphonic, as in human communication, bird song and frog calling behaviour (Bailey, 2003; Narins, 1995; Thorpe, 1975).

Johnston’s organ

The background to my research stems from the first experiments on mosquito audition by Johnston (1855) which led to his discovery of a highly mechanically-sensitive hearing organ located at the base of the antennae that was later named the Johnston’s organ (JO). The JO is a chordotonal organ, which contains thousands of mechanosensitive cells, which detect minute movements of the sound capturing flagellum. In mosquitoes the JO consists of up to 14,000 (Boo *et al*., 1975) sensory cells (Göpfert *et al*., 1999) in males but only about half this number in females. The sensitivity of the JO is such that it can detect

angular displacements of the flagellum down to $1X10^{-4}$ degrees, which is the equivalent to a 7 nanometer displacement at the flagellar tip (Göpfert *et al.*, 1999).

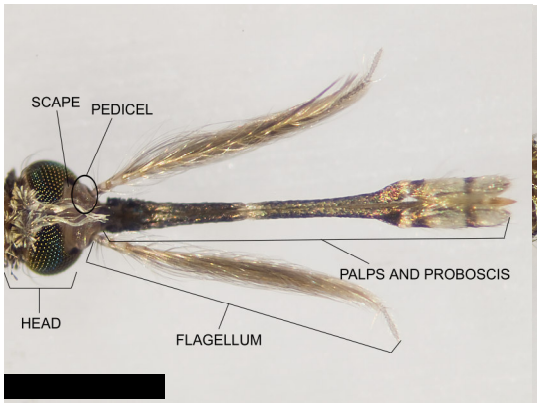

Figure I.1a

An. gambiae fibrillae folded.
Scale bar 1mm
(Photo courtesy of Gareth Jones)

Figure I.1b

An. gambiae fibrillae erect during swarming periods

The antenna is composed of 3 major divisions. The flagellum is a segmented appendage which bears fine hair-like fibrillae and is involved with capturing sound in the form of particle displacement (Fig. I.1a). The base of the flagellum is inserted into the pedicel, which forms a second segment of the antenna and is shaped like a donut and houses the Johnston's organ (Johnston, 1855). The flagellum tapers at its base into about 60-80 prongs. The prongs are cuticular appendages, which curve upwards, into the pedicel, and narrow distally so that they resemble the spokes of an upturned umbrella (Fig. I.2a). Attached to the prongs are the mechanosensitive sensory cells and other supporting cells, which surround the sensory cells, which a functional unit known as a scolopidium (Fig. I.2b). These scolopidial units are attached predominantly on the posterior side of the prongs (as depicted in Fig. I.2a) but are also attached to the anterior side, in both cases to detect displacement of the prongs. There are up to 4 different types of scolopidia. The majority (97%) of the mechanically sensitive scolopidia, type A, are attached to the posterior side of the prongs in groups of about 120 and form the 'outer ring' (McIver, 1982). Type B scolopidia form the inner ring by attaching to the anterior side of the prongs. Type C and D

are attached to the posterior of the epidermis under the base of the flagellum termed the basal plate (McIver, 1982). Type A, C and D contain two sensory cells, type B has 3 sensory cells although one of the sensory cells does not produce a cilium (Fig. I.2b).

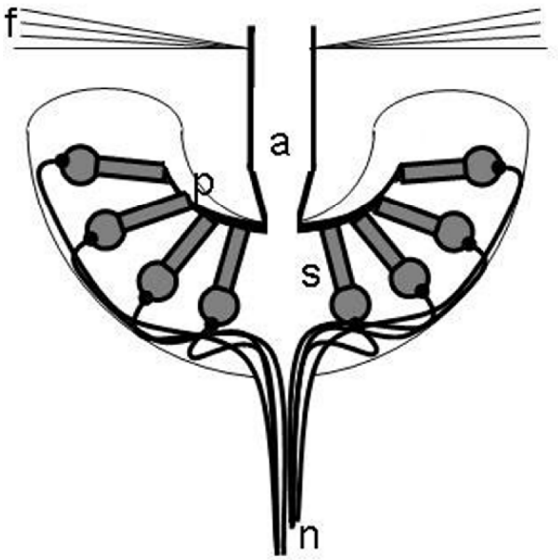

Figure I.2a

A schematized cross section of the Mosquito antennae (a=flagellum, p=prongs, s=scolopidium, f=fibrillae). For simplicity only type A scolopidia are indicated.

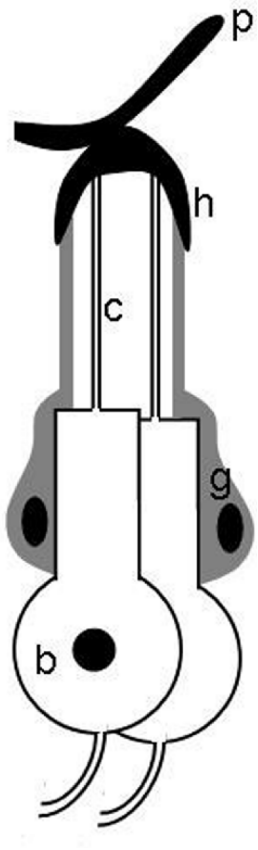

Figure I.2b

A schematized cross section of a scolopidium (b=sensory cell, c=cilium of sensory cell g=scolopale/supporting cell, h=cuticular cap, p=prong)

The axons, from the bipolar mechanosensitive cells, form the JO nerve which exits the antennae through the base of the pedicel and then through a first antennal segment; the ring-like scape which attaches the pedicel to the head. Impulses transmitted along the axons of the JO nerve are propagated to the Johnston's organ centre and the antennal motor and mechanosensory centre in the deutocerebrum (Fig. I.3) and possibly directly through to thoracic motor command areas, which control flight (Ignell *et al.*, 2005).

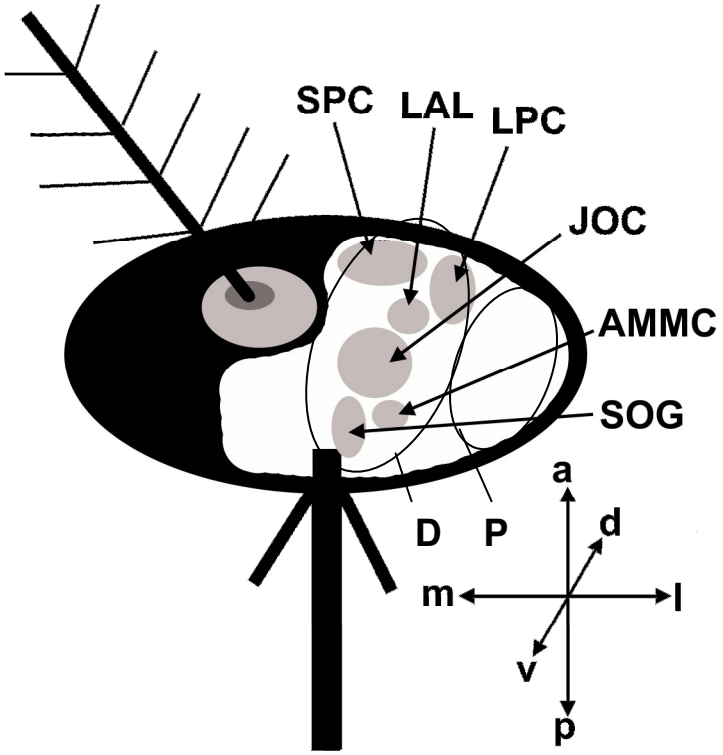

Figure I.3

Basic architecture of the mosquito brain showing the three main olfactory and mechanosensory organs. a, anterior; d, dorsal; l, lateral; p, posterior; v, ventral; m, medial. Only one antennae and left side of the brain is shown. D, Deutocerebrum; P, Protocerebrum; SPC, superior protocerebrum; LAL, lateral accessory lobe; LPC, lateral protocerebrum; JOC Johnston's organ center; AMMC, antennal motor and mechanosensory center; SOG, subesophageal ganglion (Adapted from Ignell *et al...* 2005).

Antenna

flagellum

Sound is received by the flagellum which protrudes from the pedicel. The flagellum is subdivided into 13 flagellomeres along its length. The length of the flagellum, measured from its base in the pedicel to the flagella tip, varies from 2.5 mm for *Tx. brevepalpis* to 1.8 mm *An. stephensi* (Boo, 1980; McIver, 1980). For *An. stephensi* the 12th flagellomere is the longest at 410 µm followed by the 13th 250 µm then the 1st 170 µm, the rest are all about 100 µm (Boo, 1980). The last two flagellomeres are commonly the longest for mosquitoes of the *Culex, Anopheles, Toxorynchityes* and *Aedes* genus (Boo, 1980; McIver, 1971; Slifer

and Sekhon, 1962). There is a groove along the length of the flagellum (Nijhout and Sheffield, 1979). The flagellum of the male bears whorls of hair-like sensilla, called fibrillae (Fig. I.1b). These extend out of from the flagellum in all directions, like the branches of a pine tree, decreasing in length distally along the flagellum from the base of flagellomeres 1 to 11. Each fibrillum is inserted into a cup shaped socket in the flagellum and is supported by raised cuticle at the base of the fibrillum (Fig. I.4) (Slifer and Sekhon, 1962). These fibrillae also contain longitudinal grooves along its length, which give it a star-shape in cross-section (Slifer and Sekhon, 1962).

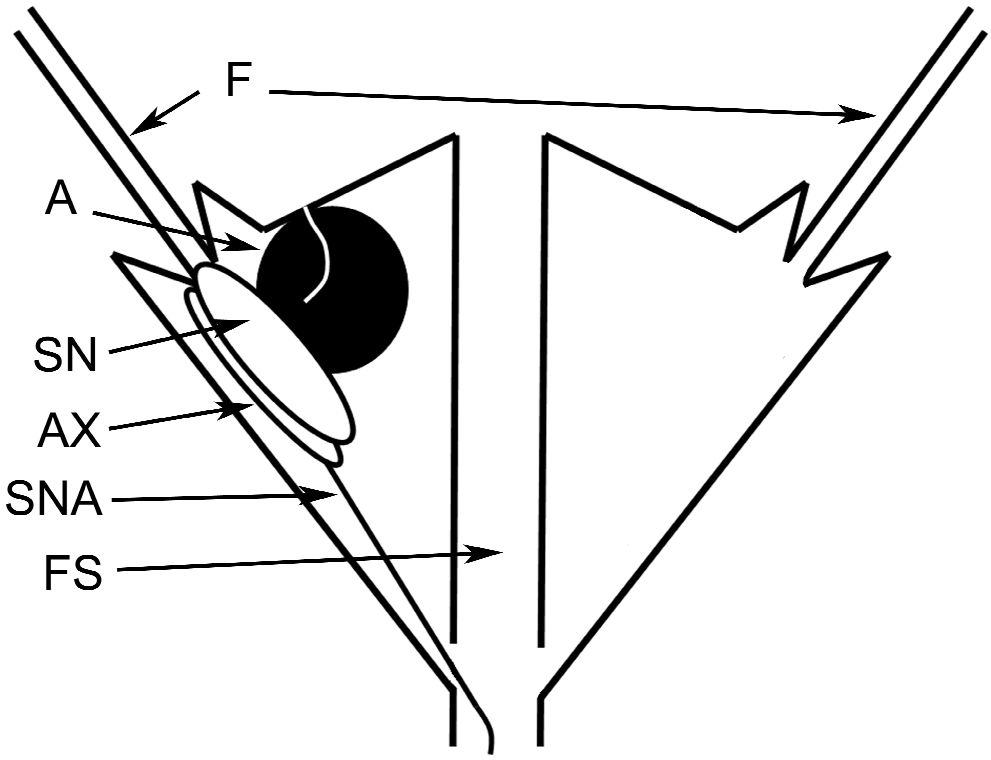

Figure I.4

Schematic diagram of a fibrillum. F, fibrillum; A, annulus; SN, sensory neuron; AX outer auxillary cell; SNA, sensory neuron axon; FS, flagellar shaft (Adapted from Clements, 1999).

These grooves are thought to increase the surface area and therefore windage of the flagellum making it acutely responsive to air particle displacement. A more specific role of the fibrillae has been postulated when Mayer, with the use of tuning forks, observed that each whorl of fibrillae was tuned to a specific frequency allowing males to respond to a range of female wing beat frequencies

(WBFs) (Mayer, 1874). However for the fibrillae to respond in this way they would each need to be mechanically receptive and afferently innervated. Boo (1980) revealed that only a fraction are afferently innervated by a single neuron (Boo, 1980). Of these innervated fibrillae Boo (1980) suggests that, at least for *An. stephensi,* they sense the relative position of the other antenna due to their concentrated arrangement along the medial axis of the flagellum. The possible afferent innervation of these tiny hairs, and their sensitivity to sound-induced vibrations in the kHz range (Göpfert *et al*., 1999), could implicate them as detectors of the particle displacement component of sound in the kHz range. A species of *Culex* mosquito (*Cx. territans*) is reported to prey on the green frog, *Pseudacris crucifer,* with a mating call of 2.6 to 3.5 kHz. *Cx. territans* are also attracted to loudspeakers, which emit sound in the kilohertz range. Bartlett-Healy (2008) suggest that fibrillae could be detecting these call frequencies and transmitting them to the flagella base. Indeed Göpfert *et al.* (1999) have measured the resonant frequency of fibrillae to be about 1500 Hz, they also recorded a second mode of vibration of the flagellum at 1500 Hz for female *Ae. aegypti.* If the fibrillae are mechanosensory they could induce a behavioural response by themselves, or impose movements onto the flagellum, which could be detected by the JO. Such high frequency movements of the flagellum have not yet been recorded in the phasic electrical responses of the JO. Cator *et al.* (2009) have, however, reported a sustained direct current shift when electrically recording the activity of the JO of *Ae. aegypti* in response to tones up to 2 kHz.

Although some fibrillae are indeed mechanosensitive they most probably first evolved to increase the surface area, increasing windage and driving of the flagellum to air particle displacement. Indeed some early experiments involved measuring potentials from the JO in response to sound of different frequencies. Upon stripping the antennae of fibrillae there was no change in the frequency, which elicited the largest sound evoked potentials from the JO and therefore no change in the resonant frequency but only a decrease in the receptor microphonic associated with the stimulus frequency (Wishart *et al*., 1962). In this respect, in *Anophelines* the fibrillae become erect and presumably functionally more effective during times of male swarming behaviour when

acoustic communication is likely to occur. At other times the fibrillae remain folded into the flagellum (Fig. I.1). There is an abundance of fibrillae on male flagella compared to female flagella for nearly all mosquito species, which leads to a 10 fold increase in the surface area for males (Clements and Bennett, 1969; Slifer and Sekhon, 1962). This sexual dimorphism leads to an increased acoustic sensitivity which may have evolved due to a stronger selection pressure for males to acoustically detect flying females. The mechanism of fibrillae erection was investigated by Nijhout (1977) who found it was under direct neural control and concluded that motor neurons must extend along the entire length of the flagellum. α-adrenergic agonists and α-adrenergic blockers induced and prevented this response respectively. Using electron microscopy Nijhout *et al.* (1979) located a specialised cell at the base of fibrillae, termed the annulus, which is highly vacuolated during hair erection, but becomes less vacuolated when hairs are folded into the flagellar shaft (Fig. I.4). He found that this was controlled by the pH of the tormogen cell; a possible effect of neural innervation on this cell by adrenergic type agonists mentioned above.

Pedicel and scape

The scape, which is the most proximal of the 3 divisions of the antennae, is a small ring structure, which connects the pedicel and the flagellum anchored within, to the head of the mosquito. Each antenna is moved by 3 sets of muscles. The first set connect the scape to the cranium and move the antenna in the transverse plane via two articulations located on opposite sides of the scape. The other 2 sets of muscles connect the scape to the pedicel like hinges, they are located at relative right angles to the first muscle set and allow movement of the flagellum in the vertical plane (Belton, 1989; Clements and Bennett, 1969). These muscles permit the flagellum and pedicel to move within a cone of about 45 degrees. The pedicel resembles a swollen donut shaped tube, which in males measures 100 μm high and 170 μm diameter (for male *An. stephensi*), it also bears numerous external scales (Boo, 1980). The pedicel also contains a blood vessel (served by a pulsating antennal heart (Schneider, 1964), tracheae and a thin layer of epidermal cells (McIver, 1980). The

flagellum is inserted deep in the middle of the pedicel and is anchored by a cuticular basal plate which, in males, narrows laterally to form the prongs. In females the prongs are shorter and thicker (Boo and Richards, 1975).

Scolopidia

Scolopidia are a group of cells which include the bipolar mechanosensitive sensory cells of the JO surrounded by supporting cells termed scolopale cells (Fig. I.2b). Mechanosensitive cilia protrude from the top of the sensory cells into a potassium and chloride rich lymph, which is enclosed and maintained by the surrounding scolopale cells (French, 1988). The tips of the cilia on top of the sensory cells are embedded into a cuticular cap, which is attached to the prongs (Fig. I.2b). Thus movements of the prongs are directed onto the sensory cell cilia. The scolopale cells have an actin rich cytoskeleton, which is thought to create a rigid tunnel, so that movements of the prongs will be conducted specifically onto the mechanosensitive cilia (Wolfrum, 1990). Type A scolopidia consist of two sensory cells enclosed by two scolopale cells (Fig. I.2b) and a third inner scolopale cell, which secretes an intracellular fenestrated structure, the outer sheath (Clements, 1999). For male *Ae. aegypti*, in type A scolopidia, the cilium of the sensory cells is approximately 11 µm long, 0.5 µm in diameter, the cap about 10 µm long with the sensory cells total length about 16 µm (Boo and Richards, 1975). The distal cap connects through a filamentous structure to the prongs at one end and to the distal end of the cilium at the other. NompA is a transmembrane protein with specialised zona pellucida (PZ) domains and mediates this strong connection in *Drosophila*. Perhaps, as a consequence of the absence of this crucial connection, the receptor potentials of the JO in *NompA* mutants are greatly reduced (Göpfert *et al*., 2005). About two thirds from the cilia base is a ciliary dilation characterised by a transient increase in its diameter (Fig. I.2b), which is packed with electron dense material, thought to be echinoderm microtubule associated protein (EMAP) (Albert, personal communication, 2009) (Schmidt, 1967). The distal end of the cilium is inserted into the cap with one becoming distantly swollen inside the cap (Clements, 1999). The cilium has a specialised microtubule structure with nine microtubule

doublets in a ring forming a 9X2+0 arrangement of microtubules (Boo, 1981) (Fig. I.5). Structures resembling dynein molecules bridge between the 9 microtubule doublets in a radial ring (Fig. I.5) and are present along the length of the cilium but are absent from the ciliary dilation (Boo, 1981; Stephens, 1974). A structure at the base of the cilium, termed the ciliary necklace, is formed by the microtubule doublets converting into microtubule triplets 9X3+0, which then go on to form the ciliary rootlets. The rootlets extend into the cell body and terminate near the nucleus (Boo, 1981). Wolfrum (1991) visualised actin filaments by phalloidin in the ciliary rootlets in the inner dendrite of the sensory cell. He also found alpha-actinin and centrin-like protein. The presence of actin filaments led to speculation that they were the basis for an adaptation apparatus, which responds and interacts with changes in calcium, similar to that hypothesised to underpin adaptation in the mammalian inner ear (Gillespie and Cyr, 2004). However it is the microtubule 9X2+0 ring that appears to be the crucial structure in mechanoreception. Agents which cause disassembly of microtubules interfere with sensory transduction in campaniform receptors of the cockroach *Blaberus giganteus* (Erler, 1983; Moran and Varela, 1971). Although in contrast to this, other studies performed on the bristle receptor or hair sensillum of the cricket *Acheta domesticus*, using agents to disassemble microtubules, showed that integrity of the microtubule cytoskeleton was not necessary for transduction (Erler, 1983). The apparent contradictory outcomes of measurements made from campaniform and bristle receptors might well be due to the differing mode of stimulation of these two receptor types. For campaniform receptors the mechanical stimulus is applied directly to the top of the sensory cell cilia where up to 1000 microtubule filaments terminate underneath a dome shaped cuticle (Keil, 1997), whereas for tibial bristle receptors of the cricket, deflection of the side of the cilium membrane, where there are structural specialities, is proposed to open mechanotransduction (MET) channels (Erler, 1983). There are 350-1000 microtuble filaments in campaniform receptors compared to the 9X2+0 microtubule structure indicative of bristle receptors (Keil, 1997). The abundance of microtubules in campaniform receptors attests to their functional importance and thus it should not be surprising that their removal causes disruption of receptor functioning.

Microtubules maybe more important for maintaining tension in chordotonal organs. They could generate the tension, between the membrane, which is proposed to open cation channels (Albert *et al*., 2007a), thereby allowing cations, mainly potassium into the sensory cell (Kuppers, 1974). The Nan-Iav transduction channel has been localised to the proximal sensory cilium in *Drosophila* (Gong *et al*., 2004), suggesting that forces may be transmitted down the sensory cilium before transduction channels in the base are opened. The opening of transduction channels results in the entry of cations causing depolarisation of the receptor potential.

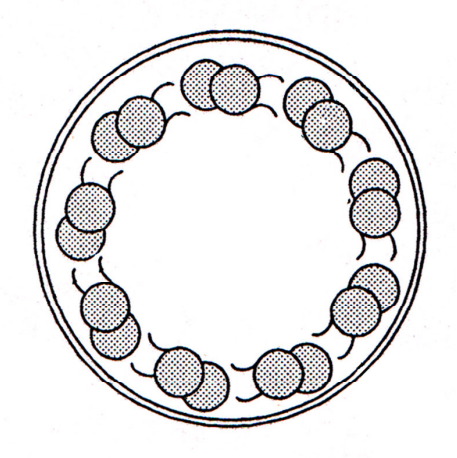

Figure I.5

Cross section of the middle part of the sensory cilium of the sensory cell in a scolopidium as found in mosquitoes and fruit flies so far examined (Adapted from (Bisgrove and Yost, 2006)).

Type B scolopidia are closely similar to type A, but have three sensory cells enclosed by 2 scolopale cells. Both A and B are termed amphinematic due to their indirect connection via a terminal filament to the cuticular prongs (Boo and Richards, 1975). The cap of the type B scolopidia is slightly longer than type A. One of the sensory neurons has different morphology having no ciliary dilation, irregular microtubule arrangement a shorter ciliary root with its cilium extending right to the tip of the cap (Clements, 1999).

Type C and D scolopidia are similar to type A in having two sensory cells. However their dendrites project into an electron dense part of an attachment cell and are thus of the mononematic type due to this direct connection. The attachment cell fuses with epidermal cells through desmosome-like connections. Type C unlike type D scolopidia have glial cells and are connected

to the antennal blood vessel. Type C connect to the edge of the basal plate whereas the single type D connects to the antennal flange (Boo and Richards, 1975).

Electrical recordings of the JO

Movements of the flagellum are conducted through the prongs which extend into the JO onto the specialised scolopidial caps that tightly envelope the cilia of the sensory cells of the scolopidia (Fig. I.2b). Our understanding of the way the sensory cells are coupled to the sound receiver comes largely from studies on *Drosophila* (Albert *et al*., 2007a; Albert *et al*., 2007b; Göpfert and Robert, 2002; Göpfert and Robert, 2003; Göpfert *et al*., 2005). The cilia of *Drosophila* appear to be under constant tension exerted through the cuticular connections to the sound receiver (Kamikouchi *et al*., 2009). If so, a decrease in the amount of tension from resting conditions would lead to hyperpolarisation through a reduction in the open probability of the mechanotransducer conductance (Kamikouchi *et al*., 2010). Conversely an increase in tension would tend to increase the open probability of the conductance resulting in a depolarising receptor potential. The essential structural similarity between the mosquito and *Drosophila* antennae indicate that they probably work in a similar way.

Intracellular recordings of the mechanosensory cells in the mosquito JO have yet to be performed. Therefore our understanding of mechanotransduction in the JO relies on extracellular recordings of the combined electrical activity of the JO made through an electrode inserted through the pedicel wall. These extracellular recordings include receptor potentials and compound action potentials but the summated receptor potentials from groups of scolopidia dominate the response (Clements, 1999). Compound potentials of the JO in response to a pure tone are typically dominated by frequencies at twice the frequency of a pure tone (Fig. I.6). These findings have been explained as being due to the summed electrical responses from two populations of sensory cells with opposite functional polarisation located at opposite sides of the JO (Fig. I.7) (Wishart *et al*., 1962). In this model it is assumed that the sensory cells

are activated upon stretching or compression of their cilia through movements of the extended flagellum.

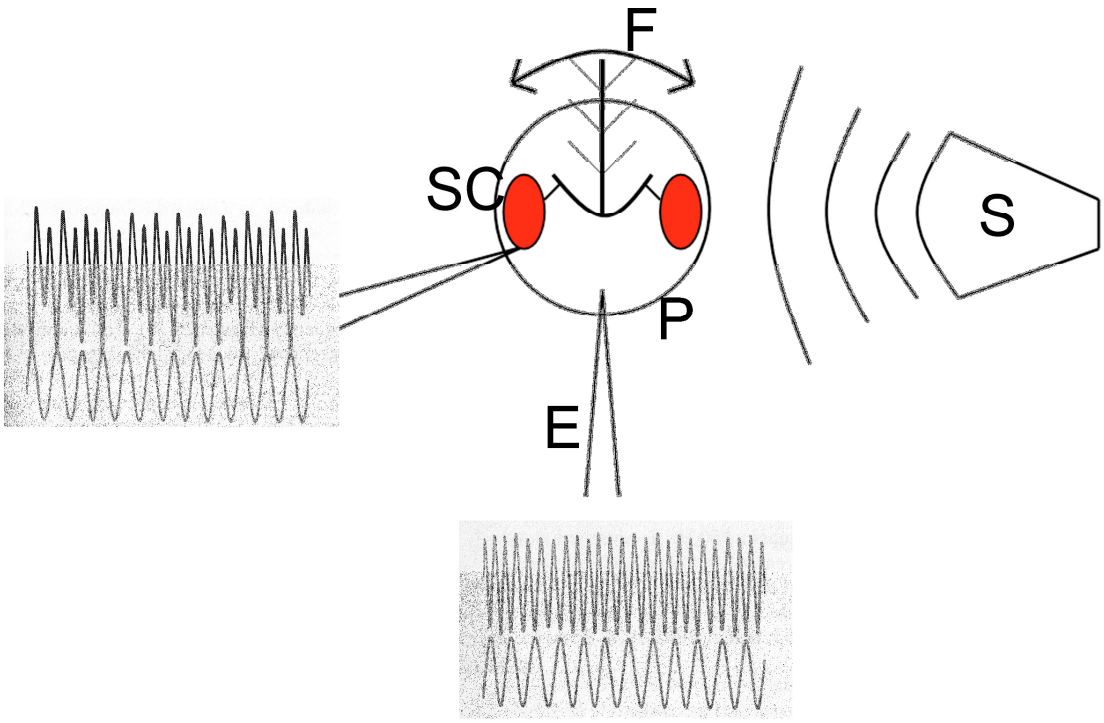

Figure I.6

Electrical recordings from the pedicel (P) with recording electrode (E) in two different locations in response to stimulation from a speaker (S). Movements of the flagellum (F) along its axis primarily stimulate two populations of scolopidia (SC) in red. If the recording electrode is positioned equidistant between the two scolopidial populations (bottom) the resulting potential, recorded from the JO, has equal amplitude. If the electrode is positioned closer to one scolopidial population a biphasic amplitude is produced. Copied and adapted from (Wishart *et al.*, 1962)).

The alternate depolarisations usually differ in amplitude (Fig. I.6). The larger potential is thought to be the receptor potential from the population of neurons closest to the electrode, whereas the smaller potential is thought to be the receptor potential from the population of neurons most distant from the electrode at the opposite end of the JO, which attenuates as it travels through the JO (Fig. I.6). There is a fundamental paradox with this explanation of recordings of compound potentials of the JO. Receptor potentials can theoretically only be recorded from the few bipolar sensory cells of the JO adjacent to the electrode. This is due to the rapid attenuation of the receptor

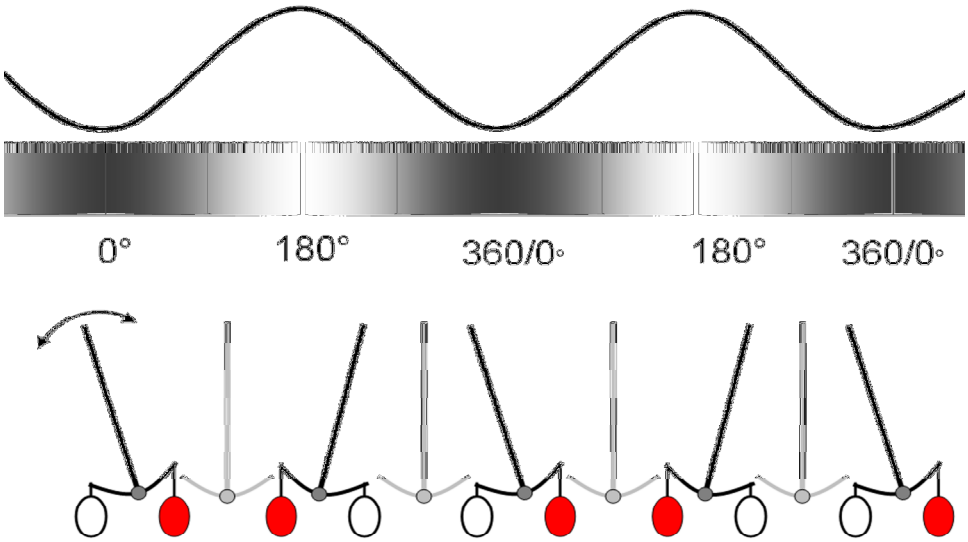

Figure I.7

Pure tone stimulus (top trace) causing the flagellum (bottom) to pivot about its base. Two distinct populations of sensory cells are stimulated for each period of oscillation, through stretching of their sensory cilia causing mechanoelectrical transduction (mechanotransducing sensory cells in red).

potential calculated from an approximated membrane length constant. Therefore depolarisations from the sensory cells at the opposite end of the JO, which explain frequency doubling, would be fully attenuated before reaching the electrode. Thus, an alternative explanation is that the sensory cells are stimulated upon stretching and compression and that only the receptor potentials from the sensory cells close to the electrode are recorded as predicted from the theoretical length constant. The asymmetric response of the sensory cells to stretching and compression once every cycle would explain frequency doubling of the compound potential. However, the fact that potentials with double the frequency can be recorded from the compound eye, at a distance far beyond the theoretical length constant, shows that receptor potentials can travel not only through the JO but well beyond it (Wishart *et al.,* 1962). Based on this finding it can be shown that sensory cells are only stimulated upon either stretch or compression because when the recording electrode is placed equally distant between the two populations of neurons the amplitude of the response is uniform, suggesting that each population of sensory cells are only stimulated once per cycle (Fig. I.6) (Wishart *et al*., 1962). How can receptor potentials travel far beyond the theoretical length constant?

This incongruity can be settled by looking at similar types of recordings made from the cochlea in mammals. In the cochlear electrical potentials from the receptor potentials (cochlear microphonic) of the outer hair cells can be recorded from fluids and tissue within and remote from the cochlea far beyond the theoretical length constant of the receptor potential from the outer hair cells. This cochlear microphonic can be explained as receptor currents, from multiple sensory cells, which induce an extracellular current flow, of the external and internal fluids and tissues of the cochlea (Cheatham *et al*., 2010). Thus receptor potentials of the sensory cells of the mosquito JO appear to induce currents in the fluids and components comprising the JO, which can be recorded at distinct locations within the pedicel.

Belton (1974) used glass microelectrodes, inserted into the pedicel, to measure the potentials only from the few sensory cells near the electrode tip in response to a single static deflection of the flagellum (Fig. I.8). The second potential was interpreted as being due to a resonant stretch of the same scolopidial population transducing the first potential (Belton, 1974). Indeed the time between these two potentials corresponded to the resonant frequency of the flagellum to sound. Thus the second potential, thought to be due to an electrical resonance of the sensory cell, could represent a form of frequency tuning of the MET channel to displacements.

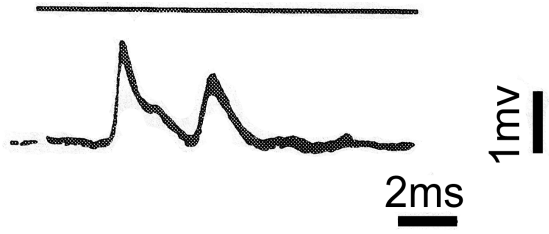

Figure I.8

Potentials recorded by a glass microelectrode to a step stimulus of the flagellum in one direction only (top line indicates duration of step stimulus) (Copied and adapted from (Belton, 1974)).

Mechanotransduction

In chordotonal organs the sensory cilium is put under tension by forces acting along the long axis of the cilium. In other insect mechanoreceptors pinching or

localised pressing against the membrane leads to stimulation, as is hypothesised to be the case for bristle and campaniform receptors (Keil, 1997). Weiderhold (1976) suggests that the surrounding scolopale rods, within the scolopale cells, would provide a rigid canal allowing tensioning forces to be conducted along the cilium. Displacement of the sensory membrane is regarded as the universal mode for stimulating mechanoreceptors (French *et al*., 1981). The MET channel is thought to be located within the membrane of the sensory cilium, but its precise whereabouts remains to be discovered.

A model proposed by Moran and Rowley (1975) assumes a population of MET channels is localised in the ciliary dilation. The ciliary dilation appears structurally to be less well coupled to the microtubule filaments and could therefore stretch and compress independently from the rigid microtubules, performing a plunger like action (Stephens, 1974). In the subgenual organ of the cochroach *Blattella germanica* the 9 microtubule doublets adhere to 9 longitudinal equally spaced invaginations on the ciliary membrane. A strong candidate for the membrane that would most effectively be displaced by tension or compression, in the subgenual organ, is that which extends between each of the 9 microtubule doublets (Fig. I.9) (Moran *et al*., 1975). In Moran and Rowley's model, the ciliary rootlets provide a strong anchor for the microtubule cytoskeleton so that tension forces exerted by the flagellum through the cuticular cap cause relative shearing between the membrane and cytoskeleton. The ciliary dilation, thus, remains a popular candidate for the localisation of transduction channels. Its role in mechanotransduction is revealed in the *beethoven* (btv) mutants of *Drosophila* where the, assumingly, essential electron dense material inside the dilation is absent and mechanoreceptor potentials of the JO are no longer produced (Eberl *et al*., 2000).

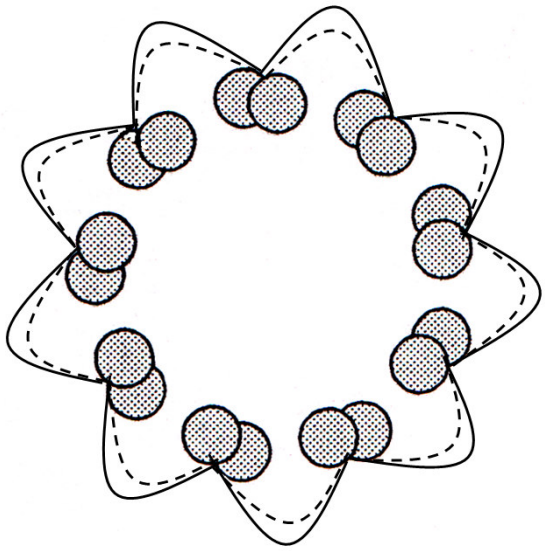

Figure I.9

Simplified cross section through the ciliary dilation of the subgenual chordotonal organ of the cochroach *Blattella germanica.* The grey circles represent the microtubule doublets. The solid line represents the membrane. The dotted lines represent the hypothetical membrane movement upon pulling of the cilium along its axis.

Another possible mechanism of channel activation involves an active cytoskeletal sliding mechanism based on the ability of dynein to slide microtubule doublets past each other along their axis. In this model mechanical forces delivered to the tip of the cilium are propagated along the cilium towards the base. This 'active wave' is mediated by the actions of dynein, which slide microtubule doublets past each other. Using high-voltage electron microscopy Moran *et al.* (1977) observed a bend near the base of the sensory cilium in response to stimulation of the grasshopper's femoral chordotonal organ. The observed bending of the cilium increased when the joint was bent at a greater angle and was presumed to be due to the induced activity of dynein sliding microtubules doublets past each other to create a bend in the microtubule cytoskeleton (Moran *et al*., 1977). This travelling wave model of the tubular body is thought to affect the MET channels in the proximal cilia membrane, which is coupled to the cytoskeleton (French, 1988; French *et al*., 1982). Indeed the Nan-Iav channel, which accounts for most of the receptor potential in *Drosophila,* has been localised to the proximal part of the cilium beneath the ciliary dilation (Chapman *et al*., 1979; Gong *et al*., 2004). This cytoskeletal contraction could be mediated by the influx of calcium through non-selective cation channels located at the distal end of the cilium such as NompC (Lee *et al*., 2010). Centrin, a calcium binding protein, which forms contractile filaments, has also been found in the sensory cells and could mediate the initiation an active wave at the distal end of the cilium upon opening of NompC, which

travels to the proximal end of the cilium (Wolfrum, 1997). Wolfrum (1997) has suggested that the ciliary rootlets, which run from deep in the sensory cells to the tip of the cilium, could undergo calcium mediated contractions, similar to those observed in green algae. These contractions are proposed to force the movement of the microtubule cytoskeleton with respect to the cilium membrane thereby causing bending of the cilium and mechanoelectrical transduction. Mechanotransduction based upon calcium mediated contractions of the ciliary rootlets is unlikely to occur because mechanotransduction in the insect bristle receptor occurs within 200 µs too quick for such 2nd messenger based transduction process (Walker *et al*., 2000). Moran *et al.* (1977) suggests that active bending caused by the sliding of microtubules could be a response of scolopidia to stimulation. In *tilB Drosophila* mutants, which are thought to lack dynein in the sensory cell cilia, mechanical responses of the antennae to sound remained linear with no power amplification (Göpfert *et al*., 2003). Dynein is not an essential component for transduction but these findings suggest that dynein's role may be to amplify small mechanical forces delivered to the cilium by sliding microtubule filaments of the cytoskeleton.

Another model proposed by Göpfert *et al.* (2006) involves the interaction between two transient receptor potential (TRP) ion channels. In this model the Nan-Iav channel mediates electrical signal propagation along the sensory cell cilium responding to tension delivered from the cap domain. The NompC channel is hypothesised to use this signal from the Nan-Iav channel to regulate the amount to which the stimulus is amplified (Fig. I.10).

Candidate mechanotransduction channels

Candidates for the MET channel have been identified by creating *Drosoplila* knockout mutants coupled with labelling studies (Göpfert *et al*., 2005; Kim, 2003). The most promising family of channels are transicent receptor potential (TRP) ion channels. The vanilloid subfamily of this group (TRPV), which appears highly conserved, has diverged in vertebrates and invertebrates from a single ancestral gene (Gong *et al*., 2004). Two TRPV's Nanchung (Nan) and

Inactive (Iav) are thought to encode the six transmembrane (TM) domain heteromultimeric Nan-Iav channel (Göpfert *et al*., 2006). The Nan-Iav channel, has been exclusively labelled to chordotonal cilia of *Drosophila*. Sound-evoked potentials in the JO of *Drosoplia* are completely absent in mutants lacking Nan (Kim, 2003). Therefore the Nan-Iav channel is an essential component of the transduction apparatus in *Drosophila*. Using HEK293 cells expressing Nan-Iav and measuring ionic currents using whole cell patch recording Gong *et al.* (2004) found that Nan-Iav forms a non-selective cation channel. Another candidate MET channel has been localised in insect bristle mechanoreceptors and in chordotonal organs such as the JO of *drosophila* (Lee *et al*., 2010). NompC (No mechanoreceptor potential C) is found to mediate the mechanoreceptor current in mechanosensory bristles, however unlike Nan and Iav it is not found anywhere in the mammalian genome but has been conserved completely in *C. elegans*, *Drosophila* and *Zebrafish* (Gong Z *et al*., 2004; Pedersen *et al*., 2005; Walker *et al*., 2000). Although the mechanoreceptor potential in the JO of *NompC* knockout mutants was found to be decreased, this effect was less dramatic than for mechanosensory bristles (Kernan *et al*., 1994; Walker *et al*., 2000). Thus, NompC was thought only to be expressed by a subset of neurons in the JO (Eberl *et al*., 2000).

Generic features of mechanosensory transduction include an adapting transduction current (Gillespie *et al*., 2001). Thus experimental studies in *Drosophila* have been focused on candidate transduction channels, such as NompC with an ability to adapt to a constant mechanical force (Walker *et al*., 2000). *NompC* was cloned and found to have four alleles, three of which produced a dramatic loss of the transduction current in bristle mechanoreceptors of *Drosophila* (Walker *et al*., 2000). The fourth (*NompC*^{4}), however, produced a near wild type transduction current with significantly faster adaptation, suggesting NompC has a role in adaptation (Walker *et al*., 2000). Adaptation of the transduction current is an integral component in the gating spring model, which fits the dynamical properties of MET channels in auditory hair cells and in the *Drosophila* JO.

Another feature of the gating-spring model is an elastic connection between the cytoskeletal framework and the membrane where the MET channel is thought to reside. This allows mechanical forces to be transmitted along the cytoskeleton, through this connection, and onto the MET channel, which can then respond by opening. In vertebrate hair cells ankyrin repeats remain a popular contender for this connection because they exist at the N-terminal regions of the two main candidates for the MET channel in vertebrate hair cells; TRPA1 and TRPN1 (Sotomayor *et al*., 2005). They also form an elastic α–helix spring by folding in on each other, which matches the stiffness estimates derived from the gating-spring model (Sotomayor *et al*., 2005). Like vertebrate MET channels the N-terminal of Nan-Iav and NompC contain 5 and 29 ankyrin repeats respectively (Kernan, 2007). Specialised microtubule integrated cones of unknown composition have been visualised between the microtubule cytoskeleton and the membrane in the region of the of the cilium that receives stimulatory force (Thurm *et al*., 1983). These microtubule integrated cones could be the ankyrin repeats themselves.

A further property of acoustical receptors is mechanical amplification of the movements of the receptor to weak acoustical stimuli compared to acoustic stimuli with a higher intensity. The only non-cuticular attachments to the antennal sound receiving structure of *Drosophila* and mosquitoes are the sensory cells of the JO (Göpfert *et al*., 2001). Thus active properties of the antennae, such as mechanical amplification of its movements to sound, are thought to be due to the combined movements of the sensory cells in the JO (Göpfert *et al*., 2006). Fitting of the gating spring model to movements of the *Drosophila* antennae suggest that movements of the sensory cells responsible for mechanical properties of the antennae are due to the MET channel themselves (Nadrowski *et al*., 2008). To investigate the involvement of the candidate MET channels of *Drosophila* in mechanical amplification Göpfert *et al.* (2006) measured the mechanical gain exhibited by the antennae of *Drosophila* mutant with knockouts of *NompC* and/or *Nan-Iav*.

Excessive mechanical amplification was found in *Nan-Iav* knockouts, whereas amplification was abolished in *NompC* knockouts. Coupled to previous findings where Knockout mutants deficient in NompC produced greatly reduced potentials and knockout of Nan-Iav abolished compound potentials (Gong *et al*., 2004; Kim, 2003) Göpfert *et al.* (2006) formed an updated model of transduction in the JO of *Drosophila*.

In this model NompC acted as the primary MET channel generating a receptor potential, at the tip of the cilium, and the Nan-Iav channel simply propagated this receptor potential to the base of the cilium where an action potential, though to dominate the compound potentials recorded from *Drosophila,* could be generated. This model is supported by findings of Gong (2004) who visualised Nan-Iav in the proximal sensory cilia, from its base up to the ciliary dilation and NompC which was localised to the distal end of the sensory cilium in chorodotonal organs of *Drosophila* (Lee *et al*., 2010; Liang *et al.*, 2010). Mechanical amplification is achieved through 'reverse mechanoelectrical transduction' where the Nan-Iav channel propagates an electrical feedback signal from the base of the cilium to the tip where NompC resides. NompC then converts this electrical signal into mechanical movements of the antennae, which combine with the movements of the antennae due to sound to produce an amplified response. Excessive mechanical amplification occurs in Nan-Iav mutants because no feedback signal is generated to regulate the runaway amplification of NompC. Such interaction between two mechanically sensitive channels of the TRPV family has been found before in the nematode (Gong *et al*., 2004). However, compound potentials are still found in *Drosophila NompC* knockouts suggesting that the Nan-Iav channel, or an undiscovered channel or protein, is able to act as a type of vestigial mechanotransducer in this system (Göpfert *et al*., 2006).

The percentage of transducer current attributed to these two candidate channels varies between studies. More recent work by Kamikouchi *et al.* (2009) sheds light on this uncertainty. In the *Drosophila* JO they found five functional groups of neurons projecting to the JO from the antennal mechanosensory and

motor centre in the brain (Kamikouchi *et al*., 2006). Neurons from subgroups AB responded maximally to sinusoidal vibrations of the *Drosophila* 'love song'. Subgroup CE responded maximally via a tonic response to static deflections for the duration of the stimulus. Labelling studies labelled Nan to almost all JO neurons, whereas NompC was exclusively labelled to AB subgroups specific for sensing sound. These different subgroups, which respond to different components of antennal movements and are distributed differently in the JO, are responsible for complicating the electrical measurements of the transducer current.

Spontaneous motility in the Johnston's organ

To date spontaneous oscillations (SOs) or antennal vibrations have been observed in *Tx. brevipalpis* and *Drosophila melanogaster* after a fatal injection of dimethyl sulfoxide or after prolonged repetitive stimulation but very rarely in uncompromised preparations (Göpfert *et al*., 2001; Göpfert *et al*., 2005). In both cases the endogenous oscillations were attributed to a system instability in the operating regime of the JO. SOs of the JO are analogous to the SOs that have been measured in the hair bundles of vertebrate hair cells, where the generation of the oscillations has been ascribed to excessive feedback between the cyclic interaction of a myosin-based adaptation motor and calcium mediated closure of the transduction channel (Fig. I.11) (Martin *et al*., 2000; Nadrowski *et al*., 2008). While the transducer apparatus contributes significantly towards the mechanical properties of the antennal receiver (Albert *et al*., 2007a; Nadrowski *et al*., 2008) the presence of a myosin–actin motor associated with transducer channels of the JO sensory neurons has not been demonstrated. Based on the microtubule rich cytoskeleton the force producing component of the adaptation motor powering these SOs has been hypothesised to be dynein (Göpfert and Robert, 2008). Indeed dynein is the known force producing molecule present in motile cilia such as human nasal and tracheal ciliated cells, sperm cells, protists and statocysts of Medusae (Clary-Meinesz *et al*., 1992; Horridge, 1969; Kamimura *et al*., 1985; Satir *et al*., 2008) and is also present in the cilia of the mechanosensitive cells of the JO (Boo, 1981).

Wiederhold (1976) suggests that the motile function of more primitive cilia could be a feature present not only in more advanced sensory cilia, but also could be a complementary aspect of transduction itself. Indeed oscillations of mechanical receptors have been demonstrated to enhance frequency selective gain and sensitivity of the system in noisy environments (Martin *et al*., 2001; Nadrowski *et al*., 2004). There are many similarities between motile cilia and sensory cilia (Fig. I.5). These include the prominent 9 microtubule doublets arranged in a ring in the cilia and dynein bridges between them. Utilising dynein to move microtubule doublets relative to each other, sensory cell cilia would theoretically still have the basic machinery to undergo a type of ciliary beat, as has been suggested by Thurm and Kuppers (1980) for insect mechanoreceptors. However, to date, no functional evidence of dynein's role in the motility of sensory cell cilia has been provided.

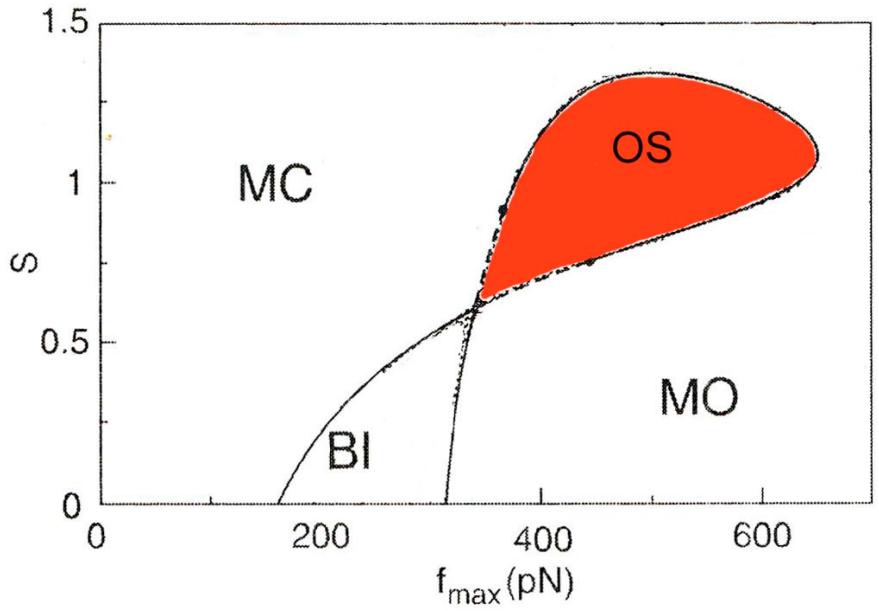

Figure I.11

State diagram of the hair bundle as a function of the force that an adaptation motor produces (f_{max}) and the force produced through the strength of Ca^{2+} feedback (S). Four states are produced, through the opening and closing of the MET channels, depending on the amount of force contributed through the two feedback mechanisms. MC; mostly closed, MO; mostly open, BI; bistable, OS; oscillations. The amount of force leading to oscillations is shaded in red. Copied and adapted from (Nadrowski *et al*., 2004).

Behaviour

Swarming behaviour

Male mosquitoes detect female mosquitoes through their WBF at close range (<15cm), with the notable exception of *Wy. smithii* who are not known to be 'active flyers' but which are assumed to meet via olfactory cues (Göpfert *et al*., 1999; McIver, 1980). Two of the three subfamilies of Culicidae: Anophelinae and Culicinae mate in swarms. However, the last of the 3 major subfamilies, *Toxorhynchitinae* compose non-blood feeding mosquitoes and do not swarm. Instead males such as *Tx. brevipalpis* rest on plant matter and, upon acoustically detecting a passing female, take flight and pursue the female until she is grasped. Mating occurs and the pair lose directional flight and begin to fall although mating is completed before reaching the ground (Bonnet *et al.,* 1951).

Culicinae and *Anophelinae* mosquitoes, such as male *Cx. quinquefasciatus* and *An. gambiae,* swarm at dawn and dusk over swarm markers. Swarm markers are a visual stimulus normally with good contrast and include edges such as river banks, tree tops, and dark objects such as rocks (Brogdon, 1998; Downes, 1969; McIver, 1980). Detection of odours and visual landmarks, which comprise swarm markers, could be responsible for long range attractants to mating swarms (Downes, 1969). The flight pattern, of swarming mosquitoes, has been extensively characterised by Gibson, (1985) and consists of large looping flights contained within the edge of the swarm (Fig. I.12). Males detect and home-in on the female WBF produced by a female mosquito entering the swarm. Typically, when entering the swarm, females will be grasped by a swarming male within seconds and will drop to the ground *in copula* (Roth, 1948). Mating takes place over about 10 seconds (Gibson, personal communication, 2010). The detection of the female WBF, by the male, is a necessary prerequisite before any mating takes place (Roth, 1948). Although in the wild only male swarms have been observed, female mosquitoes can be made to swarm in the laboratory and, like males, they do not collide mid-air whilst swarming (Gibson, personnel

communication, 2009). It is common for many different species and sub-species to be present in the same swarm (Diabate *et al*., 2009). Sub-species of *An. gambaie* are found to swarm together in Burkino, Faso, Africa but rarely hybridise (Downes, 1969). Hybridising pairs of Mopti (M) and Savanna (S) form *An. gambiae* were counted after they fell out of swarms *in copula.* The low occurrence of hybrids cannot be accounted for through hybrid inviability as such hybrids remain fertile (Tripet *et al*., 2004). However the strong, rapidly acting, premating barriers to different form mating, which exist within the swarm, suggest that such hybrids have a decrease in fitness; perhaps because hybrids are not optimally adapted to either habitat which the M and S form occupy.

The interaction between pairs of mosquitoes, attempting to mate in a swarm, is extremely brief, with the male grasping a female within seconds after the detection of her WBF. Brodgon (1998) and Wekesa *et al.* (1998) have suggested that a species specific WBF mediates strong species isolation. Differences in WBF might only explain species isolation in some

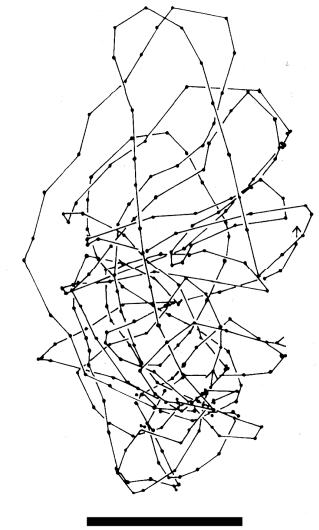

Figure I.12

Flight track of one male mosquito from a swarm of five male mosquitoes; duration 12 seconds (scale bar represents 10cm) (Copied and adapted from (Gibson, 1985).

cases. Tripet *et al.* (2004), however, highlights the fact that the WBFs of the *An. gambiae* complex overlap, so that they cannot be a reliable indicator of their sub-species. Further to this, the tuning of the JO appears too variable and too broad to be used for assortative mating (Clements *et al*., 1969). Visual cues seem unlikely to form the basis of speices recognition due to the poor resolution

of the compound eye, which for the diurnal *Tx. brevipalpis* is 5.2 degrees, which is comparable to more advanced Dipteria (minimum resolvable angle for a grating) (Clements, 1999). There is no evidence for sexual discrimination based on olfactory odours or pheromones acting at a distance. However contact pheromones are used by *Aedes* mosquitoes to discriminate species (Clements, 1999; Duhrkopf *et al*., 1992). Such a cue would be detected only after the male had grasped the female and would result in the pair splitting before falling to the ground *in copula* (Clements, 1999).

Behaviour in response to acoustic cues

There are numerous documented cases where male mosquito flight patterns have been altered by the presence of sound with frequencies close to the female WBF (Roth, 1948 and references within). The most common of these behaviours is phonotaxis towards the sound emitting structure such as a tuning fork, loud speaker or man singing! The sound emitting structure was, in some cases, grasped by the *Ae. aegypti* males typifying the first stages of their mating response (Roth, 1948).

Gibson (1985) studied the effects of sound on swarms of *Cx. pipiens* of both sexes. Diffuse sound presented at 500-600 Hz induced a decrease in the velocity of swarming male mosquitoes, which still performed looping turns at the same intervals in time, therefore the swarm as a whole occupied less space. The females showed no response to sound whilst swarming. Renewed interest in the behavioural response of mosquitoes to sound was sparked by a novel experimental design. To investigate the auditory sense and behaviour of the nectar feeding mosquito *Tx. brevipalpis,* Gibson and Russell (2006) flew mosquitoes on tethers whilst recording their flight tones. Male and female *Tx. brevipalpis* are similar in size and fly at similar overlapping WBF's (Gibson *et al*., 2006). They found that upon acoustic stimulation, through sounds delivered through a speaker or that of another tethered flying mosquito, that the tethered

mosquito altered its wing beat frequency (Fig. I.12, I.13, I.14). Data for figures I.12, I.13, I.14 were collected as part of my undergraduate project.

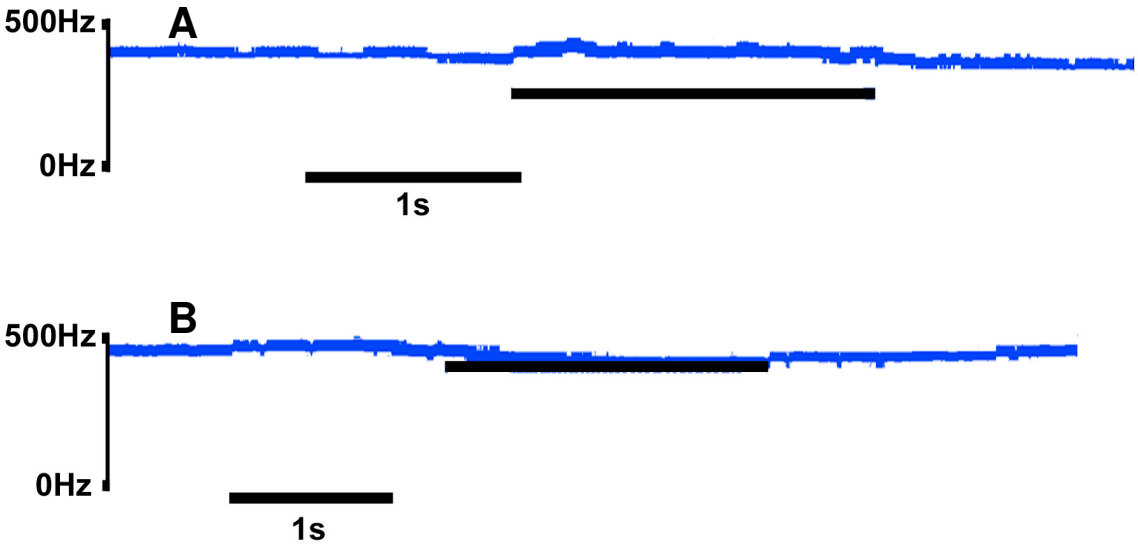

Figure I.12

Fundamental WBF of Male *Tx. Brevipalpis* (blue trace) in response to a A: 300 Hz and B: 420 Hz pure tone (black bars) from a loud speaker at 2.65X10^{-4} m/s. The frequency and time resolution is 2.7 Hz and 45 msec.

The tethered flying mosquito often altered its WBF to coincide and match that of a tone delivered from a speaker (Fig. I.12 B). When flown together, in pairs, within each other's acoustic field, opposite sex pairs of *Tx. brevipalpis* matched their WBF for extended periods of time (Fig. I.13). Same sex pairs did not match their WBF's for any significant length of time (Fig. I.14). Thus the auditory-motor responses of *Tx. brevipalpis* was sexually distinct with opposite sex pairs frequency matching and same sex pairs avoiding matching their WBF's. This novel form of signalling is distinct from other forms of caller-receiver communication which are normally antiphonic. It is not known if this continuous auditory dialogue between pairs of flying mosquitoes occurs for more economically relevant blood feeding mosquitoes.

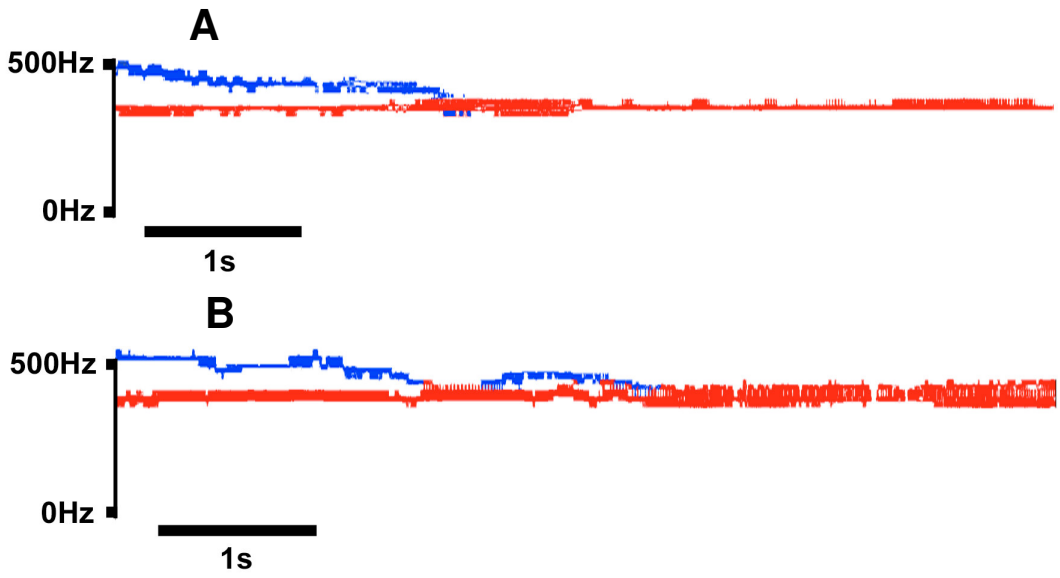

Figure I.13(A-B)

Spectrograms displaying frequency matching behaviour of male (blue) and female (red) during paired flight. Frequency matching at 340 and 390 Hz occurs between 2 and 3 seconds after flight onset, at the beginning of the spectrogram for A and B respectively.

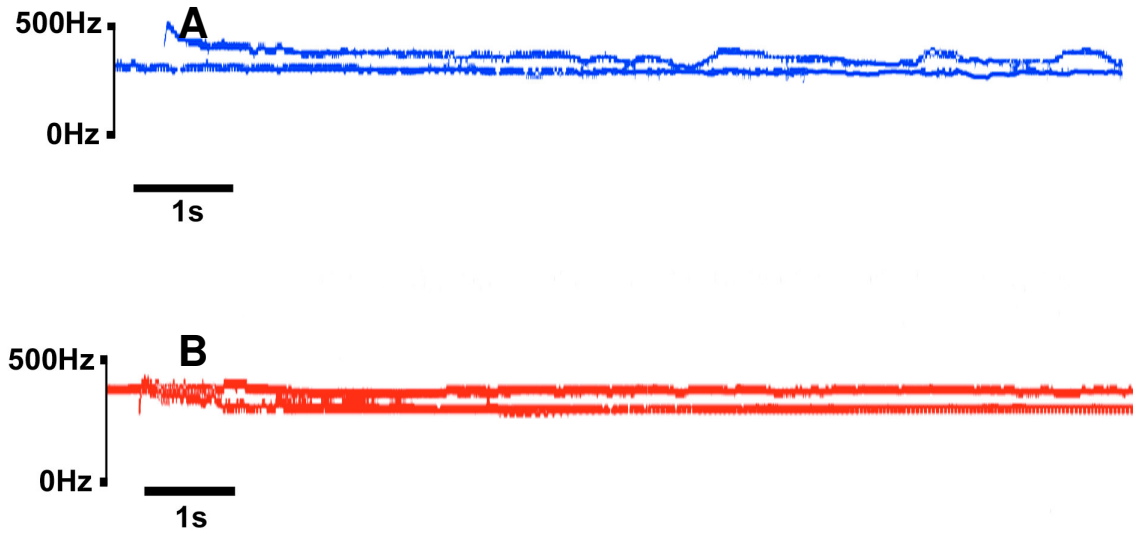

Figure I .14(A-B)

Spectrograms displaying frequency avoidance behaviour of same sex pairs of male (blue) and female (red) during paired flight.

Aims

The aims of the research presented in this thesis are:

- To measure and record the responses of tethered flying mosquitoes to acoustic stimulation and auditory interactions between tethered flying mosquitoes.

- Use electrophysiology and laser interferometry to measure the electrical and mechanical properties of the JO and flagellum in its quiescent state and in response to sound delivered from a speaker.

- Measure the mechanical and electrical spontaneous oscillations of the antennae as functions of temperature and apply specific blocking agents to the JO as a means for understanding the molecular basis of the spontaneous oscillations of the antenna.

Through these measurements I will

Re-evaluate the frequency limits and sensitivity of the JO and the mosquito to sound by:

- Analysing the behavioural responses of tethered flying mosquitoes to acoustical stimulation (Chapter II-III).

- Measuring frequency components of the electrical responses of the JO and measuring mechanical displacements of the flagellum to acoustic stimulation (Chapter IV)

- Decipher the ability of mosquitoes to respond to tones outside their auditory limits using distortion generated by the antenna (Chapter V)

Identify the molecular mechanism underlying spontaneous oscillations of the antenna by:

- Measuring the temperature dependence of the oscillations (Chapter VI).

- Measuring the effects of solutions delivered into the JO designed to affect specific functions of the JO (Chapter VI).

CHAPTER I MATERIALS AND METHODS

Mosquito care and preparation

Culex quinquefasciatus Say 'Muheza' strain and *Toxorhynchites brevipalpis* Theobald were obtained from the London School of Hygiene and Tropical Medicine. *Anopheles gambiae* Giles s.s. were collected from the wild whilst swarming in Burkina Faso. Adult mosquitoes were fed on concentrated sugar water soaked in cotton wool. To produce offspring adult female mosquitoes were fed on a defibrinated horse blood (supplied by TCS Biosciences, Butolph Claydon, Bucks, UK) delivered through membrane feeders (Hemotek 5W1). Mosquito eggs were obtained from pots of water, inside the cage, and were then transferred to another container where the larvae hatched. The larvae were fed Olli © cat biscuits (fresh chicken with duck and liver variety). Pupae were obtained and transferred back into the cage where adult mosquitoes hatched. The mosquitoes were maintained on a 12 hour rotating cycle of light and dark at 21℃.

Cold narcosis was used to prepare mosquitoes for experiments. Mosquitoes were captured and placed in a coffee cup, then placed in a fridge at 4℃ for 2 minutes and then directly transferred to a Petri dish resting on top of a tub of ice. For tethered experiments mosquitoes were tethered with bee's wax by their dorsal thorax to a 3 cm length of annealed 100 µm diameter stainless steel wire and mounted in a micropositioner so their body axis was parallel with the speaker (Fig. 1.1). For physiological measurements mosquitoes were secured to a brass metal block 4x3x3 mm in size, using low melting point bone wax (Figure 1.5). A fine stainless steel wire (0.1 mm diameter) was used to apply a small bead of superglue between the head and thorax and between both pedicels, thereby securing the pedicel to the head. The palps and proboscis were also fixed to the head in the same way. All experiments were performed on a vibration isolation table (VHT3636W-OPT, Newport corp.). Normal physiological condition of mosquitoes was confirmed by the existence of the

tarsal reflex, abdominal contractions and motor activity elicited throughout and after all experiments.

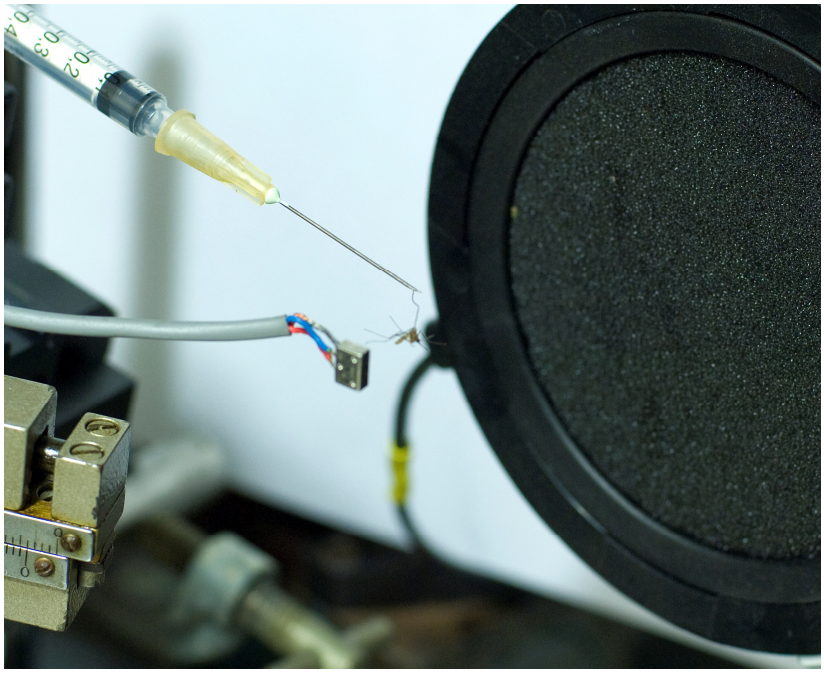

Figure 1.1

Experimental set up for tethered recordings from one female *Cx. quinquefasciatus.* To the left is the particle velocity microphone (5mm in height) (Knowles NR-23158-000). To the right is the Beyer DT770 Headphone used for acoustic stimulation.

Electrophysiological recordings

For electrical recordings, the metal block, to which the mosquito was attached, was clamped with a plastic screw onto a thin layer of electrode gel (Signa gel, Parker Laboratories INC) atop a ground electrode, (EL212, WPI) ensuring the gel contacted the mosquito (Fig. 1.5). To record receptor potentials and motor activity, electrolytically sharpened tungsten electrodes (World Precision Instruments, Inc.), with 2 MΩ resistance, mounted on micropositioners were advanced into the mosquito. To record receptor potentials from the JO one electrode was inserted 10µm into the lateral side of the pedicel using a piezoelectric stepper (Scientific products GMBH), the other electrode was inserted 50 µm into the lateral thorax. To record motor activity one electrode was inserted in the thorax near the legs, the other electrode was inserted in the

contralateral thorax close to the wing base. The voltage output from the tungsten electrodes were inserted into a differential amplifier where the difference between the voltage was amplified 10,000 times with reference to the ground electrode.

Solutions

Solutions injected into the JO and thorax were made from *Drosophila* insect saline (Ruiz-Sanchez *et al*., 2007) adjusted to pH 7.2 using sodium bicarbonate. *Drosophila* insect saline contained 117.5 mM NaCl, 20 mM KCl, 8.5 mM $MgCl_2$, 2 mM $CaCl_2$, 20 mM Glucose, 10.2 mM $NaHCO_3$, 4.3 mM NaH_2PO_4, 8.6 mM Hepes, 10 mM Glutamine. Colchicine solution contained 10 mM of colchicine and 9 mM methylene blue. Control colchicine-free solution contained 9 mM of methylene blue. Tetrodotoxin solution contained 10 mM of Tetrodotoxin. All solutions were delivered through a quartz glass microelectrode (1mm in diameter and tapered down to ~20 µm) stepped just through the pedicel wall using a peizoelectric stepper (Scientific products GMBH).

Laser interferometer measurements

A self-mixing laser diode interferometer (Lukashkin *et al*., 2005) was used to measure displacement ~240 µm from the base of the flagellum where it inserts into the pedicel. The laser was focused at the base, as opposed to the distal end of the flagellum in order to stay within the ~84 nm operating range of the laser interferometer for particle velocity values up to 2×10^{-4} m/s. This allowed a large range of particle velocity values used to displace the flagellum. It was positioned so that its optical axis was perpendicular to the length of the flagellum and directly opposite or in line with the speaker. The interferometer design consists of a Fabry-Perot (homodyne) laser-diode (DL3149-057, Thorlabs) whose light is collimated (aspheric lenses, NA=0.25, C220TME-B, Thorlabs) and focused (NA=0.125, T45-234, Edmund Optics) so that it can produce a 5 µm spot in diameter at about 45 mm from the surface of the focusing lens. For the focusing lens used (NA=0.125) the depth of focus is

about 20 μm. The interferometer is housed on top of a micromanipulator. Light reflected back from the surface onto which it is focused alters the laser intensity when the surface is displaced. If the target is linearly displaced along the axis of the beam, the intensity of the laser varies sinusoidally with a period $\lambda_{laser}/2$ (Fig. 1.3). The reflected signal interferes with the laser intensity, which depends on the delay and phase differences between the outgoing and reflected signal. Changes in the lasing power are measured with the photodetector (Fig. 1.4). The photodiode converts the signal into voltage with a cut-off frequency of 200 kHz. The voltage output from the photodetector is linear for displacements measured by the interferometer of ~ 0.15 to 84 nm (Fig. 1.2). Movements of the flagellum, on which the laser is focused, may shift the interferometer transfer function onto a nonlinear region where voltage output from the photodiode is not proportional to displacement (Fig. 1.3). Therefore a total of 10 recordings for each stimulus presentation were recorded but only the largest displacements were collected. The largest displacements occurred only when the interferometer passed through the linear, most sensitive point of the transfer function (Fig. 1.3).

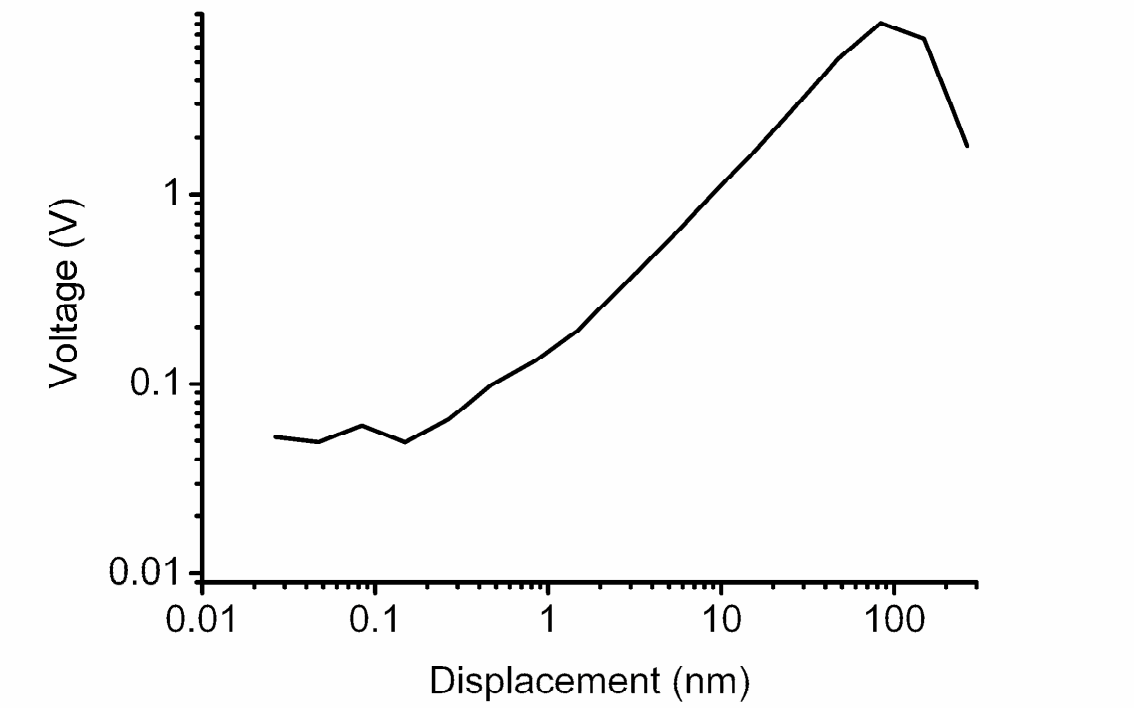

Figure 1.2

Voltage output from the laser interferometer in response to known displacements from a piezoelectric crystal on which is was housed.

The voltage from the laser is amplified by 40 dB. The voltage is calibrated by vibrating the piezo manipulator, on which the laser diode assembly sits, by increasing displacements from 1 to 84 nm. The maximum voltage output is obtained when the laser records an 84 nm displacement. This analysis provides a coefficient in nm/V of the laser sensitivity for each experiment. This allows the voltage recorded from the laser to be converted into displacement. A schematic of the interferometer signal-processing set-up is displayed in Fig. 1.4.

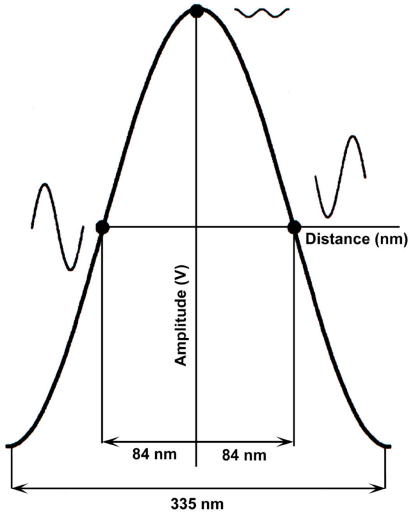

Figure 1.3

Schematic of the interferometer transfer function, as it is predicted theoretically (Lukashkin *et al.*, 2005). The period will correspond to $\lambda_{laser}/2$ (335 nm) displacement of the target. The largest self-mixing signal (as shown in the insets) will be obtained when the target moves 84 nm ($\lambda_{laser}/8$) from its centre position.

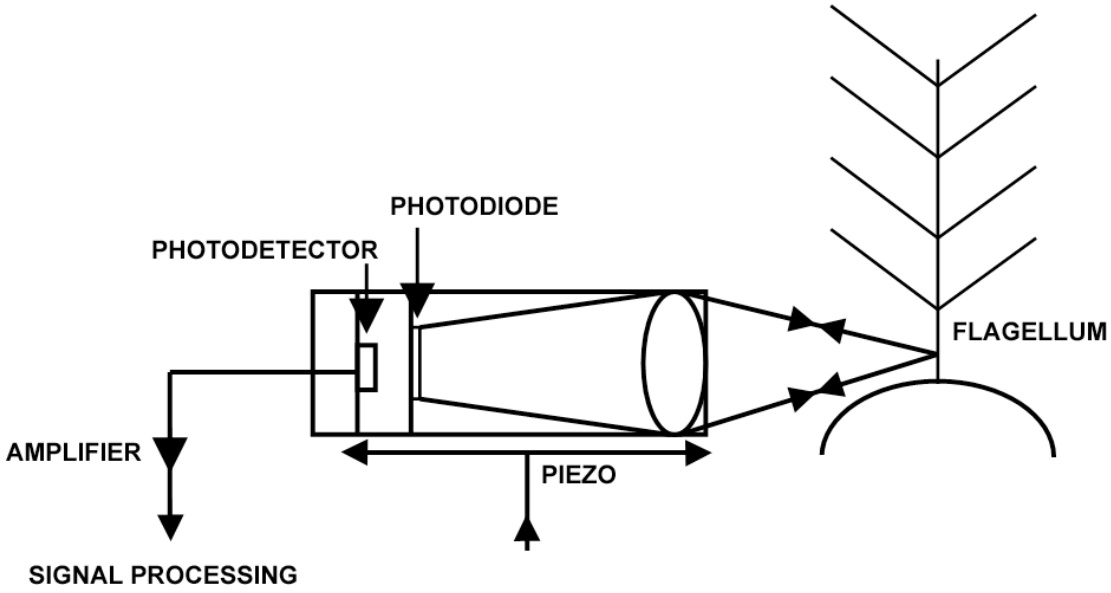

Figure 1.4

Schematic diagram of the interferometer signal-processing set-up

Acoustic recording, stimulation and sound system

For recording WBFs in tethered experiments a particle velocity microphone (Knowles NR-23158-000) was positioned about 3cm from flying mosquitoes. The voltage output from the microphone was sampled at 44.1 kHz. Factors known to affect wing-beat frequency (Clements, 1999) were controlled for. Room temperature between 20-22℃ was used for all experiments, mosquitoes were between 3 and 10 days old and experiments were performed within a 3 hour period. The 3 hour experimental period started an hour before the lights were switched off in their 12 hour light cycle.

For acoustic stimulation during tethered experiments acoustic stimuli were delivered through a Beyer DT770 Headphone (6 cm cone diameter) (Total Harmonic Distortion <0.2%) placed about 5 cm from the mosquito (Fig. 1.1). For tethered experiments all tones were presented at a particle velocity level between 1 – 9 $X10^{-4}$ m/s. For physiological recordings acoustic stimuli were delivered by a Beyer headphone coupled to the preparation through 1 cm tubing ~70 cm long. The tubing was necessary in order to position the speakers far enough away to minimise electromagnetic pick up of the speaker magnet by the recording electrodes. The output from the tube connected to the speaker was placed about 1 cm from the head of the mosquito. The highest particle velocity level emitted from the speaker was limited to the highest particle velocity level recorded from a tethered flying mosquito ($5X10^{-3}$ m/s) (Göpfert *et al*., 1999). Thus all particle velocity levels remained within the behaviourally relevant range. The largest particle velocity level emitted from the speaker caused distortion for sinusoidal signals below 100 Hz due to physical constraints of the speaker (Fig. 1.5). For mechanical measurements pure tones of 100 ms duration and a rise/fall time of 14 ms were generated using a DT3010 board. For electrical measurements pure tones of duration 400ms were used with a rise fall time of 8ms.

Acoustic stimuli were expressed in particle velocity (pV). A pressure difference microphone, (Knowles NR-23158-000) the voltage output of which increases

linearly with particle velocity, was used to measure particle velocity. In the near field of a sound source (within λ/6, where λ is the wavelength of a pure tone) there is a nonlinear relationship between pV and Sound Pressure Level (SPL). However in the far field at a distance of more than λ /6 the relationship is linear.

SPL was measured in the far field in response to a 1 kHz tone at 1.5 meters using a pressure microphone (Brüel and Kjaer 1/2" type: 2669). pV was calculated from the SPL using equation (1). Voltage was obtained from the Knowles microphone to the same 1 kHz tone at 1.5 meters. This allowed a coefficient (0.0379) to convert voltage output from the Knowles microphone into pV.

$$\text{Particle velocity (m/s)} = \frac{\text{Pressure (Nm}^{-2}\text{ [pascal])}}{\text{Acoustic impedance (Pa.s/m [z])}} \qquad (1)$$

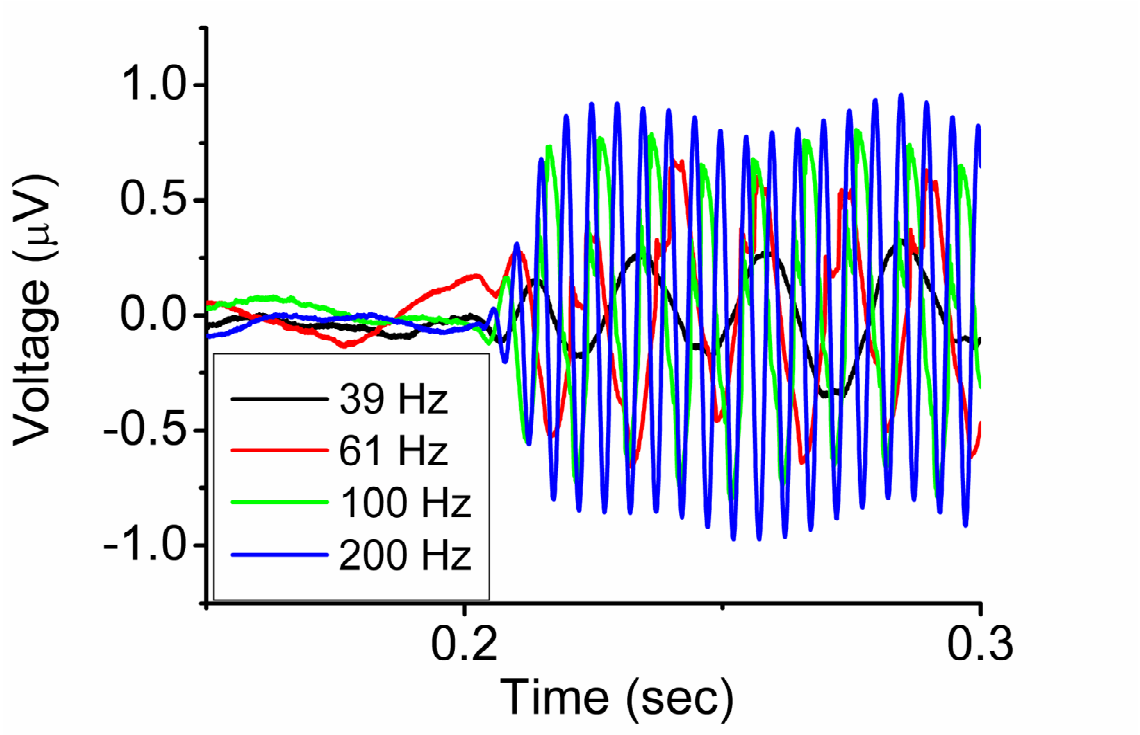

Figure 1.5

Recording of pure tones emitted from a Beyer DT770 speaker, using a low distortion low frequency response pressure microphone (Brüel and Kjaer 1/2" type: 2669) at the maximum particle velocity level used in all experiments

($5X10^{-3}$ m/s). Particle velocity amplitude varies nonlinearly with respect to the voltage obtained from the pressure microphone, therefore changes in amplitude are not due to distortion of the sound system. The Brüel and Kjaer 1/2" type: 2669 microphone was used because it has a very low level of distortion in its response to sound.

Temperature controlled system

For temperature controlled experiments the metal block with attached mosquito was clamped to the bottom of a stainless steel chamber, which was attached to a Peltier element and a heatsink (Fig. 1.6). Temperature was controlled by a custom made device with a negative feedback loop, which altered the current fed through the Peltier element in response to the temperature read by a thermal resistor (Fig. 1.6). A 2-minute stabilization period was left after a new temperature was set. The exact temperature of the mosquito was measured by fixing a thermocouple modulator with a resolution of ±0.1 °C (80TK, Fluke©, www.fluke.co.uk) to the brass block with bone wax imitating the mosquito. The display temperature and the temperature of the thermocouple modulator were measured simultaneously (Fig. 1.7) and the difference between their readings was used to calibrate the temperature during the experiments (Fig. 1.8). A polynomial was fitted to the data (Fig. 1.8) in order to convert the temperature recorded from the power supply into temperature of the mosquito. The error in temperature readings of the thermocouple modulator (±0.1 °C) and the error through a non-perfect fit of the polynomial (Fig. 1.8, difference between black and red trace at 20°C) makes the combined error in the temperature measurements ± 0.3 °C.

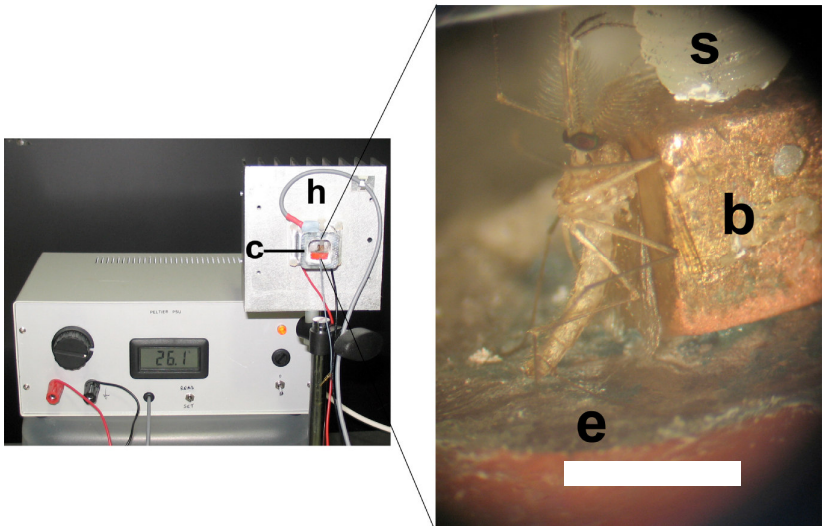

Figure 1.6

Experimental setup showing a metal chamber **c** where mosquitoes were housed during the temperature control experiments. The chamber is attached via a Peltier element to a heat sink **h**. The current fed through the Peltier is controlled via a power supply with feedback control from a thermistor attached to the metal chamber. Mosquitoes were attached to a brass block **b**, which was clamped with a screw **s** to a ground electrode **e** situated at the bottom of the chamber **c**. Scale bar 3mm.

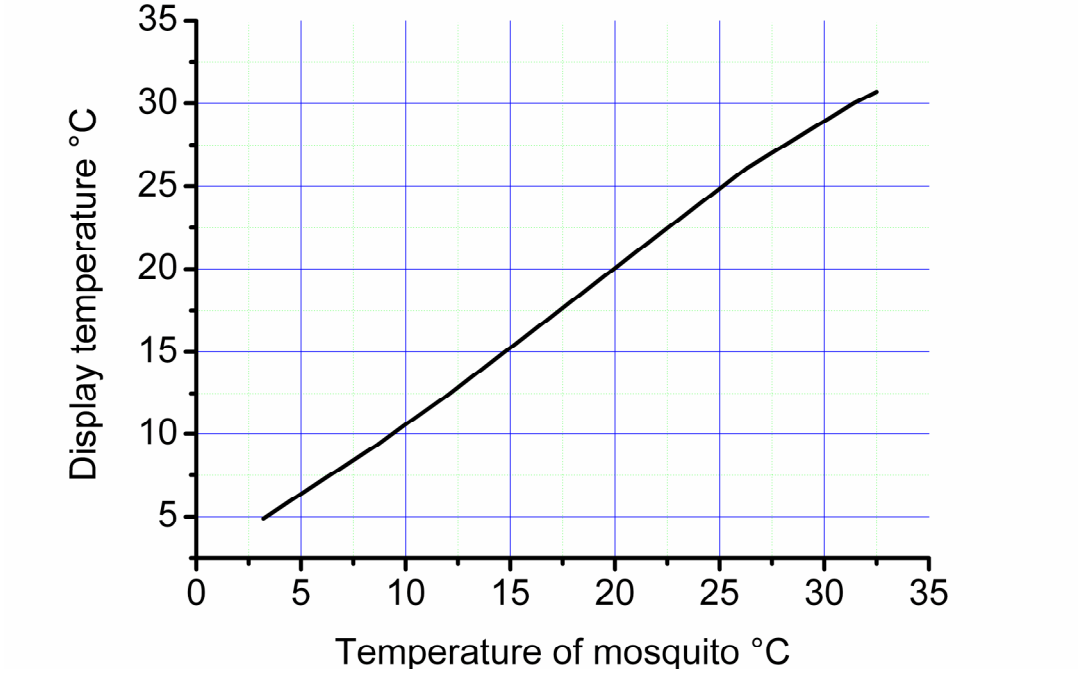

Figure 1.7

Relationship between the display temperature as read on the power supply (Fig. 1.5) and the temperature read by a thermocouple modulator (80TK, Fluke©, www.fluke.co.uk) fixed to the brass block with bone wax imitating the mosquito in Figure 1.5.

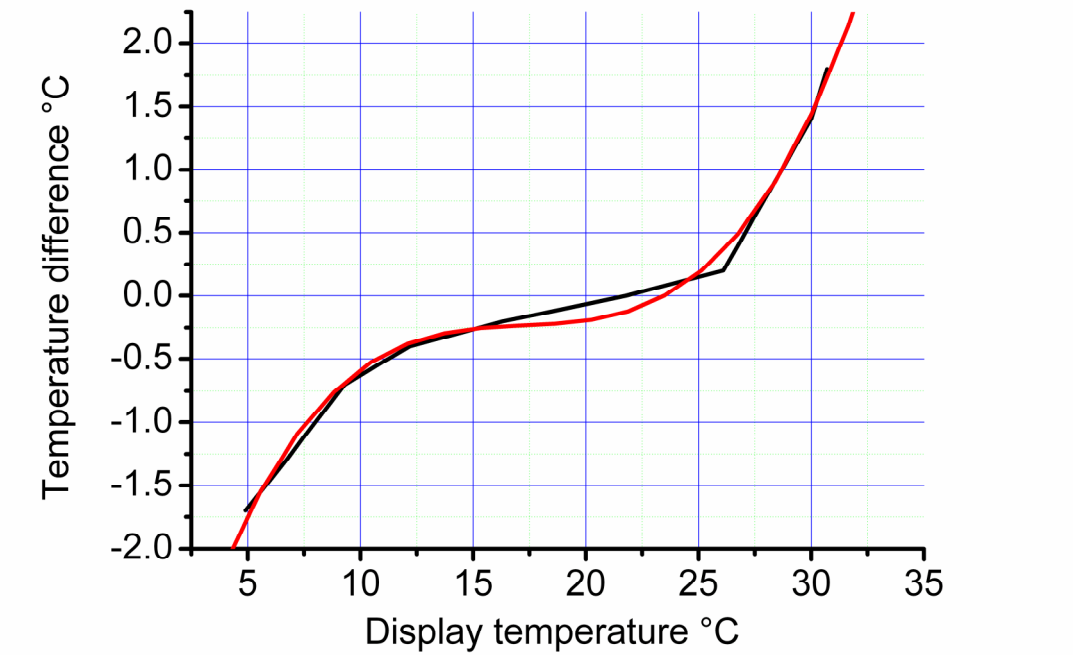

Figure 1.8

The temperature difference between that read on the power supply and that read by a thermocouple modulator (black trace) (80TK, Fluke©, www.fluke.co.uk) fixed to the brass block with bone wax imitating the mosquito in Figure 1.5. A polynomial (red trace) was fitted to the data in order to allow the temperature to be calibrated.

Data analysis

Spectrograms for *Tx. brevipalpis* were manually digitized using origin (v.7). The WBF was manually extracted by taking the WBF every 10 msec from a spectrogram plotted in Spectrogram v.16. The frequency and time resolution of WBF's manually digitised was 2.7 Hz and 45 msec. Spectrograms for *An. gambiae* and *Cx. quinquefasciatus* were digitized using a custom made programme written in Matlab R2006b (The MathWorks. Inc.). Where the programme failed to follow the WBF's because they overlapped or were too weak, manual analysis was performed for recordings from *Cx. quinquefasciatus* as explained for *Tx. brevipalpis* and is stated in the figure captions for that chapter.

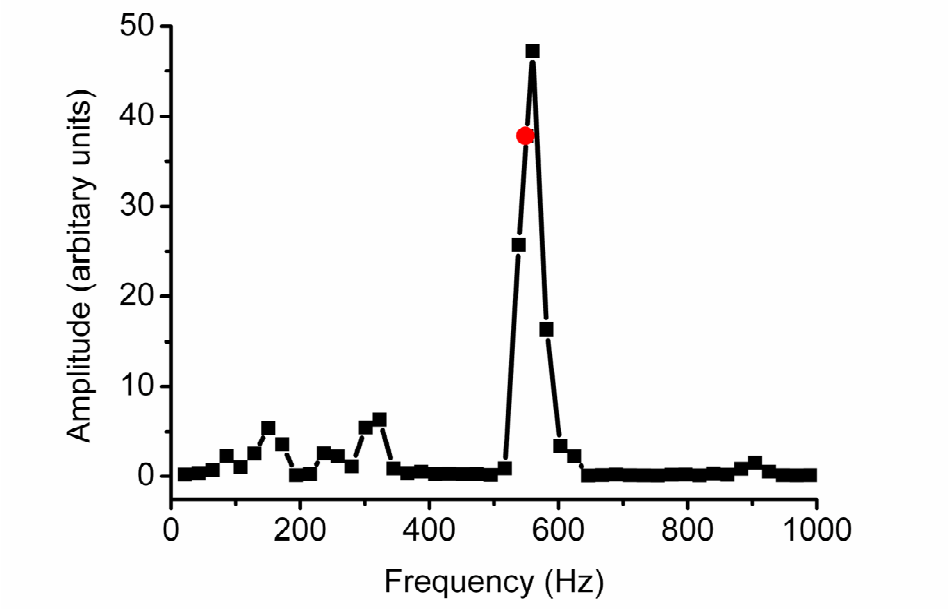

Figure 1.9

Fourier transform (2048 points) of sound file recording of a solo flying male at ~550 Hz. Although the frequency resolution is only ~25 Hz, by calculating the average of the 3 points defining the WBF (red circle), (as done when automatically calculating the WBF using a custom made programme in matlab ©) the frequency resolution can be increased.

To extract the WBF's from sound recordings of tethered flight a custom made programme was developed which performed a Fourier transform at every 2048 points (every 46 msec) along the sound file to extract up to 3 WBF's. The WBF was plotted as an average of the amplitude of the highest point on the Fourier transform and two points either side (Fig. 1.9). Thus, even though the Fourier transform only had a frequency resolution of ~25 Hz, by taking the amplitude at three frequency points on the Fourier transform into consideration high frequency resolution was obtained (Fig. 1.10, Fig. 1.12, Fig. 1.13). Figure 1.11 shows a spectrogram plotted in Spectrogram v.16. Figure 1.12 and 1.13 show the manually digitised and automatically digitised data displayed in Figure 1.11.

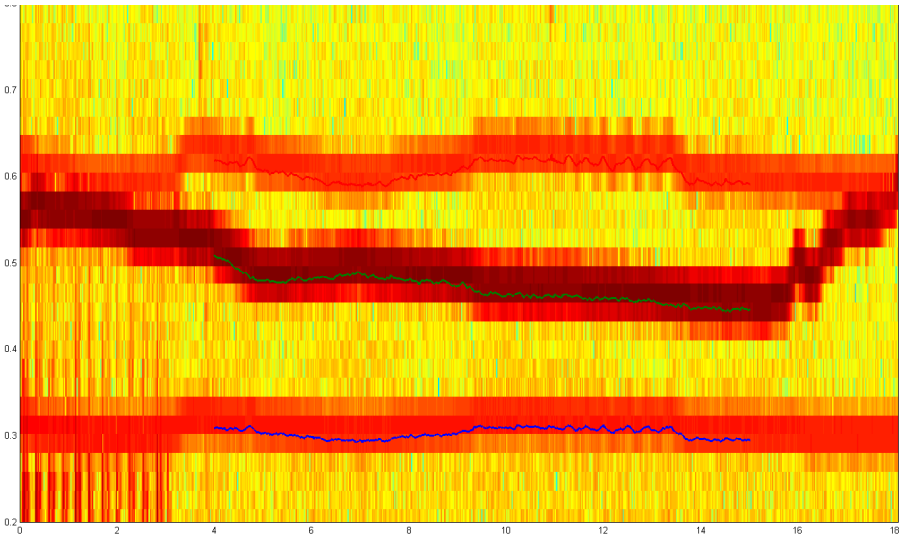

Figure 1.10

Spectrogram performed by Matlab programme with the calculated WBF shown as thin blue, green and red lines.

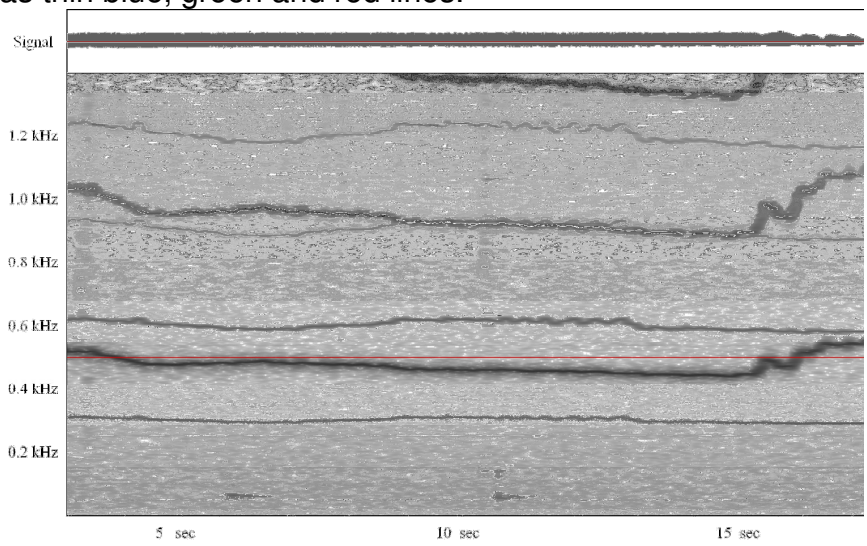

Figure 1.11

Spectrogram of a sound recording showing the WBF's of a tethered male and female *Cx. quinquefasciatus*, generated in Spectrogram v.16 ©.

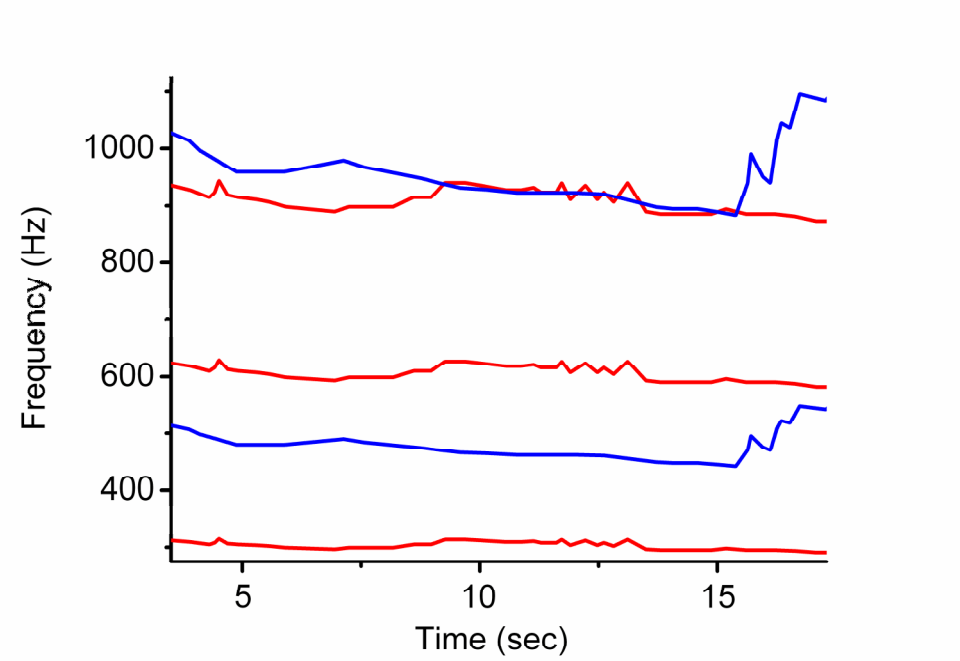

Figure 1.12

Spectrogram of sound file with the WBF's of a tethered male and female *Cx. quinquefasciatus*, manually obtained from spectrogram in Fig. 3.5. The male's first and second harmonics are in blue. The female's first three harmonics are in red.

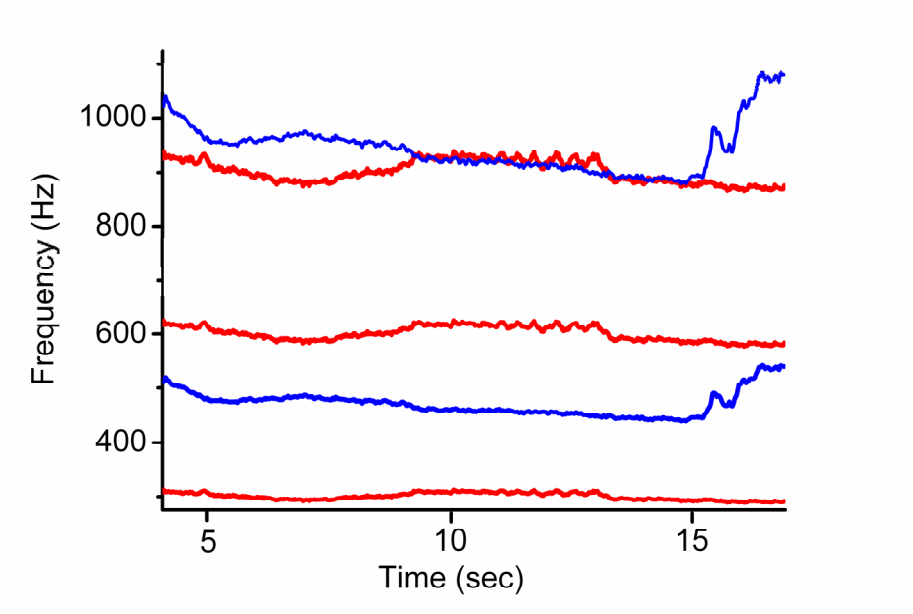

Figure 1.13

Spectrogram showing frequency matching between the 2nd harmonic of the male and 3rd harmonic of the female *Cx. quinquefasciatus* WBF when flown in pairs. The male's first and second harmonics are in blue. The female's first three harmonics are in red. Spectrogram automatically obtained from spectrogram in Fig. 3.5 using custom made programme written in matlab ©.

Mechanical and electrical isoresponse tuning curves are derived using level runs, whereby the particle velocity of tones emitted from a loud speaker, at a fixed frequency was increased, until an isoresponse or ‘threshold’ level was reached. For isolevel tuning curves the same particle velocity level was used across all frequencies. The isoresponse levels derived from recordings of the receptor potential were obtained by measuring the amplitude at a specific frequency after a Fourier transform. Isoresponse levels were obtained when the potential, at the specified frequency, was 1.4 times higher than the noise floor. The noise floor was calculated by the average of the noise floor either side and within the vicinity of the measured frequency.

The isoresponse level derived from mechanical recordings with the laser interferometer were obtained by measuring displacement as the peak to peak voltage recorded from the laser after the laser signal was band –pass filtered in the time domain with a filter width of 100 Hz (i.e. for a stimulus of 500 Hz a band-pass filter between 450 and 550 Hz was used). Noise was calculated as the average amplitude of the peak-to-peak signal in the time domain before stimulation.

For mechanical distortion product tuning curves the signal was converted into the frequency domain via a Fourier transform. Isoresponse levels or ‘thresholds’ were processed as described above for electrical tuning curves. Displacement of the laser was calibrated by measuring the point at which a sinusoidal signal of increasing amplitude produced harmonics (i.e. outside the 84 nm operating range of the laser). The voltage recorded from the photodiode at this level was equivalent to 84 nm.

CHAPTER II ACOUSTIC INTERACTION IN *CX. QUINQUEFASCIATUS*

ABSTRACT

Mosquitoes are endowed with a highly acute auditory sense underpinned by the auditory JO at the base of the antennae. Detection of acoustic stimuli through the JO leads the mosquitoes to alter their WBF. Such acoustic interactions between pairs of tethered flying mosquitoes has been shown for nectar feeding mosquitoes (Gibson *et al*., 2006). This included sexual recognition based on frequency matching for *Tx. brevipalpis* where the wing beat frequencies of males and females are similar. Here I show that frequency matching also occurs in the blood feeding mosquito *Cx. quinquefasciatus* even though the wing beat frequencies, of males and females, differ significantly ($P<0.001$) and do not overlap. The wing beat frequencies of a tethered flying male-female pair converge not on their fundamental but on their nearest shared harmonic (for instance the female's third and male's second). Criteria were established to quantitatively assess the amount of frequency matching between pairs of tethered flying *Cx. quinquefasciatus*. When flown together in pairs, *Cx. quinquefasciatus* (like *Tx. brevipalpis*), show significantly more frequency matching between opposite sex pairs than same sex pairs. This chapter is largely based on work from Warren *et al*. (2009).

INTRODUCTION

It has been known for some time that flying mosquitoes are attracted towards a sound source that emits a frequency similar to the fundamental of its WBF (Roth, 1948). Sounds are detected by the JO, which transduce auditory stimuli into electrical signals (Tischner *et al*., 1955). The JO of female mosquitoes has been found to be only slightly less sensitive than that of the male JO but, somewhat surprisingly, auditory behaviour in females has only recently been shown (Gibson *et al*., 2006). Acoustical stimulation, provided by the WBF of female mosquitoes, is a necessary prerequisite to initiate a mating response by the male in many mosquito species. In the case of *Ae. aegypti*, the male will not enter into a mating response without acoustic stimulation (Roth, 1948). This was proved convincingly by using tuning forks and a loud-speaker to produce pure tones, which triggered the typical mating response in *Ae. aegypti* (Roth, 1948). Previous to Gibson and Russell's (2006) analysis of mosquito flight behaviour, in response to sound, only phonotactic responses of mosquitoes were shown. By flying mosquitoes on tethers, Gibson and Russell (2006) were able to make auditory recordings of their WBFs over a period of time and show that *Tx. brevepalpis* females can respond to the WBF of other mosquitoes during tethered flight (Gibson *et al*., 2006). When *Tx. brevipalpis* are tethered and flown they respond to acoustic stimulation by altering their WBF (Gibson *et al*., 2006). *Tx. brevipalpis* also change their WBF so that it matches that of a tone presented from a speaker (Fig. I.12 B) or matches the WBF of another tethered flying mosquito (Fig. I.13). The ability of *Tx. brevipalpis* to match its WBF with that of another mosquito depends of the sex of the other mosquito such that only opposite sex pairs enter into a prolonged flight where both their WBF's are matched. The WBF of male and female *Tx. brevipalpis* do not significantly differ but the WBF of male and female haematophagous species are significantly different. This is due to the necessity of female haematophagous mosquitoes to take a blood meal and carry eggs for ovipositioning. They are typically larger than their conspecific males and fly at significantly lower wing beat frequencies. This allows sexual identification based on the fundamental wing beat frequency and is especially important for male

mosquitoes when detecting, approaching and grasping females entering the swarm. Using the experimental design of Gibson and Russell (2006) auditory interactions between mating pairs of another haematophagous species blood feeding mosquito has been recently demonstrated for *Ae. aegypti* (Cator *et al*., 2009). Surprisingly, *Ae. aegypti* opposite sex pairs frequency match through their higher harmonics (the female's third harmonic with the male's second). Cator *et al*'s (2009) study reveals that frequency matching is not restricted to mosquitoes with similar wing beat frequencies such as that demonstrated in *Tx. brevipalpis* (Gibson *et al*., 2006). Thus, frequency matching appears to be important across, at least, two genera of mosquitoes.

RESULTS

Individual responses to acoustic stimulation

In order to record the fundamental WBF of *Cx. quinquefasciatus* a particle velocity microphone (Knowles NR-23158-000) was positioned in the middle of a cage, above a swarm marker, (30X30 cm) of either male or female mosquitoes for 10 minutes in their active period at dusk. Measurements of the WBF were taken whenever the mosquito flew within 6 cm of the microphone by performing a Fourier transform (with 16384 points) of the sound file and measuring the frequency, at which the peak voltage was obtained (Fig. 2.1). The measurement of WBF's from the same mosquito could not be ruled out because each mosquito in the cage could not be individually identified. Thus a lower estimate of the number of WBF's recorded from individual mosquitoes was made by dividing the number of flying individuals in the cage by two.

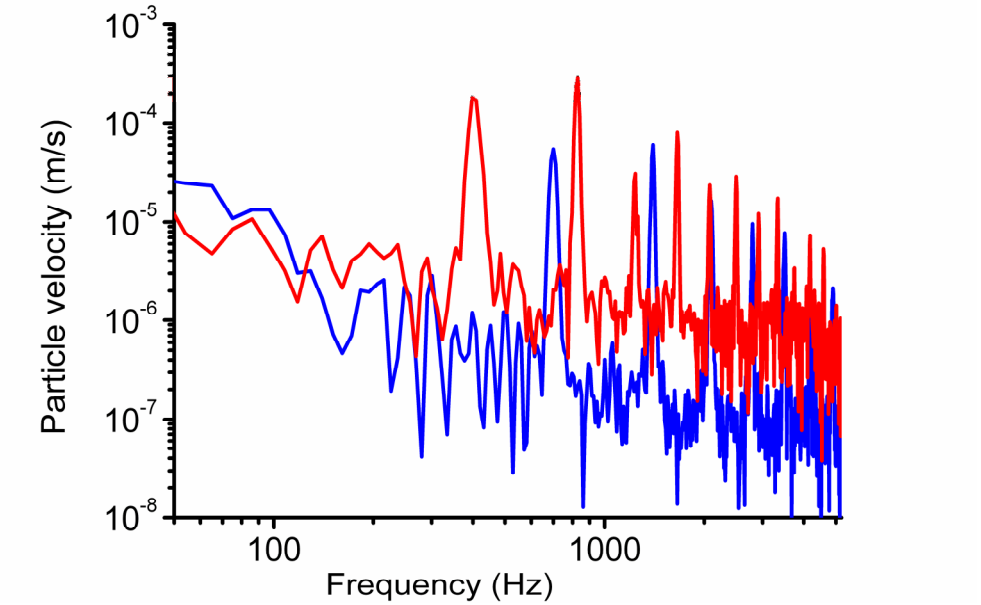

Figure 2.1

Fourier transform of a flight tone recording of free flying male (blue) and female (red) *Cx. quinquefasciatus* at ~3 cm from a particle velocity microphone (Knowles NR-23158-000).

The fundamental WBF of female *Cx. quinquefasciatus* is significantly lower than for males (401 ± 27 Hz female (n~10), 708 ± 41 Hz male (n~12) (untethered 'free' flight)). These measurements were repeated for *Cx. quinquefasciatus* that

were tethered which decreased the WBF of each sex to 346 ± 40 Hz for female's and 525 ± 47 Hz for male's (Table 2.2). The change in WBF with tethering was significant (Tukey's test P<0.001) as was the difference in WBF between the male and female for tethered and free flying *Cx. quinquefasciatus* (Tukey's test P<0.001).

	Female	Male
Free flying	401 ± 27 (n~10)	708 ± 41 (n~12)
Tethered	346 ± 40 (n=16)	525 ± 47 (n=14)

Table 2.2

Wing beat frequencies of free flying and tethered *Cx. quinquefasciatus* (each n number is an individual).

To assess the ability of *Cx. quinquefasciatus* to frequency match artificially generated sounds, pure tones were delivered from a loud speaker within 3 cm of tethered flying male mosquitoes (Fig. 2.3). Frequency matching of their flight tone to the tone delivered by the speaker occurred at their fundamental (~675 Hz) and also at their 2nd harmonic (~1200 Hz) (Fig. 2.3 A).

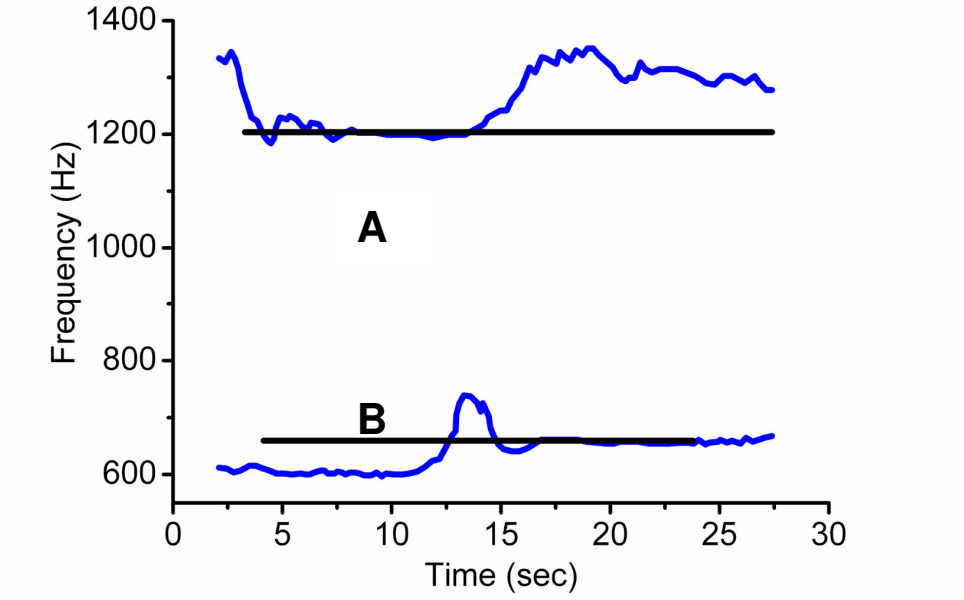

Figure 2.3

Spectrograms of two separate male *Cx. quinquefasciatus* frequency matching a pure tone from a loud speaker. A The second harmonic of the male frequency matching a 1200 Hz tone at $1.5X10^{-3}$m/s. B The fundamental of the male frequency matching a 675 Hz tone at $4.6X10^{-4}$m/s. Spectrograms were manually digitised.

Paired recordings

Frequency matching was observed between opposite sex pairs despite the large and non-overlapping difference in their mean fundamental WBF of both sexes (Fig. 2.4, 2.5). Similar to *Tx. brevipalpis* same sex pairs avoided matching their fundamental WBF (Fig. 2.6 – 2.8). Frequency matching was observed between the harmonic components of the WBF such that frequency matching commonly occurred between the 2nd harmonic of the male and 3rd harmonic of the female (Fig. 2.4) or less commonly between the fundamental of the male and 2nd harmonic of the female (Fig. 2.5). This incredible behaviour challenges the current understanding of mosquito audition because the JO of mosquitoes is thought not to respond to frequencies exceeding 800 Hz (Clements, 1999; Roth, 1948). The frequency tuning of the JO is reviewed in Chapter IV and a mechanism for frequency matching at such high frequencies is proposed in chapter V.

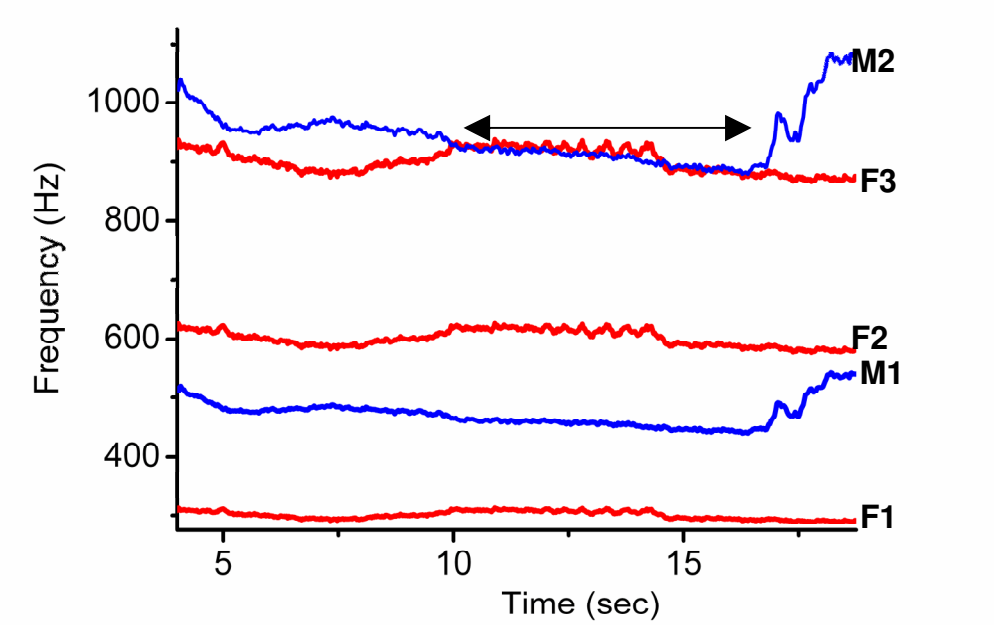

Figure 2.4

Spectrogram showing frequency matching between the 2nd harmonic of the male (M2) and 3rd harmonic of the female (F3) *Cx. quinquefasciatus* WBF when flown in pairs. The male's first and second harmonics are in blue. The female's first three harmonics are in red. Spectrogram automatically obtained from spectrogram using custom made programme written in matlab ©. Period of frequency matching indicated by two-headed arrow.

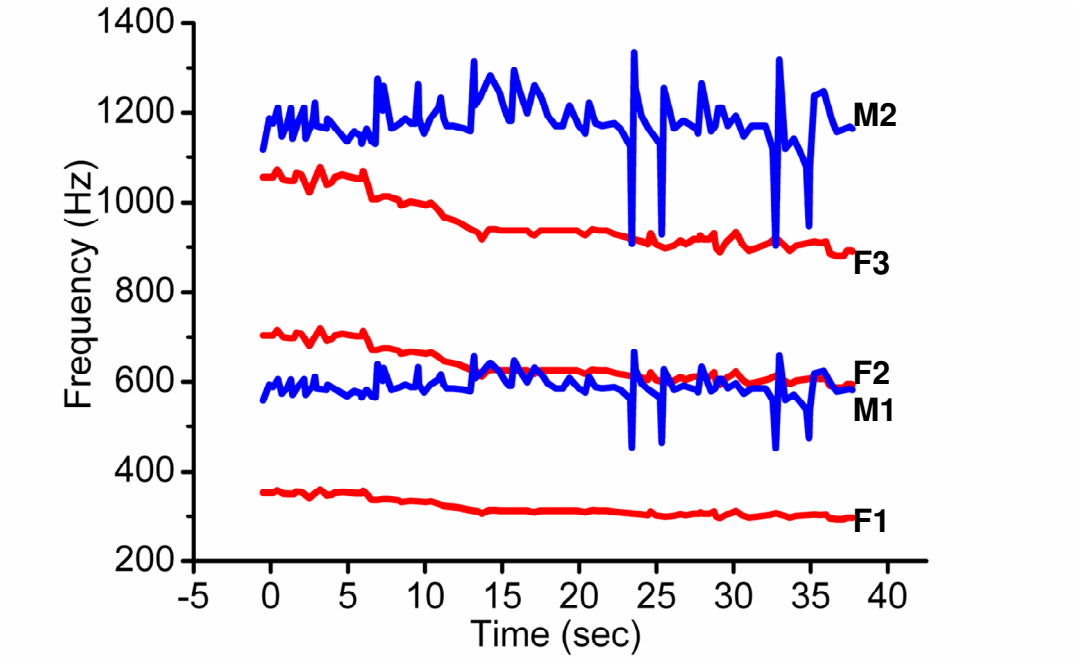

Figure 2.5

Spectrogram showing frequency matching between the 1st harmonic of the male (M1) and 2nd harmonic of the female (F2) *Cx. quinquefasciatus* WBF when flown in pairs. The male's first and second harmonics are in blue. The female's first three harmonics are in red. This spectrogram was manually digitised.

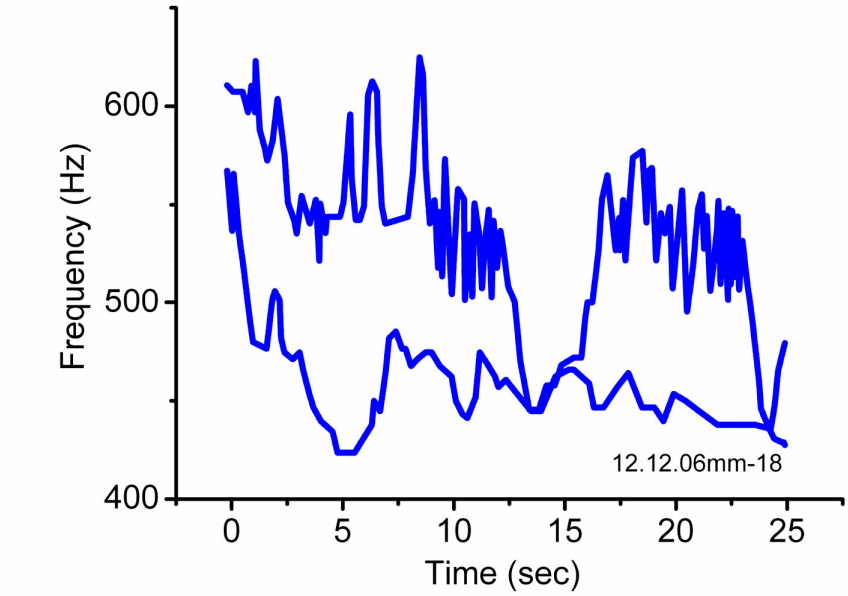

Figure 2.6

Spectrogram showing frequency matching avoidance for the first harmonic of a pair of male *Cx. quinquefasciatus*. This spectrogram was manually digitised.

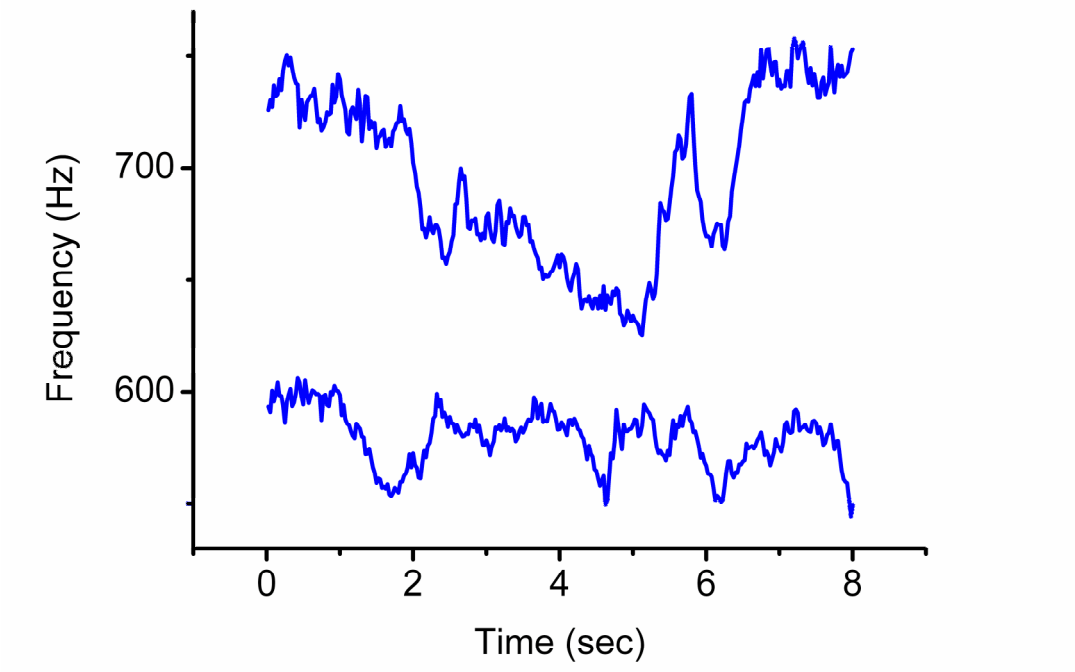

Figure 2.7

Spectrogram showing frequency matching avoidance for the first harmonic of a pair of male *Cx. quinquefasciatus*.

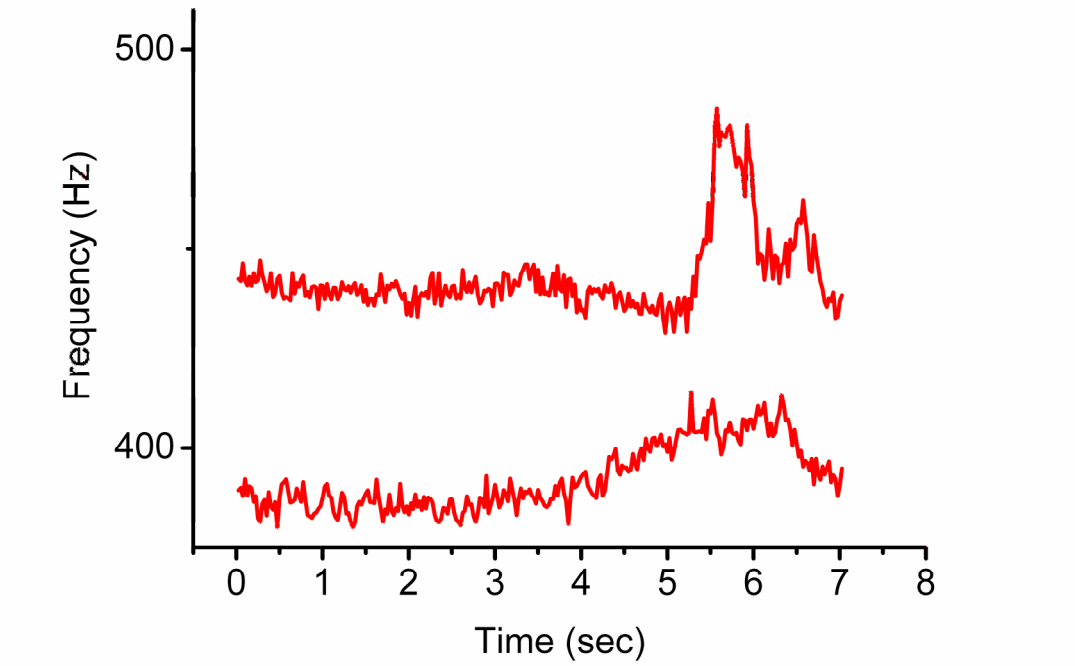

Figure 2.8

Spectrogram showing frequency matching avoidance for the first harmonic of a pair of female *Cx. quinquefasciatus*.

To quantitatively assess the amount of frequency matching between pairs of flying mosquitoes the ratio between the fundamental WBF's were obtained for

paired recordings between 6 and 10 seconds in length for 40 separate mosquitoes. Frequency ratios that are integer based ratios indicate that frequency matching between two mosquitoes will occur at the specified harmonic of each mosquito. For example, a frequency ratio of 1.5 is the inverse of 3:2, which means that the 3rd harmonic of one mosquito will be the same frequency as the 2nd harmonic of the other mosquito. Accordingly, frequency ratios that are not integer-based indicate frequency avoidance, where two mosquitoes do not share frequencies at any harmonic. Figure 2.9 displays the ratio obtained from dividing the fundamental male WBF by the fundamental female WBF for Figure 2.4. The frequency distribution of the ratios between the 1st harmonics of each mosquito in a pair were plotted and fitted with a Gaussian curve by an Origin 7 programme to test for the occurrence of significant peaks (Fig. 2.10).

Out of 20 male-female pairs, 17 had significant peaks in their frequency ratios (r^2>0.90, P<0.05); 15 pairs had a significant peak centered at a ratio of 1.50 (3:2), as shown in Fig 2.9 and Fig. 2.10 and the other 2 had a significant peak centered at a ratio of 2.0 (2:1). Three pairs did not show any significant peaks in the distribution of their frequency ratios. Overall, we conclude that male-female pairs frequency-match at shared harmonic frequencies. All 10 male-male pairs had significant peaks (r^2 >0.88, *P*< 0.05), centered at a ratio of either 1.13 or 1.07 (Fig. SD 2). All 10 pairs of female-female pairs had significant peaks (r^2 >0.89, *P*< 0.05), centered at a ratio of 1.10. These are non-integer ratios, and therefore, we conclude that same-sex pairs frequency-avoid.

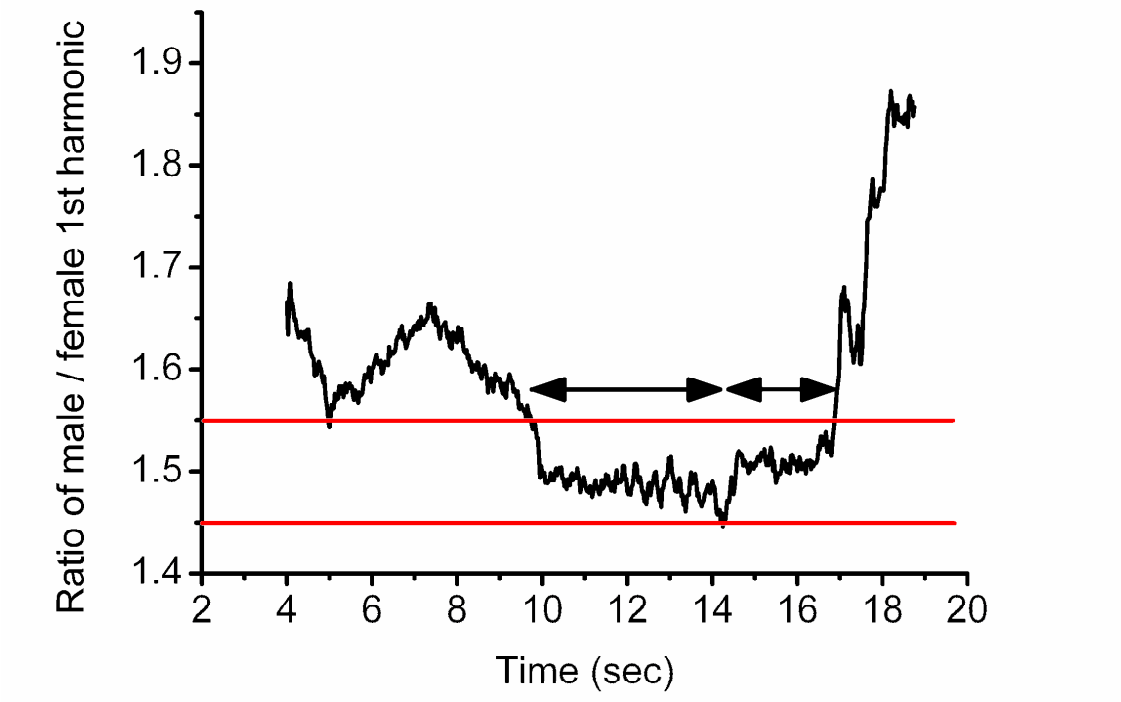

Figure 2.9

Ratio of male's 1st harmonic / females 1st harmonic (data from Fig. 3.4). Frequency matching limits are displayed in red and arrows depict when the ratio between the WBF's is between these limits.

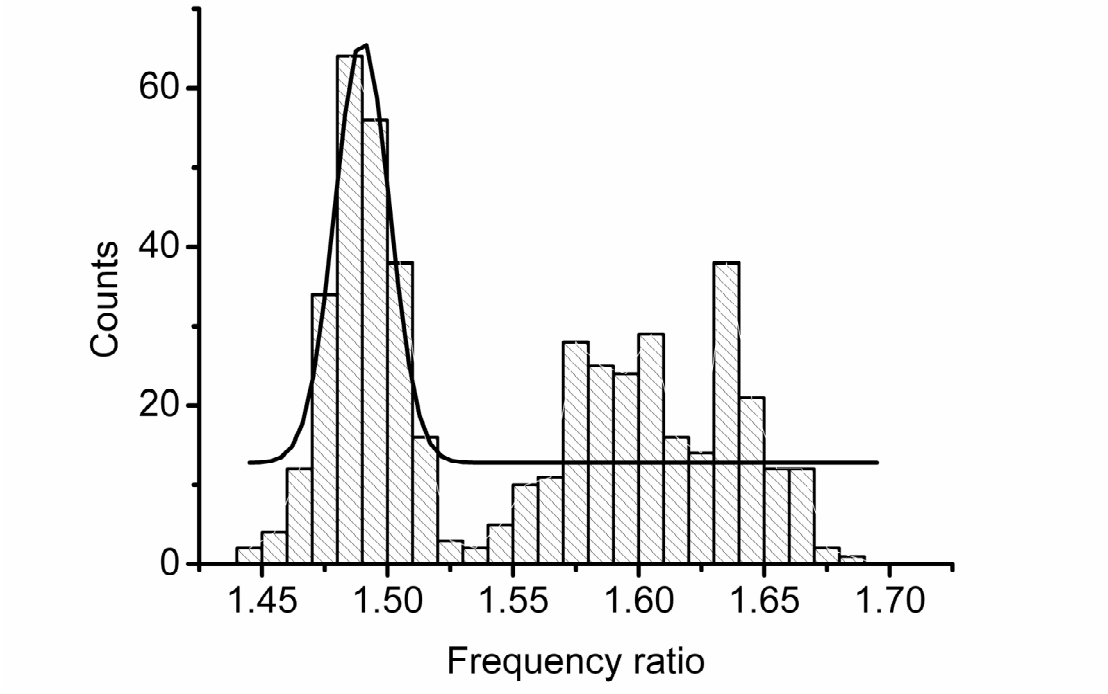

Figure 2.10

The frequency distribution of interactions between a male and female *Cx. quinquefasciatus* put into frequency ratio bin sizes of 0.01 and then fitted with a Gaussian curve, which has a peak at a frequency ratio of 1.49 Data from Warren *et al.* (2009).

DISCUSSION

Although *Cx. quinquefasciatus* swarming flight patterns have been shown to be consistently altered by sound, (Gibson, 1985) tethered *Cx. quinquefasciatus* respond less readily to pure tones emitted from a loud-speaker. However Figure 2.3 shows that males are not only able to respond to tones around the female fundamental WBF but also at higher frequencies, which are thought to be outside the frequency range of the JO (Clements, 1999; Wishart *et al*., 1959). Frequency matching of a tone at 1200 Hz occurred with the 2nd harmonic of the male WBF (Fig. 2.3A).

Frequency matching occurred between the harmonic components of the male and female WBFs. In Figure 2.5 matching occurred between the 2nd harmonic of the male and the fundamental of the female, whereas in Figure 2.4 matching occurred between the male's 2nd and female's 3rd harmonic. The frequency at which matching occurred was dynamic and not at a fixed frequency as shown in figure 2.4 where matching occurred between 15 and 20 seconds whilst the matching frequency shifted down over 50 Hz. The behaviour of same sex pairs mirrored that of *Tx. brevipalpis* showing frequency avoidance (Figure 2.6-2.8). Opposite sex pairs frequency match significantly more that same sex pairs. Based on the frequency tuning of the male JO (Chapter IV) it seems probable that males can detect the sex of another airborne mosquito based on its fundamental WBF. What appears to be the role of frequency matching? Frequency matching could form a possible cue for females to assess the fitness of advancing male mosquitoes with only genetically fit males able to maintain frequency matching for extended periods. Another consideration stems from the problem an airborne male has when approaching and grasping a female in the face of the turbulent airflow generated by the flapping of her wings. By frequency matching the male's 2nd with the female's 3rd harmonic every 2nd stroke of the male's wing beats will coincide with every 3rd stroke of the females. If frequency matching between the male's 1st and female's 2nd harmonic occurs then every stroke of the male's wing beats will coincide with every 2nd stroke of the females. Thus, frequency matching may help the male to approach and

grasp the female by drafting off her wing beats like migrating birds in flight. If the WBF is correlated to flight speed, which is suggested to be the case if the wing stroke amplitude remains the same (Taylor *et al*., 2003), then frequency matching may lead to opposite sex pairs maintaining a similar speed which would be important for mating on-the-wing. Frequency avoidance as shown by same sex pairs would therefore lead to separation in space of airborne same sex pairs. It would be interesting to know if frequency matching occurs when mosquitoes meet in swarms or if frequency matching is simply an epiphenomenon created through the unique conditions during tethered flight.

CHAPTER III ACOUSTIC INTERACTION IN AN. GAMBIAE

ABSTRACT

Tethered flight recordings of the malaria vector *An. gambiae* were conducted on two chromosomal forms of *An. gambiae*; M and S. The chromosomal form of each mosquito was determined by Dr Dabire after each experiment through genotyping the mosquito. It was found that opposite sex pairs of the same chromosomal form frequency matched significantly more then opposite sex pairs of different molecular forms when tethered and flown together. This is the first phenotypic difference found between these two forms that could account for reproductive isolation in mixed form swarms. Acoustic stimulation is the first necessary stimulus, to initiate mating behaviour (Roth 1948). Thus differences found in the acoustic interaction of tethered Anophelines suggest that acoustic cues may be involved in initiating or maintaining subspecies identity. This chapter is largely based on work in Pennetier *et al.* (2010).

INTRODUCTION

Malaria is spread by up to 7 sibling species of *An. gambiae*, which are morphologically indistinguishable. Two sub-species M and S, which are in the process of speciation, commonly swarm together in Bobo Dioulasso, Burkina Faso (Diabate *et al*., 2009), but few hybrids are found in the mixed swarms suggesting that a strong premating barrier must exist between the M and S chromosomal forms (Diabate *et al*., 2009). These two chromosomal forms differ in about 60 genes, however previous to this study no phenotypic differences have been found that can account for reproductive isolation in mixed swarms (Wondji *et al*., 2002). The difference in WBF between the M and S chromosomal form has been proposed to act as the subspecies specific cue allowing males to detect its conspecific form based on the frequency of her wing beats (Brogdon, 1998). However, the WBF was found to overlap significantly between forms and could therefore not account for the low amount of hybrid pairs (Tripet *et al*, 2009). Frequency matching occurs in the blood feeding mosquito *Cx. quinquefasciatus* (Chapter II) and is shown to be sexually specific. We wanted to explore the possibility of WBF matching acting as a reproductive isolation mechanism between the M and S subspecies of *An. gambiae*.

RESULTS

Paired recordings

An. gambiae were tethered and flown in pairs, within each other's auditory range at 21℃. Opposite sex pairs were both the same (MM and SS) or different (MS and SM) molecular form. Similar to all blood feeding mosquitoes the WBF is significantly different between the sexes (Table 3.1). In agreement with previous studies by Tripet *et al.* (2004) the WBF between the two molecular forms is not significantly different for either males or females (Tukey's test $p>0.05$).

	M female	M male	S female	S male
Solo	466 ± 25 Hz n=6	703 ± 99 Hz n=4	461 ± 38 Hz n=3	682 ± 60 Hz n=5
Paired	485 ± 35 Hz n=20	761 ± 54 Hz n=31	470 ± 34Hz n=24	733 ± 58 Hz n=13

Table 3.1

WBF of tethered flying *An. gambiae* M and S form when flying solo and when paired (data from (Pennetier *et al.*, 2010)). Each n number is a different mosquito.

The WBF appears to change upon presentation of the mosquito to another irrespective of form. However, this is not significant (Tukey's test $p>0.05$). The large standard deviation of the WBF in solo flight is due to the low number of mosquitoes recorded.

Like *Cx. Quinquefasiatus* and *Ae. aegypti* (Cator *et al* 2009), *An. gambiae* frequency match with their higher harmonics (typically the female's 3rd and male's 2nd). Frequency matching classification follows the same criteria as laid down for *Cx. quinquefasciatus*. Same form pairs (SS and MM) frequency matched more than opposite form pairs (SM and MS) (Table 3.2). The difference in frequency matching, between same and different form pairs, is statistically significantly different. (Fisher's exact test $P=0.0014$).

MM	SS	MS	SM
10/17	4/7	1/7	1/13
Same form 14/24		**Mixed form** 2/20	

Table 3.2

The proportion of opposite sex pairs classified as frequency matching (first and second letter denotes the female's and male's molecular form) (data from (Pennetier *et al*., 2010)).

Frequency matching

A mechanism to explain the difference in the proportion of same and different form pairs that frequency matched is principally based on each form occupying distinct but overlapping areas of frequency space, with their frequency matching harmonics (Fig. 3.3). When flown individually *An. gambiae* fly at very similar fundamental WBF frequencies (Table 3.1). Due to this, when acoustically interacting with other mosquitoes, irrespective of form, the frequency matching harmonic of M and S form occupy different frequency space. Same form mosquitoes occupying similar frequencies have less difference between their frequency matching harmonics. Therefore, same form mosquitoes can more easily frequency match by changing their WBF by less, than if attempting to frequency match with a different form partner.

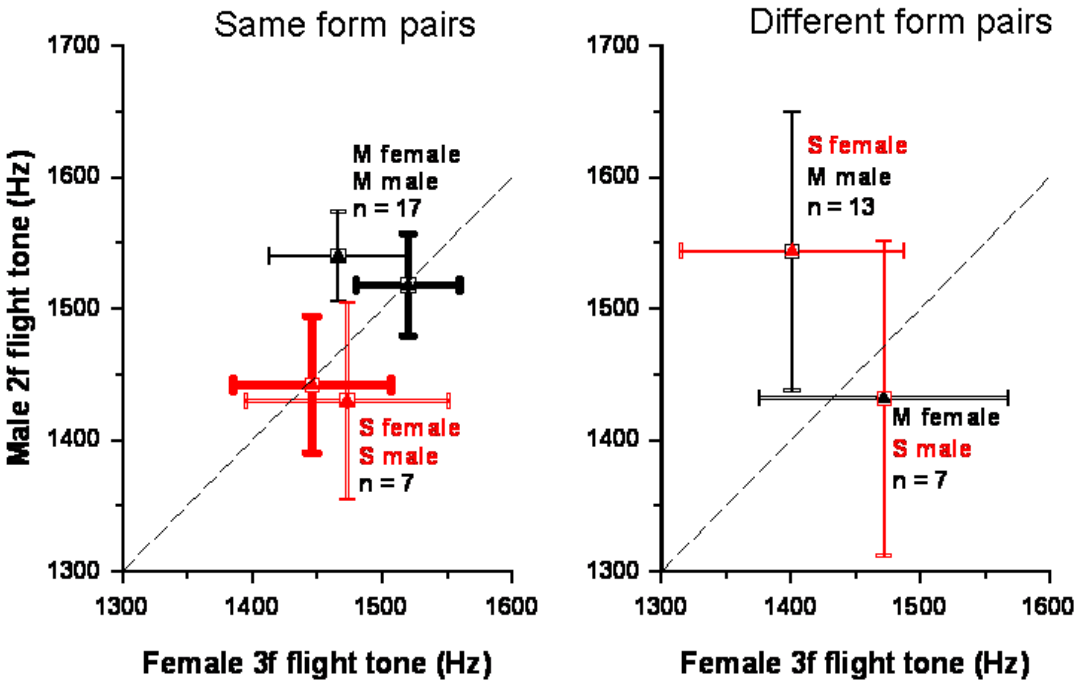

Figure 3.3
Frequency occupied by the male's 2nd and female's 3rd harmonic, during tethered paired flight for same form (left) and different form (right) pairs when frequency matching (thick lines) and not frequency matching (thin lines). Bars indicate standard deviation; dashed diagonal line indicates perfect frequency matching. Data from (Pennetier *et al*., 2010).

To quantify the likelihood of frequency matching between pairs of mosquitoes the frequency occupied by the second and third harmonic of the male and female (where 92% of frequency matching occurred), respectively was plotted (Fig. 3.3). Although the frequency occupied by the frequency matching harmonic of each form of mosquito overlapped the M form males tended to fly at higher frequencies compared to S form males irrespective of the molecular form of its tethered female partner. Similar to this the frequency occupied by the frequency matching harmonic of S form female mosquitoes tended to fly at lower frequencies than M form female mosquitoes.

DISCUSSION

Previous studies revealed no significant difference between the fundamental WBF of *An. gambiae* M and S form (Tripet *et al* 2004). However, differences in the WBF occur when *An. gambiae* are flown in pairs within each other's acoustic near field (Table 4.1). Like *Cx. quinquefasciatus, Tx. breviaplpis, and Ae. aegypti* opposite sex pairs of *An. gambiae* frequency match when flown on tethers. *An. gambiae* frequency match using their higher harmonics (usually the female's 3rd with the male's 2nd) like all other blood feeding mosquitoes studied to date (Cator *et al*., 2009) (Chapter II). The same molecular form frequency matched significantly more than opposite form, when tethered and flown in opposite sex pairs. This is the first phenotypic difference found between these two forms, which could potentially form a premating barrier. A plausible mechanism underpinning the difference in frequency matching between subspecies is based on the frequency occupied by the frequency matching harmonics (Pennetier *et al*., 2009). The matching harmonics occupied different yet overlapping parts of frequency space (Fig. 3.3). *An. gambiae* mosquitoes frequency match at a higher rate when their frequency matching harmonic is closer in frequency to their tethered partner. This is presumably because *An. gambiae*, of the same form, can frequency match easier with a smaller change in their WBF compared to different form pairs where a larger change in WBF is needed. Indeed theoretical calculations state that flight efficiency decreases as WBF deviates from an optimal frequency (Thomas *et al*., 2003). However, there is a very low occurrence of hybrid mating pairs of *An. gambiae* (Diabate *et al*., 2009) and it appears that the overlapping differences in the frequency matching harmonics cannot alone account for robust reproductive isolation in *An. gambiae.* Evidently there is a mechanism, or behavioural strategy yet to be identified, that favours same-form frequency matching. For example, having increased their mean WBFs on hearing the sound of a nearby mosquito, if M-form males then decrease and M-form females further increase their respective mean WBFs, they would increase the likelihood of frequency matching, whereas the reverse is true for S-form mosquitoes (after the initial increase in WBFs, females decrease and males further increase their respective WBFs to match). Would each type of mosquito to respond, through a change in its WBF,

always as if it were flying in a same-form pair, the chance of frequency matching in mixed-form pairs would be much reduced because the difference between their respective 3:2 WBFs would increase. Previous attempts to detect potential mate recognition characteristics in the mean WBFs of *An. gambiae* species may have failed because WBFs were measured only in solo-flying mosquitoes. Findings that mosquitoes increase the overall frequency of their wing beats when encountering others and the potential importance of the relative WBFs of male's and female's at higher harmonic ratios were not yet known (Clements, 1999; Tripet *et al*., 2004).

CHAPTER IV MECHANICAL AND ELECTRICAL TUNING OF THE FLAGELLUM AND JOHNSTON'S ORGAN

ABSTRACT

The physiology of the antennae of *Cx. quinquefasciatus* and *An. gambiae* were investigated using optical and electrical techniques to measure mechanical displacements of the flagellum and electrical potentials from the JO in response to sound stimulation. The mechanical vibrations of the sound capturing flagellum of the males were found to be broadly tuned and were most sensitive to frequencies below the WBF's of female mosquitoes. The flagella of female mosquitoes were also broadly tuned to frequencies below those of the male's. Mechanical vibrations of the flagellum could be measured up to 5 kHz for behaviourally relevant sound intensities. Although the electrical responses of the JO for both male and female mosquitoes matched the frequency tuning of the flagellum their range was limited to <1000 Hz. Therefore the JO of male of *Cx. quinquefasciatus* was not tuned optimally to detect the WBF of their female conspecific. The frequency tuning of the JO of female mosquitoes was not matched to any component of the male flight tone. In male *An. gambiae* the fibrillae of the flagellum become erect at times of swarming and presumably function in the acoustic detection of females. Fibrillae erection caused an upward shift in the most sensitive frequency of the male's flagellum and JO towards the WBF of females. Thus fibrillae erection appears to increase the sensitivity of male *An. gambiae* to airborne females. The nature of the neural response of the JO to sound was investigated through the injection of TTX into the mosquito and through the measurement of different components of the evoked electrical potentials. Finally, action potentials were measured from the thoracic wing and leg areas of male mosquitoes, in response to sound, and was used as a measure of the behaviourally relevant sound frequencies and intensities, to which a mosquito responds.

INTRODUCTION

The mosquito antenna is an anatomically simple, yet intricate, hearing organ designed principally to detect conspecific WBFs and is the most sensitive arthropod detector known (Göpfert *et al*., 1999; Mayer, 1874). The sound capturing flagellum of the antennae pivots about its base in response to the particle displacement component of sound. Movements of the flagellum are transduced into receptor potentials by the JO. Previous studies have found that the flagellum of male mosquitoes is mechanically tuned to its conspecific female WBF (Gibson *et al*., 2006; Göpfert *et al*., 1999; Göpfert and Robert, 2000). Similarly potentials recorded from the JO, in response to sound, match the most sensitive frequency of mechanical displacements of the flagellum (Belton, 1974; Clements, 1999; Göpfert *et al*., 2000).

The mechanical properties of the anatomically similar but less complex flagellum of *Drosophila* has been modelled as a simple damped harmonic oscillator (Nadrowski *et al*., 2008). However the simple harmonic oscillator model only captures the basic characteristics of the mosquito antenna. This is due to the complex anatomy and physiology of the flagellum. For instance, it has been shown previously that the flagellum's fine hair-like fibrillae can influence its mechanical properties (Göpfert *et al*., 1999). The presence of the fibrillae tend to increase the mechanical sensitivity of the flagellum at higher frequencies, as has been shown for *Ae. aegypti* by Göpfert *et al.* (1999). For *Anophelines*, physiological processes result in diurnal movements of the fibrillae. Fibrillae are folded into the flagellum during periods of rest but become erect, and presumably function in the detection of WBFs, during periods of swarming activity (McIver, 1982). Fibrillae erection itself should alter only the sensitivity of the flagellum to the particle displacement component of sound through the predicted increase in surface area. The effect of fibrillae erection on the mechanical and/or electrical properties of the flagellum and JO remains to be investigated.

RESULTS

Mechanical tuning of the flagellum of the antenna

Isoresponse and isolevel mechanical tuning curves were obtained from measurements of the sound-induced vibrations of the flagella of *Cx. quinquefasciatus* mosquitoes. Isoresponse mechanical tuning curves are used in order to determine the frequency specific response of the flagellum at a relatively low level of stimulation by measuring the particle velocity level sufficient to displace the flagellum by 6 nm ~240 µm from its base. The 6 nm criterion was detemined by the noise floor measured at 300 Hz (close to the resonance of the flagellum). Displacements of 6 nm were clearly discernable above the noise floor for all mosquitoes and the particle velocity required to elicit a 6 nm displacement was ~20 times that required to elicit a potential response of the JO at 300 Hz. The flagellum is most sensitive to frequencies at ~300 Hz (Fig. 4.1) but displacements of the flagellum of 6 nm could be measured up to 5000 Hz in frequency. The flagella of male mosquitoes are tuned to about 300 Hz with a Q_{10}dB bandwidth of 520 Hz. The Q_{10}dB bandwidth is an indicator of the sharpness of tuning and was calculated by measuring the frequency range at which a response could be elicited 10 dB above the particle velocity level at the most sensitive frequency (Fig. 4.1, inset). The flagellum of the female is most sensitive to a frequency of 200 Hz with a Q_{10}dB bandwidth of 675 Hz. Thus the female flagellum is sensitive to frequencies considerably below the WBF's produced by either male or female during flight (Fig. 4.1). Frequency tuning of the female flagellum is broader and an order of magnitude more sensitive than that of the male, with a peak sensitivity of $1.5X10^{-6}$ m/s. The particle velocity level required to displace the flagellum by 6 nm increases above and below the most sensitive frequency by ~10 dB per octave and ~6dB per octave respectively (Fig. 4.1). However, there are secondary, high frequency resonances (minima) in the frequency tuning of the flagella of both male and female *Cx. quinquefasciatus* at about 1500 Hz (arrow in Fig. 4.1).

Isolevel tuning curves were obtained by measuring displacement of the flagellum to a broad range of frequencies of the same intensity (Fig. 4.2). Displacement of the flagellum increased nonlinearily with sound pressure level (SPL). At the resonant frequency rate of change of displacement with level is steepest between 40 and 60 dB SPL (4.5 nm dB^{-1}) compared with 0.3 nm dB^{-1} and 2 nm dB^{-1} for levels between 30-40 and 60-70 dB SPL for example (Fig. 4.2). The resonant frequency of the flagellum was level dependant and increased by about 30 Hz with an increase in SPL of 40 dB (Fig. 4.2).

Measurements of the displacement of the flagellum due to thermal noise along the 1.8 mm length of the flagellum, provides an indicator of its flexibility (Fig. 4.3). Thermal noise increased from the base of the flagellum to the tip. Noise scaled linearly with distance from the base of the flagellum up to 1500 µm, as has be predicted for simple insect hairs (Fletcher, 1978). Distal to 1500 µm, thermal noise increased nonlinearly with distance from the base of the flagellum indicating that the tip is comparatively more flexible than the rest of the flagella shaft.

In *Anopheline* mosquitoes the structure of the flagellum undergoes diurnal activity associated with periods of swarming. At dawn and dusk the fibrillae become erect extending out from the flagellum. During periods of inactivity the fibrillae are folded into the flagellum (Fig. I.2). Mechanical isoresponse tuning curves measured from the flagellum, of *An. gambiae* M form, with both folded and erect fibrillae reveal that these changes are associated with changes in frequency tuning rather than with changes in mechanical sensitivity. When the fibrillae are folded the most sensitive (characteristic) frequency is 200 Hz (Fig. 4.4 red). This shifts significantly to 400 Hz (Fig. 4.4 black) when the fibrillae are extended (t-test, p=0.0013 [from 4 mosquitoes with erect fibrillae and 6 mosquitoes with folded fibrillae]), but with little change in sensitivity ($1.2X10^{-5}$ m/s, folded vs $1.9X10^{-5}$ m/s extended [from 4 mosquitoes with erect fibrillae and 6 mosquitoes with folded fibrillae]). Unlike the flagellum of their male counterparts, the characteristic frequency of the flagellum of female *An. gambiae* does not undergo diurnal change.

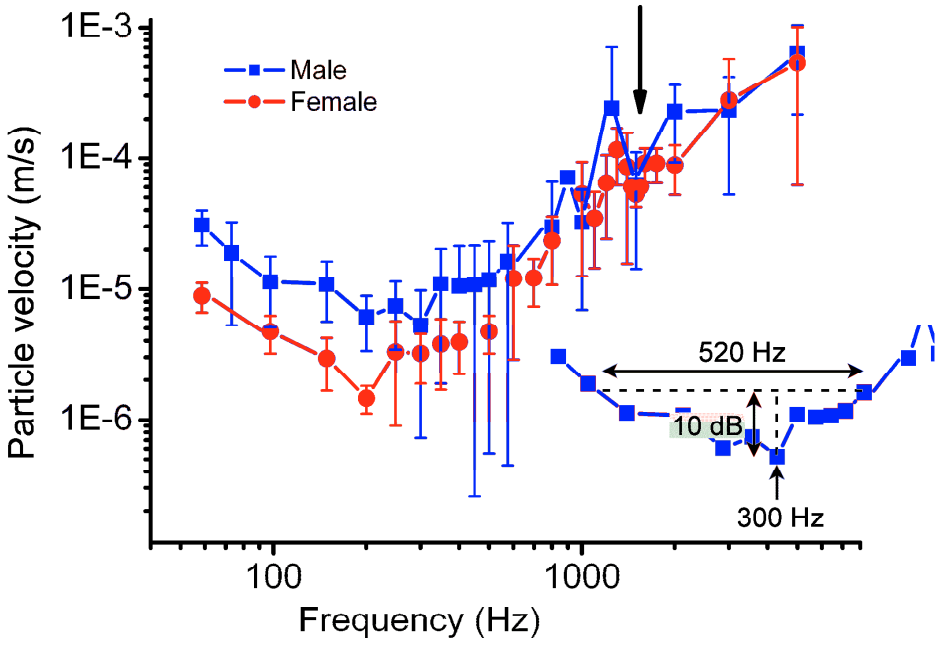

Figure 4.1

Isoresponse ('Threshold' or isoresponse criterion, 6nm) mechanical tuning curves of the flagellum of 7 Male and 5 female (error bars indicate ± 1 standard deviation) *Cx. quinquefasciatus* to acoustic pure tone stimuli. Arrow shows the second sensitivity dip at 1500 Hz for both sexes. For clarity only positive or negative standard deviation is shown. Inset: enlarged section of the male's tuning curve without standard deviation bars showing how the Q_{10}dB bandwidth of 520 Hz is calculated.

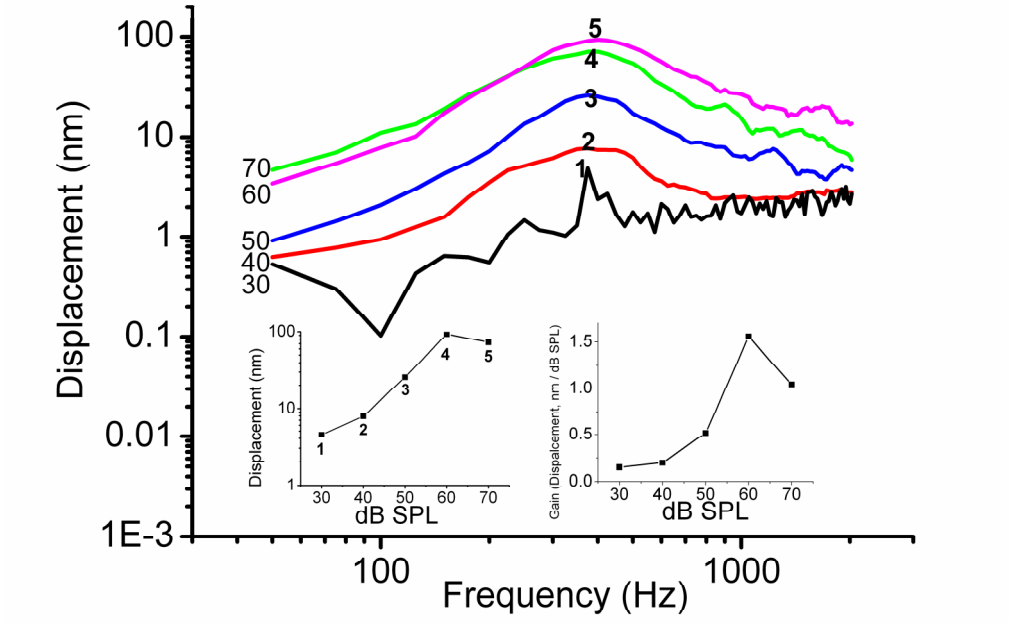

Figure 4.2

Isolevel mechanical tuning curves showing the displacement of the flagellum to pure tones at the SPL's shown adjacent to each trace. Inset left: Displacement as a function of SPL and Inset right gain as a function of SPL.

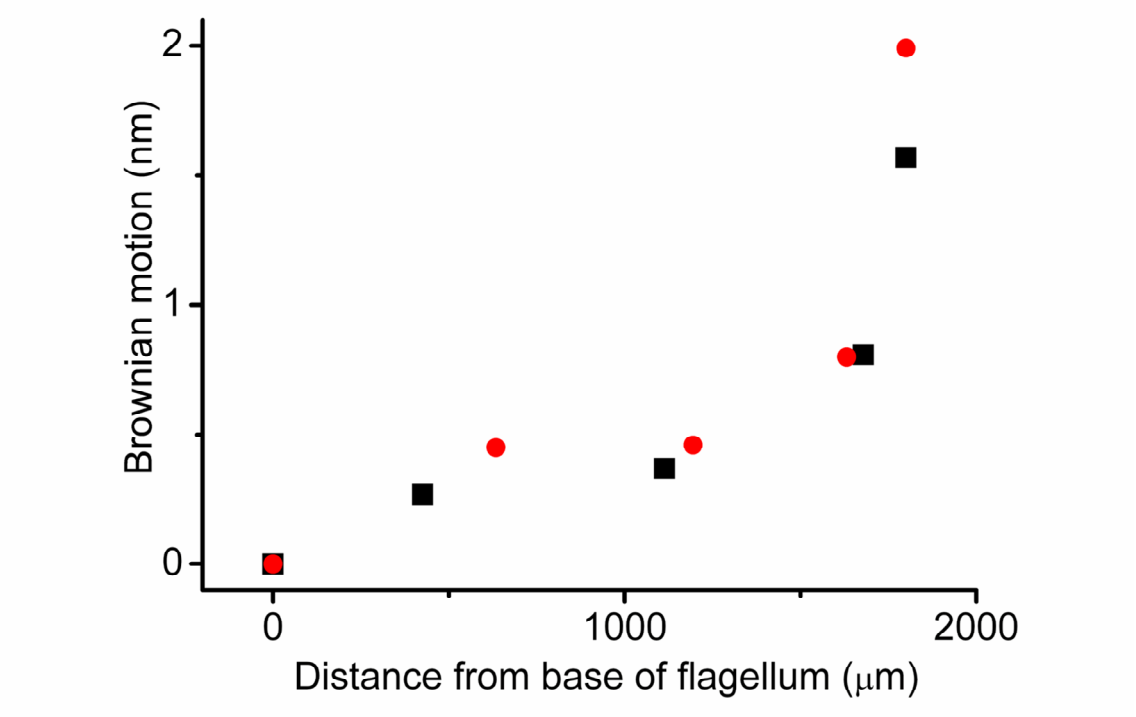

Figure 4.3

Thermal noise of the flagellum for two female mosquitoes.

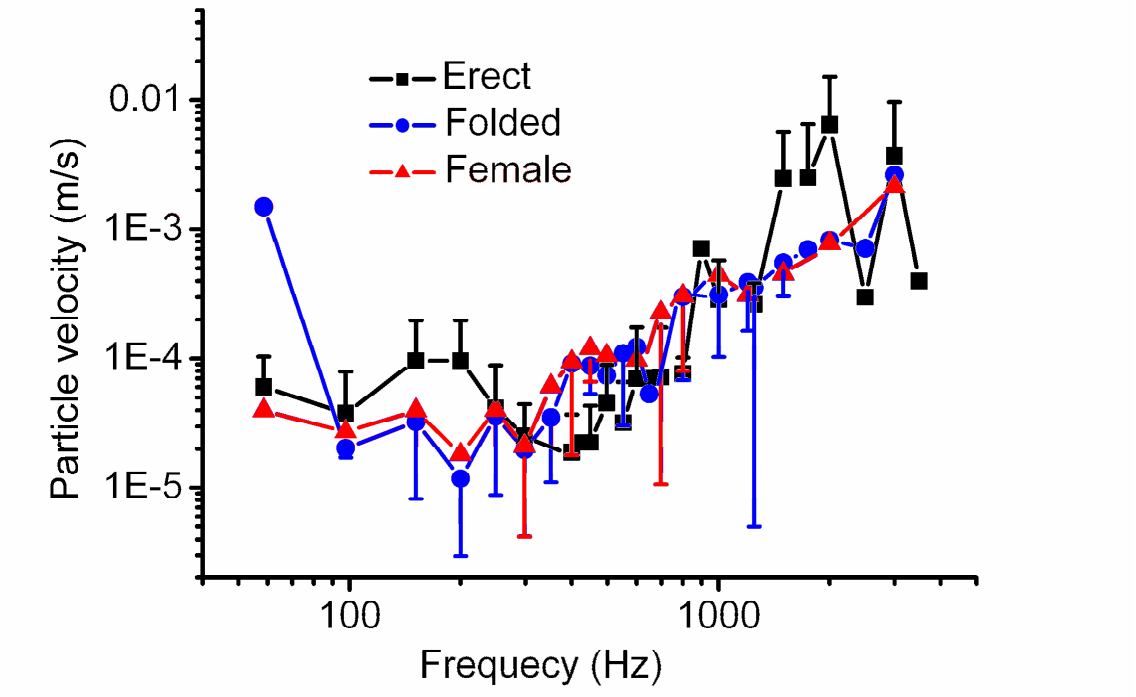

Figure 4.4

Isoresponse (Criterion 6nm) mechanical tuning curves of the flagellum of 10 male and 3 female (blue) *An. gambiae* to acoustic pure tone stimuli. Recordings were made from 4 male mosquitoes with fibrillae erect (black) and 6 males with folded fibrillae (blue). Error bars indicate ± 1 standard deviation and show only positive or negative standard deviation for clarity.

Electrical tuning of the JO of the antennae

Compound electrical responses to tones can be recorded with an extracellular electrode inserted through the cuticle in the vicinity of the JO. The electrical responses of the JO are comprised of phasic components, entrained with the stimulus frequency, and a direct current (DC) component with transients at tone onset and tone offset. The phasic component is dominated by the 2F component (i.e. at twice the frequency of the forcing stimulus (Fig. 4.5B). Electrical recordings from the JO have been explained as the summed receptor potentials from the sensory cells of the scolopidia (Clements 1999, Wishart *et al*, 1962). Receptor potentials can theoretically be recorded only from the few bipolar sensory cells of the JO adjacent to the electrode. This is because the receptor potential is rapidly attenuated with distance from its source. In view of estimates of this hypothesised rapid attenuation of the receptor potential it has been proposed that the electrical recordings from the JO are comprised of summated action potentials from the bipolar sensory cells of the scolopidia (Nadrowski *et al*., 2008). Due to this, it is not known to what extent extracellular electrical responses from the JO are composed of receptor currents from the mechanotransducing ciliated region of the sensory cell and/or compound neural responses from the axons of the same sensory cells, which form the JO nerve. As a means of investigating the contribution of neural activity to the compound action potentials, Tetrodotoxin (TTX) was injected into the thorax of a mosquito through a pipette because TTX eliminates action potentials by blocking sodium voltage-gated channels (Narahashi *et al*., 1960). Extracellular recordings of the JO, in response to a 300.3 Hz tone, were taken after all observable motor activity of the mosquito ceased (Fig.4.7) (within 10 minutes). Motor activity included abdominal contractions, leg, palp and proboscis movements. TTX injection significantly reduced the large transient negative potential at tone onset, however phasic and DC voltage responses to the tone remained unchanged (Fig. 4.7). Accordingly, the phasic F2 extracellular electrical component of the JO appears to be dominated by the receptor current of the sensory cells, which does not require sodium voltage-gated channels, and the

negative onset transient is dominated by the stimulated compound action potentials from the JO nerve.

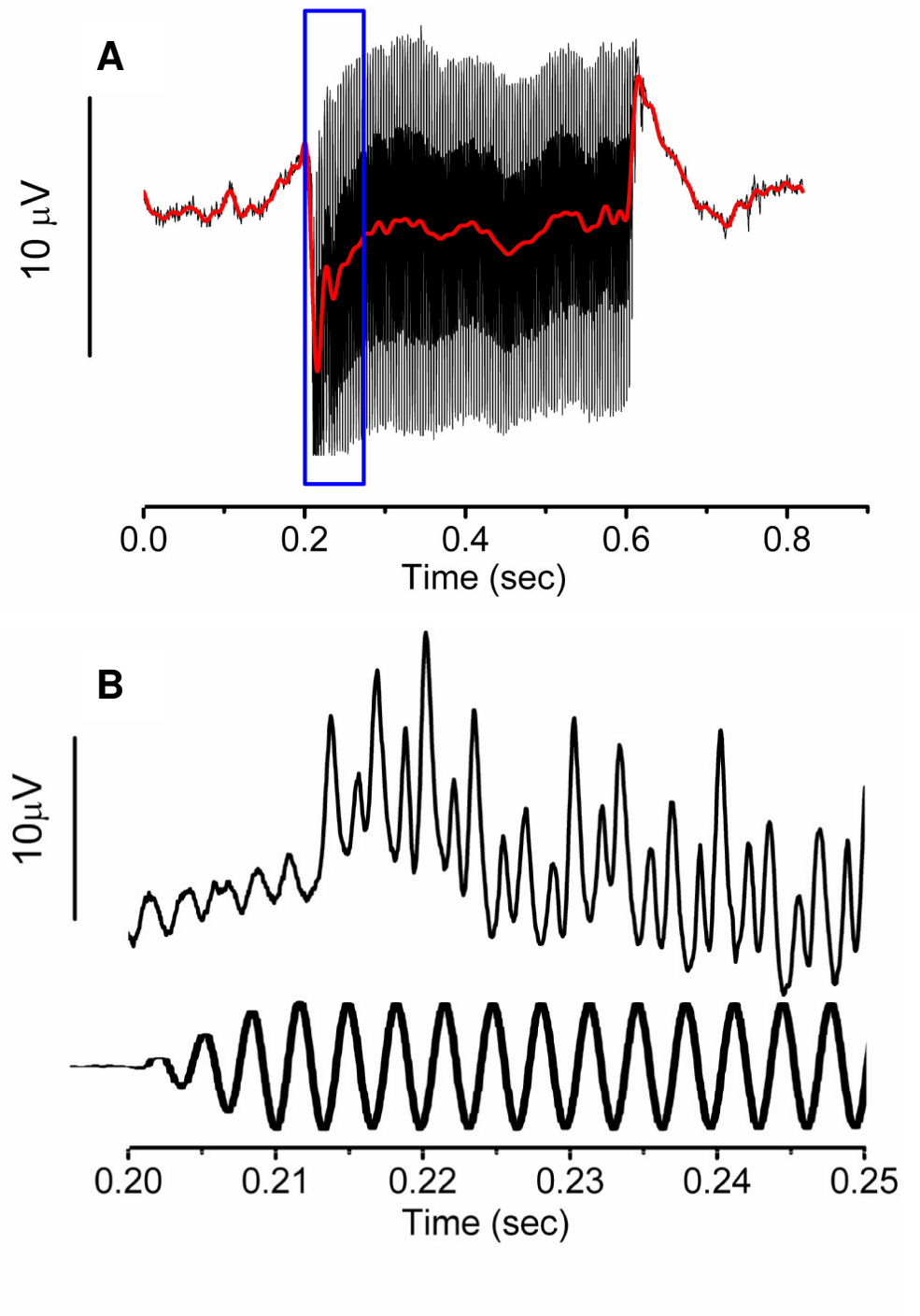

Figure 4.5

A: Oscillogram of the compound electrical response of the JO (black trace) to a pure tone at 300.3 Hz at $4X10^{-5}$ m/s started at 0.20 seconds with a rise time of 14 ms. Red line is a low pass filter showing the DC component.

B: Top trace shows the 2F component of the receptor potential, lower trace is the acoustic stimulus.

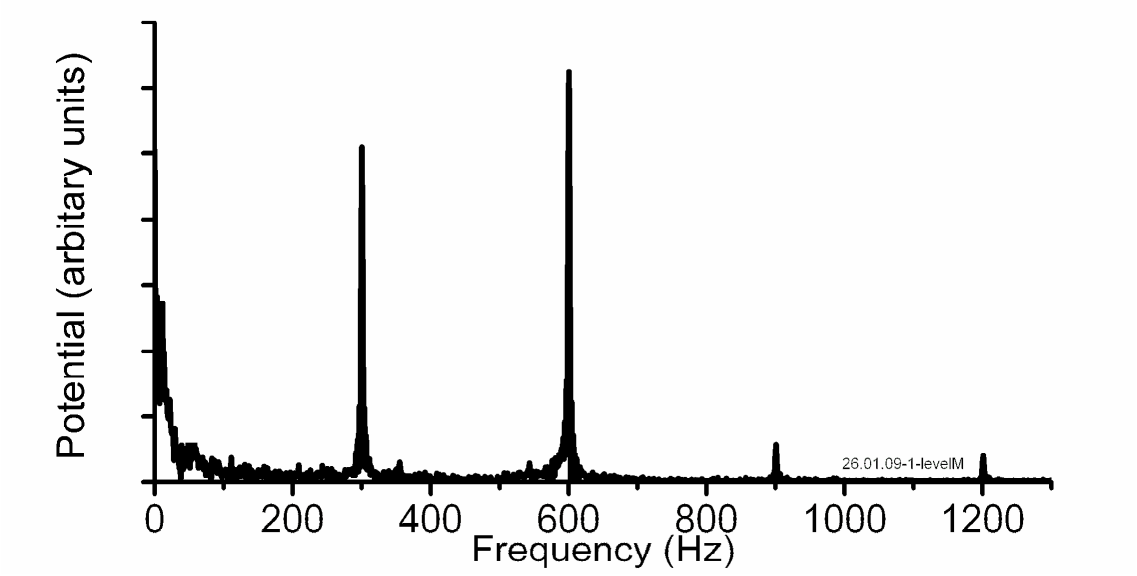

Figure 4.6

Fourier Transform of Fig. 5.5 showing the F1 and F2 components and other harmonic components.

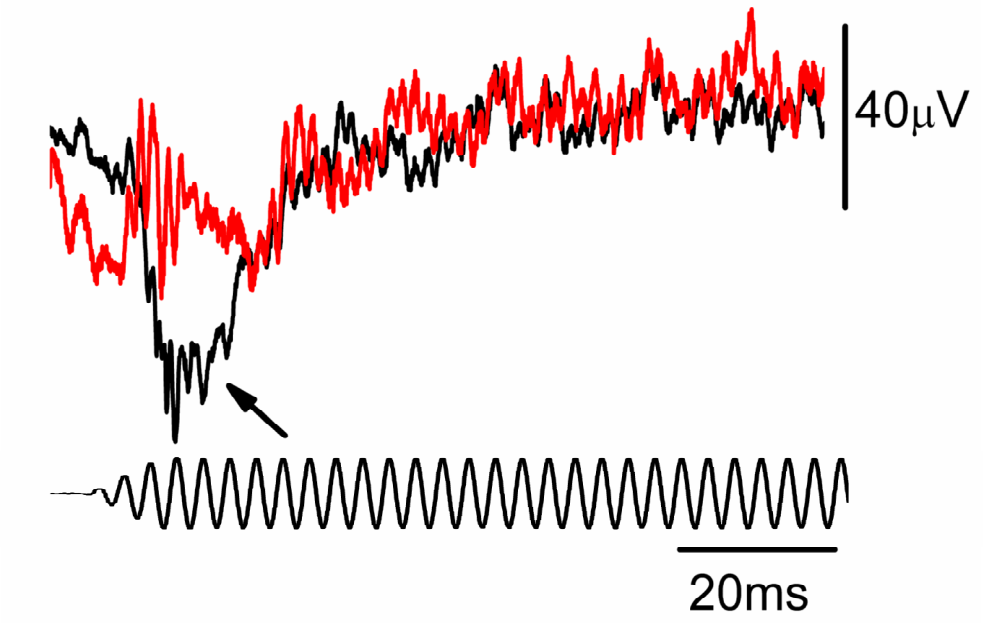

Figure 4.7

Voltage responses recorded from the JO of male M-form *An. gambiae* mosquito in response to a 300.3 Hz tone at $5.6X10^{-4}$ m/s before (black) and after (red) injecting 1 µM tetrodotoxin (TTX, Sigma-Aldrich) in insect saline into the thorax.

Isoresponse tuning curves were derived from measurements of the compound receptor potential in the JO (Fig. 4.8-4.10). Isoresponse 'threshold' responses were classified as the stimulus level needed to elicit an F1 or F2 component 1.4 times above the noise floor when analysed in the frequency domain (Figure 4.6). The DC isoresponse or 'threshold' was attained when the potential, within 15 ms following stimulus onset, exceeded 1 standard deviation of the baseline potential measured within the 20 ms preceding stimulus onset.

Tuning curves based on the 2F component of the receptor potential were most sensitive at 300 Hz (Fig. 4.8), which is similar to that of the mechanical tuning (Fig. 4.1). The particle velocity needed to achieve the isoresponse criterion of the receptor potential of the JO at this frequency was 26 dB below that required to achieve the mechanical isoresponse criterion of 6 nm. The sensitivity decreases at a rate of 13 dB per octave for frequencies below the best frequency and at 35 dB per octave for frequencies above the best frequency. Electrical noise due to intrinsic motor activity by the mosquito including the pulsating antennal heart (Clements, 1956) masked electrical responses at frequencies below 30 Hz. Corresponding low and high frequency slopes, above and below the best frequency, of the electrical tuning curve based on measurement of the F1 component are both 22 dB per octave. Further to this, responses based on the F1 components could be elicited at frequencies (up to 1000 Hz) higher than those based on the F2 component. The different slopes and sensitivities derived from the F1 and F2 phasic components can be attributed to the attenuation of the receptor current in the JO. The F2 component is due to receptor currents recorded from two populations of sensory cells, at opposing sides of the JO in the plane of stimulation, whereas the F1 component is recorded from the population of sensory cells nearest the electrode. Due to this, when the receptor current is small; at low stimulus levels or at a high frequency of stimulation, the receptor current from the furthest population of sensory cells, which contributes to the F2 component only, is completely attenuated before reaching the recording electrode, whilst the F1 component, which is elicited by the receptor current from the population of sensory cells nearest the electrode, is still recorded. Thus, the highest

frequency at which an F2 and F1 component can be recorded, at behaviourally relevant intensities, is limited to about 800 Hz and 1000 Hz respectively (Fig. 4.8). Attenuation of the receptor current also provides an explanation for the different slopes of the electrical tuning curves based on the F1 and F2 components.

The electrical isoresponse tuning curve based on the DC component follows a similar shape and sensitivity to those derived from the F1 and F2 components. The origin of the DC component has not yet been established and was not investigated in the experiments reported here. Although various untested suggestions have been put forward by Arthur *et al.* (2010), no attempt was made to investigate the origins of the DC component of the receptor potential in experiments reported here because we employed an AC coupled amplifier with a low pass filter set at 5 Hz, which filtered slow waveforms such as the DC potential.

The best frequency of the electrical isoresponse tuning curves reported for *An. gambiae* (Fig. 4.10), like those of the mechanical isoresponse tuning curves (Fig. 4.1), are shifted to higher frequencies when the fibrillae are erect (two tailed t-test p=0.0013 [from 4 mosquitoes with erect fibrillae and 6 mosquitoes with folded fibrillae]). The most sensitive frequencies for folded and erect fibrillae were 200 and 300 Hz, respectively, with corresponding particle velocity levels needed to elicit an isoresonse level of $1.4X10^{-6}$ and $1.5X10^{-7}$ m/s (Fig. 4.10). Thus, during fibrillae erection the sensitivity of the JO at the best frequency is increased by about an order of magnitude (Fig. 4.10). However, the mechanical sensitivity of the flagellum does not change upon fibrillae erection (Fig. 4.4).

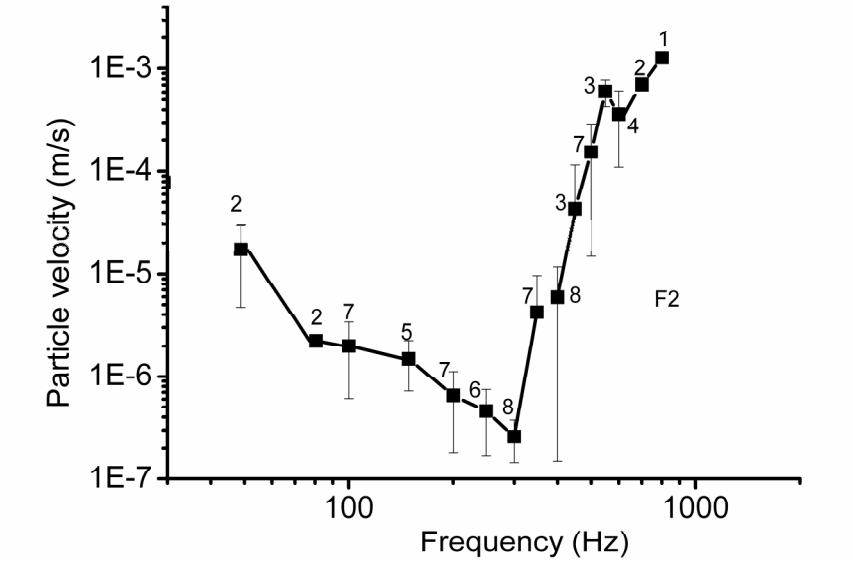

Figure 4.8

Isoresponse electrical tuning curve based from recordings of the receptor potential of Male *Cx. quinquefasciatus* (n numbers ± 1 standard deviation shown for each point, where each n number is a different mosquito). Isoresponse levels were determined by measuring the amplitude of a Fourier transform of the receptor potential at twice the frequency of the stimulus frequency (the stimulus frequency is plotted).

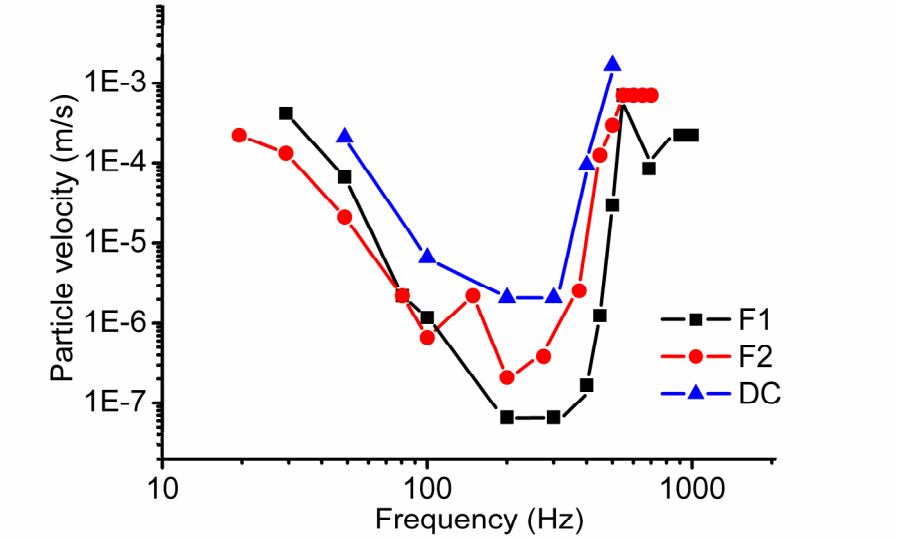

Figure 4.9

Isoresponse electrical tuning curve based from recordings of the receptor potential of a Male *Cx. quinquefasciatus*. Isoresponse levels were determined by measuring the amplitude of a Fourier transform of the receptor potential at the same frequency and at twice the frequency of the stimulus frequency for the F1 and F2 components respectively (the stimulus frequency is plotted). The DC isoresponse level was defined as when the baseline of the potential, within 15 ms following stimulus onset, exceeded 1 standard deviation of the baseline potential measured within the 20 ms preceding stimulus onset. (23.01.09).

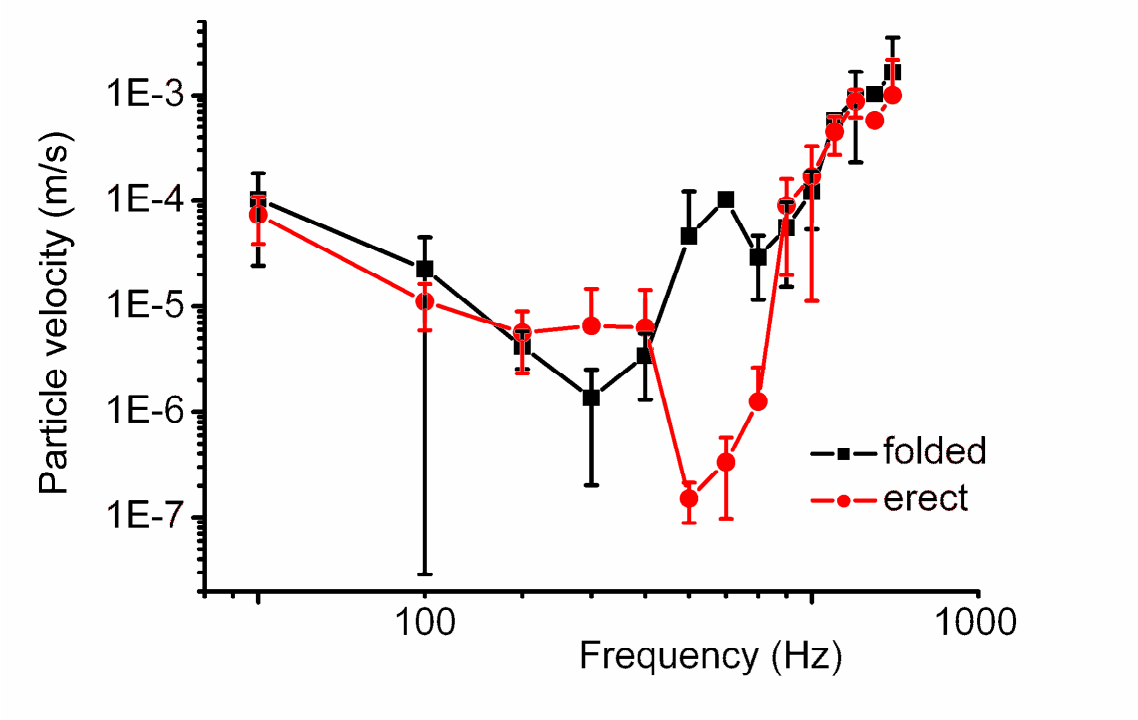

Figure 4.10

Isoresponse electrical tuning curves of *An. gambiae* before (4) and during fibrillae erection (5 individuals). Error bars indicate ± 1 standard deviation. Isoresponse levels were determined by measuring the amplitude of a Fourier transform of the receptor potential at twice the frequency of the stimulus frequency (the stimulus frequency is plotted).

Motor tuning curves

Isoresponse tuning curves derived from electrical motor activity recorded through differential electrodes placed in the wing and thorax near the wing and leg muscles provided a measure of the behavioural sensitivity of the mosquito to acoustic stimulation. Stimulation of the JO causes a train of biphasic action potentials which propagates through to thoracic and wing motor areas with a delay of ~6 ms (Fig. 4.11). Motor responses to tones at different frequencies and levels delivered to the JO via a loud speaker were used to derive isoresponse tuning curves (Fig. 4.12). An isoresponse tuning curve was derived in this way for frequencies up to 1200 Hz for a single male *Cx. quinquefasciatus*. The sensitivity decreases at a rate of 14 dB per octave for frequencies below the best frequency and at 32 dB per octave for frequencies above the best frequency.

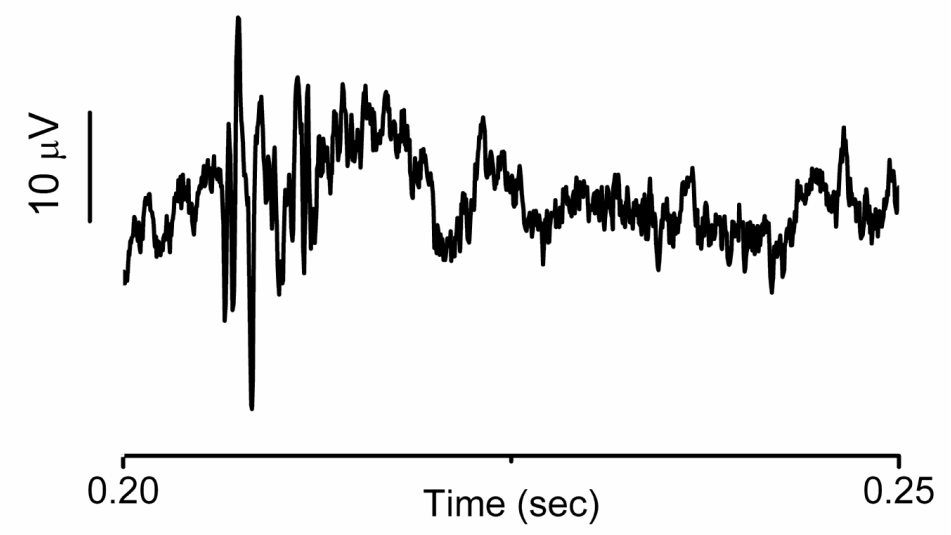

Figure 4.11
Electrical activity from thoracic motor areas of a *Cx. quinquefasciatus* to a 300.3 Hz tone at $4X10^{-5}$ m/s started at 0.20 seconds with a rise time of 14 ms.

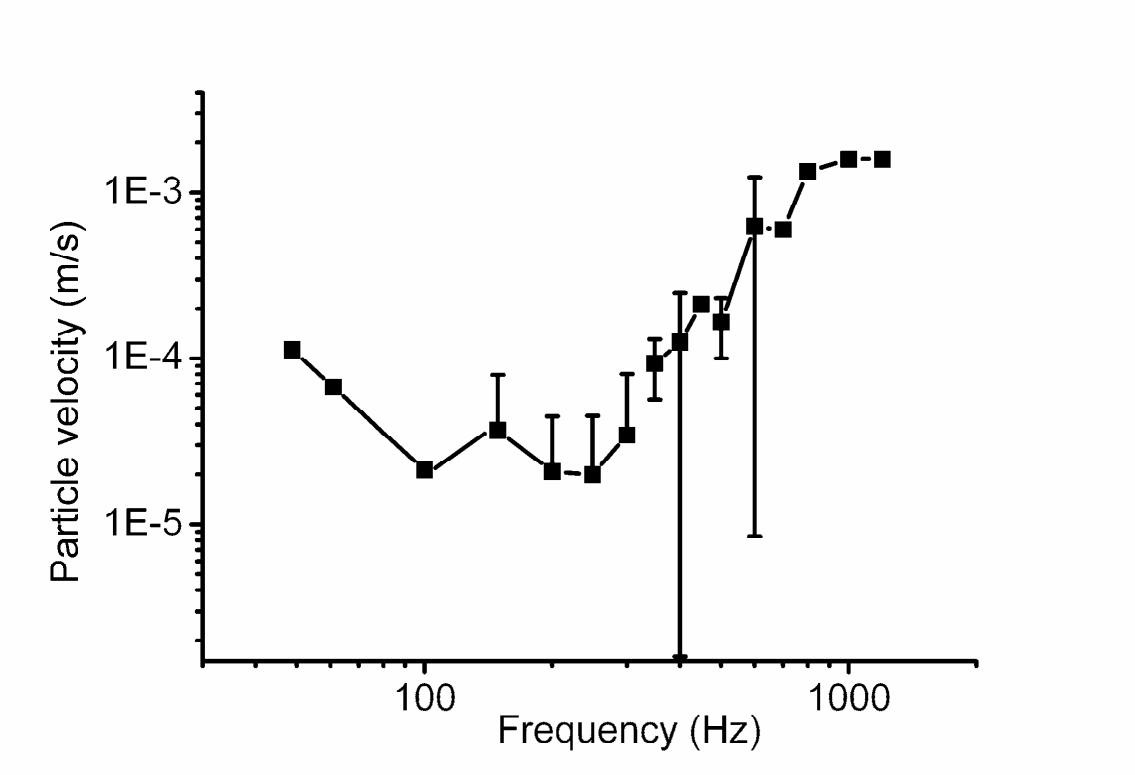

Figure 4.12
Isoresponse electrical tuning curve based on the motor response of 3 Male *Cx. quinquefasciatus.* Error bars indicate ± 1 standard deviation. Isoresponse or 'threshold' defined as when the biphasic spike exceeded 1.5 X standard deviation (peak to peak) of the 0.2 second period of electrical activity before stimulus presentation.

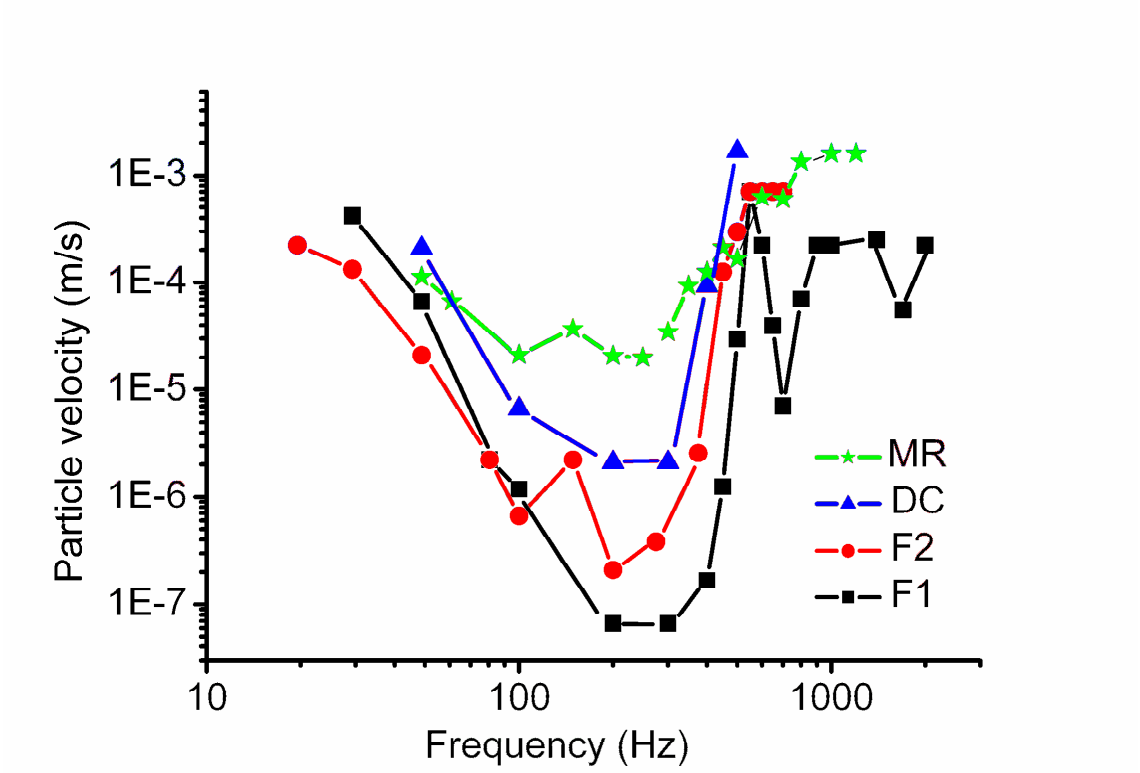

Figure 4.13
Isoresponse electrical tuning curve based from recordings of the receptor potential of a Male *Cx. quinquefasciatus* (Composite of Figure 4.9). Isoresponse levels were determined by measuring the amplitude of a Fourier transform of the receptor potential at the same frequency and at twice the frequency of the stimulus frequency for the F1 and F2 components respectively (the stimulus frequency is plotted). The DC isoresponse level was defined as when the baseline of the potential, within 15 ms following stimulus onset, exceeded 1 standard deviation of the baseline potential measured within the 20 ms preceding stimulus onset. The 'threshold' isoresponse level of the motor response (MR) was defined as when the biphasic spike exceeded 1.5 X standard deviation (peak to peak) of the 0.2 second period of electrical activity before stimulus presentation.

DISCUSSION

Mechanical properties of the flagellum of the antenna

The mechanical tuning curves of the flagellum of male *Cx. quinquefasciatus* are most sensitive for frequencies around 300 ± 50 Hz (Fig.4.1) and are similar in shape, with similar high and low frequency slopes, to those measured from *Ae. aegypti* (Göpfert *et al*., 1999). The mechanical resonance of the flagellum of *Cx. quinquefasciatus* males falls well below the WBF of its conspecific female of ~401 Hz, in free flight, (see Chapter II) as has also been reported for *Ae. aegypti* (Göpfert *et al*., 1999). A number of factors influence the frequency tuning of the antenna. These include age of the mosquito, humidity and temperature (Tischner *et al*., 1955). The mechanical tuning of the flagellum is rather broad so that, at the female WBF of 401 Hz, the particle velocity level required to elicit a mechanical isoresponse (6 nm displacement 240 µm from the flagella base) of the male flagellum is only 6dB less sensitive than at its most sensitive frequency of 300 Hz. The inverse relationship between the sharpness of tuning of a passive resonant structure and the time required for it to develop a maximal response to a sinusoidal, oscillating, stimulus is well known (e.g. Jackson *et al*., 2009). Thus broad tuning of the mosquito flagellum facilitates fast maximal responses to acoustic stimuli.

The male antenna, compared to that of the female, is more specialised and elaborate, presumably due to higher selection pressures for acoustic detection. This elaboration is most noticeable for the pedicel containing the JO of the male, which is about twice the size of the female's and contains about twice the number of mechanosensitive scolopidia (Boo and Richards, 1975). Despite this, the mechanical isoresponse level of the female flagellum to sound is lower than that of the male, according to isoresponse levels derived in Fig. 4.1. This would lead to the invalid conclusion that the female is mechanically more sensitive than the male. Indeed, Tischner and Schief (1955) found that the female flagellum is displaced more than the male flagellum for the same intensity of sound for *Ae. aegypti*. This counterintuitive result can be explained by

understanding how the sexually dimorphic anatomy of the flagellum and physiology of the JO leads to a sexually different function.

The male flagellum bears whorls of long grooved fibrillae, whereas the female's flagellum contains relatively few fibrillae. Fibrillae increase the windage of the flagellum by increasing the surface area able to detect air particle movements (Risler, 1955; Slifer and Sekhon, 1962). Fibrillae in turn also increase damping due to increased friction from air particles. Thus, the elaborate dense fibrillae of the male flagella, which increases acoustic sensitivity, is compromised by increased damping, which tends to decrease flagella movements. Although the fibrillae contribute to the damping of the antennae to displacements, Göpfert and Robert (2002) has shown that the stiffness and damping imposed by the scolopidia, which attach to the extended flagellum, dominate the mechanical response of the flagellum to displacements in *Drosophila*. This is most probably also the case for mosquito antennae due to the similar anatomy and function. By comparison with the JO of mosquitoes that of the male is more elaborate with about twice the number of scolopidia, compared to the female's (Boo and Richards, 1975; Clements, 1999). The greater number of scolopidia of the male JO appears to increase the stiffness and damping of the flagellum compared to that of the female which is displaced to a greater extent by the same intensity of sound (Tischner and Schief, 1955). Therefore constraints imposed by the anatomy of the flagellum and the physiology of the JO, lead to increased windage, stiffness and damping of the male flagellum in comparison to the female flagellum. These sexual differences in the antennae lead to the increased neural sensitivity of males compared to females in spite of smaller displacements of the male flagellum (Göpfert and Robert, 2000). Thus a smaller particle velocity level is need to elicit a 6 nm displacement ~240 µm from the base of the female flagellum compared to the male flagellum (Fig. 4.1). The male flagella are mechanically more sensitive for only very small displacements, which are presumably below the particle velocity level used to elicit a 6nm displacement of the flagellum ~240 µm from the base.

The flagellum is mechanically most sensitive at its resonant frequency of 200 and 300 Hz for female and male flagella respectively (Fig. 4.1). However, there are regions of increased sensitivity at higher frequencies about 1500 Hz for both male and female flagella which appear to interrupt the other smooth decrease in sensitivity from the most sensitive frequency. To test if this high frequency dip at ~1500 Hz was significant the particle velocity level necessary to elicit a response of the male flagellum was compared between 1501, 1251 and 2001 Hz and found not be significant (ANOVA p=0.43, 6 mosquitoes). In relation to the findings reported here, Göpfert *et al*. (1999) reported broad increases in the mechanical sensitivity of the flagella of male and female *Ae. aegypti* at about 1500 and 3000 Hz, which could be attributed to the different length of the fibrillae. Further mechanical recordings are needed to determine if these high frequency dips are significant and therefore similar to *Ae. Aegypti* antennae. These apparent dips in the mechanical sensitivity of the flagella of *Cx. quinquefasciatus* females falls within the range of the second and third harmonic of the male and female WBF respectively. They could perhaps help with the mechanical detection of harmonic components of wing beats (See Chapter II). In this sense, although fibrillae may well have first evolved to increase windage and detectability of air particles they appear to possibly serve a secondary role in increasing mechanical sensitivity at functionally specific frequencies used to detect the flight tone harmonics of airborne conspecifics.

Acoustically elicited mechanical displacements of the flagellum are nonlinear. For instance, at low levels of acoustic stimulation the displacement of the flagellum is comparatively larger than at higher levels of stimulation (Fig. 4.2, left inset 30-40dB and 40-50dB respectively). This has also been found for *Tx. brevipalpis* and for the similar antennae of *Drosophila melanogaster* (Göpfert and Robert, 2002; Göpfert and Robert, 2001; Jackson and Robert, 2006). The mechanism of the nonlinearity has been explained in Drosophila as due to force generating properties of the MET channels themselves (Nadrowski *et al*., 2004; Nadrowski *et al*., 2008). The force is produced by the interplay between the adaptation motors, most probably dynein, and the MET channel. The force generated by the MET complex is fed into oscillations of the sound receiver with

the correct phase to enhance and amplify these movements. As such, there is a nonlinear relationship between displacement of the sound receiver and the force used to move it (Nadrowski *et al*., 2008). The sensitivity of the *Drosophila* antenna is large for small displacement but decreases for larger displacements, thus the transducer-based force generation manifests itself as nonlinear stiffness changes. The nonlinear properties that make the sound receiving structure comparatively more sensitive for small displacements, as has been shown for male *Tx. brevipalpis,* when detecting a flying female (Jackson and Robert, 2006). An increase in differential sensitivity at low sound intensities aids the detection of faint sounds, whereas a decrease in differential sensitivity at high sound intensities leads to an extension of the mechanical range of the flagellum, which would otherwise saturate.

Another dynamical mechanical property of the antennae is the upward shift in resonant frequency in response to increasing sound intensity (Fig. 4.2) which increases by about 28 Hz for a 40 dB increase in sound intensity (Fig. 4.2). Such a change in the resonance of a system is brought about by either a change in mass or in stiffness. Assuming that mass stays relatively constant, the change in resonance is caused by an increase in the stiffness. A stiffness change is also thought to account for the significant increase in the resonant frequency from ~200 to ~400 Hz, which occurs during diurnal erection of the fibrillae of *An. gambiae* (Fig. 4.4) (t-test p=0.0013, from 4 mosquitoes with erect fibrillae and 6 mosquitoes with folded fibrillae). A level dependant resonant frequency has been shown before for *Drosophila melanogaster* however, in *Drosophila,* the frequency shift is more severe, at about 300 Hz over a 36 dB range (Göpfert and Robert, 2002), compared to that reported here. Stiffness of the flagellum has two sources; the cuticular attachment of the flagellum, at the flagellar base, and the scolopidia, of the JO, that attach to the extended flagellum. The likely increased stiffness of the flagellum of *An. gambiae* with erect fibrillae is not thought to be due to changes in the cuticle as the cuticle is not physiologically vulnerable to changes over such short time scales (Andersen, 1979). However, stiffness of scolopidia dominate the resonance of the antennae of *Drosophila* and is physiologically vulnerable as demonstrated

by CO_2 hypoxia (Göpfert *et al*., 2005). If this is the case for *An. gambiae*, then there must be some physiological change in the JO, which increases the stiffness of the scolopidia, and occurs simultaneously with fibrillae erection. In *Culex* where the fibrillae do not undergo diurnal changes the level dependent change in the resonant frequency occurs on a fast timescale. In *Drosophila* a level dependence change in the resonant frequency is proposed to be due to stiffening of the scolopidia mediated by the relative decrease of open MET channels for high displacements (Nadrowski *et al*., 2008). This suggests that both fibrillae erection and increasing the level of acoustic stimulation lead to stiffening of the scolopidial units in the JO. Although stiffening due to an increase in level is thought to be due to the nonlinear nature of the MET complex, stiffening upon fibrillae erection appears to be mediated by a separate mechanism. It would be interesting to see if the adrenergic type molecules, which cause fibrillae erection also stiffen the scolopidia of the JO (Nijhout, 1977).

The predicted increase in windage and damping of the flagellum upon fibrillae erection is thought to lead to an increase in sensitivity of the JO to sound (Fig. 4.10) however this is not significant (t-test p=0.078, from 4 mosquitoes with erect fibrillae and 6 mosquitoes with folded fibrillae). However, erection of the fibrillae makes the flagellum shifts the most sensitive frequency to 400 Hz; closer to frequencies produced by flying mosquitoes. Thus, during fibrillae erection there is an increase in the mechanical sensitivity to WBFs, produced by both sexes, at the expense of low frequency sensitivity. The use of folding them during periods of inactivity might be to help in the detection of approaching predators whose acoustic presence may be dominated by low frequencies.

When stimulated with frequencies of sound around the resonant frequency the flagellum moves like a stiff rod clamped at one end. However, when stimulated with higher frequencies the distal tip of the flagellum moves out-of-phase with the rest of the flagellar shaft (Göpfert *et al*., 1999). This frequency specific flexibility can be easily observed through a bifocal microscope with low magnification (X40) when stimulated with puffs of air (unpublished

observations). Movements of the flagellum in the absence of external stimulation have not been measured. Measurements of the flagellum without stimulation reveal that the last two flagellomeres are especially flexible in comparison to the other 11 flagellomeres, which form the flagellar shaft. Such a sharp change in stiffness indicates that the tip may move 180° out of phase with the rest of the shaft. This is the case for high frequencies approaching the resonance of the fibrillae for *Ae. aegypti* (Göpfert *et al*., 1999).

Electrical properties of the JO of the antenna

In an effort to clarify that potentials from the JO are due to summated receptor potentials and not due to summated action potentials from the bipolar sensory cells TTX was injected into the ventral body of a mosquito in an effort to block compound action potentials. The contribution of receptor potentials and compound action potentials to the sound evoked potentials recorded from the JO can then be determined. The large transient negative potential at tone onset was reduced after TTX treatment (Fig. 4.7). The onset of the transient potential is, therefore hypothesised to be, due to the synchronised action potentials of sensory cells producing compound potentials, whereas the unaffected phasic response is due to the receptor potentials from sensory cells. This observation bears many similarities with the recording of potentials from the cochlea, where the a transient potential upon stimulus onset is due to compound action potentials of the auditory nerve and the phasic potentials are due to the receptor potentials of the sensory outer hear cells (Cheatham *et al*., 2010). Although these measurements were conducted only on one mosquito they are supported by conclusions drawn from previous measurements of the compound potential of the JO (Wishart *et al*., 1962).

In conjunction with earlier reports the isoresponse electrical tuning curve (Fig. 4.8) has been derived from this F2 component (Clements, 1999; Keppler, 1958; Tischner and Schief, 1955). The F2 component is not detectable past 800 Hz in agreement with studies by Belton (1974). The most sensitive frequency at which

an electrical response can be detected is 300Hz in agreement with the mechanical resonance of the male flagellum (Fig. 4.1). The low frequency roll-off of the electrical tuning curve has a shallow slope allowing the mosquito to detect frequencies well below 20 Hz. Isoresponse electrical tuning curves based on the F1, F2 and DC components of the response were plotted (Fig. 4.9). Receptor components derived from the F1 component were detected up to 1000 Hz suggesting that mosquito's auditory range could extend to these frequencies. F2 components were not detected at these frequencies because the rather small receptor potential from the scolopidia population more distance from the recording electrode is completely attenuated before reaching the electrode. The DC component appears to be bounded and proportional to the F1 and F2 components. The recording of receptor potentials below 20 Hz was confounded by low frequency electrical noise (possibly caused by the antennal pulsating heart (Clements, 1956)).

The electrical sensitivity of the JO of male *An. gambaie* upon fibrillae erection (Fig. 4.10) is very similar to the change in mechanical sensitivity (Fig. 4.4). After fibrillae erection the most sensitive frequency at which a receptor potential can be elicited shifts upwards by 100 Hz and becomes more sensitive by an order of magnitude. Although sensitivity is reduced at about 200 Hz it remains similar to the flagellum in the folded state at all other frequencies. Although the receptor potential of the JO shows similar tuning to the mechanical properties of the flagellum, receptor potentials could only be recorded up to 1000 Hz thus the frequency response of the JO is limited to lower frequencies than mechanical movements of the flagellum.

Behavioural properties determined from motor neuron recordings

Action potentials from presumably motor neurons, near the wing and leg areas were recorded in response to sound delivered from a loud-speaker. Motor potentials are the basis of behaviour thus these were used to assess the behaviourally relevant sound frequencies and intensities, to which a mosquito responds. Motor isoresponse tuning curves were derived which best follow

isoresponse tuning curves of the 2F component of the receptor potential (Fig. 4.13). However responses are recorded up to 1200 Hz suggesting that *Cx. quinquefasciatus* can detect frequencies above the previously determined threshold of hearing of about 800 Hz based on the 2F component of the receptor potential (Clements,1999). Thus action potentials measured in the thorax bear similar frequency specificity to the JO, confirming that acoustically elicited behaviour of mosquitoes is underpinned by the JO. Motor responses were only recorded in response to acoustic stimuli over two orders of magnitude, compared to the four orders of magnitude of the receptor potential based on the F1 and F2 component. However this may be due to the detectability of action potentials in the thorax of mosquitoes, in a noisy environment.

CHAPTER V THE GENERATION OF MECHANICAL AND ELECTRICAL DISTORTION PRODUCTS IN THE FLAGELLUM AND JO

ABSTRACT

The response of the antennae to sound of *Cx. quinquefasciatus* and *An. gambiae* is characteristically nonlinear. A signature of nonlinearity is the generation of frequencies present in a system which were not present at the input. For instance, in response to two tones (donated F1 and F2, where F1<F2) delivered onto the flagellum, the flagellum vibrates at a frequency difference of the tones (F2 – F1). Distortion products can, not only, be recorded as mechanical movements of the sound capturing flagellum but also as potentials of the JO. The largest distortion product generated on the male flagellum and recorded from the JO is F2 – F1. The flagellum is able to mechanically respond to two tones, above the high frequency limit, at which movements of the flagellum can be encoded into receptor potentials. Remarkably the resulting low frequency F2 – F1 distortion product generated between these two frequencies can be transduced by the JO because it is within the auditory range of the JO. It is demonstrated that the generation of mechanical distortion products is limited by the mechanical tuning of the flagellum not only at the frequency of the two primary tones (F1 and F2) but also at the frequency of the generated F2 – F1 distortion product. Further to this the encoding of the distortion product is also limited by the frequency tuning of the JO. In order to investigate the metabolic contribution of the sensory cells in the generation of mechanical distortion, *Cx. quinquefasciatus* were cooled to 5.5℃. Cooling severely disrupted metabolic processes of the JO (Chapter VI). It was found that the generation of distortion in the antennae of *Cx. quinquefasciatusi* could be mechanical in nature and generated passively without energy input from the sensory cells of the JO.

INTRODUCTION

The response of ears to sound is nonlinear. A hallmark of nonlinear processing of sound is the generation of distortion products. In response to two tones (donated F1 and F2, where F1<F2) distortion products are generated at a distinct frequency through the interaction of these two tones during nonlinear auditory processing. These distortion products can be measured with a sensitive microphone in the ear canal of humans (Kemp, 1978) and are used to assess normal auditory function. As such they can give insight into the inner mechanism of auditory processing. The largest distortion product measured from the acoustical organs of all animals is 2F1 – F2 (Coro and Kössl, 1998; Kemp, 1978; Kössl and Boyan, 1998; Mockel *et al.,* 2007; Rosowski *et al*., 1984; Van Dijk and Meenderink, 2006). In response to two tones the F2 – F1 distortion product dominates in the JO of mosquitoes, which is different to all auditory systems measured to date, including the similar JO of *Drosophila* (Albert, personal communication, 2009). Distortion of the mosquito antennae can be measured mechanically as movements of the flagellum but can also be measured electronically as potentials in the JO. The unique tuning properties of the mosquito antennae allow mechanical displacements of the flagellum to be recorded for frequencies up to 5 kHz (for behaviourally relevant sound intensities) but potentials from the JO to only be recorded for comparatively lower frequencies; up to ~1000 Hz. The flagellum is able to mechanically respond to two tones, above the high frequency limit, at which movements of the flagellum can be encoded into receptor potentials. Remarkably, for certain frequencies of two tones delivered onto the antennae, the resulting low frequency F2 – F1 distortion product which is generated can be transduced by the JO because it is within the auditory range of the JO. The generation of distortion products has been proposed to be due to an active energy contributing process of the sensory cells (Kössl *et al*., 2007). This train of thought is inspired by properties of the MET complex, which is highly nonlinear and can account for the dynamical properties of acoustical receivers from hair bundles (Howard and Hudspeth, 1987; Martin and Hudspeth, 1999) to *Drosophila* antennae (Albert and Göpfert, 2006). Thus, the basis for the

nonlinearity in acoustical receivers is thought to be primarily from the mechanical effects of the nonlinear processing of the MET channels. This view is also based on experiments where the amount of distortion was greatly decreased upon hypoxia (Kössl and Boyan, 1998). This finding led people to believe that distortion is only created by an active force producing process, such as that encapsulated by the MET channels (Kössl *et al*., 2008). Unfortunately the disappearance of distortion upon hypoxia does not rule out the possibility that the distortion was generated passively without the energy contribution of the sensory cells. The hypoxic dependant distortion could be explained through the sensory cells holding the tympanum in a mechanical state where distortion is optimally created.

RESULTS

The generation of electrical distortion products in the JO of the antenna

To investigate distortion generated by the response of the antennae to sound two tones were delivered simultaneously onto the flagellum of male *Cx. quinquefasciatus*. Receptor potentials from the JO were recorded using metal electrodes inserted into the pedicel. Distortion products were electrically recorded in the receptor potentials of the JO in response to two tones for five male *Cx. quinquefasciatus* mosquitoes and three *An. gambiae* mosquitoes. All mosquitoes, in normal physiological conditions, showed large F2 – F1 distortion components. The understanding of distortion generation in the mosquito antennae is developed from recordings from single mosquitoes. For instance, the electrical recording of one mosquito to two tones at 250 and 310 Hz is shown (Fig. 5.1, Fig. 5.2). The largest distortion components, typically produced by a quadratic nonlinearity, are F2 ± F1, were F1 and F2 donated the stimulus tones with a lower and higher frequency, respectively. When the antenna is stimulated with two tones at 250 and 310 Hz a large F2-F1 component is clearly visible in the oscillogram trace of the receptor potential (Fig. 5.1). It is important to note that the receptor potential amplitude of the F2 – F1 component is larger than the receptor potential elicited by the two primary tones or their harmonics (Fig. 5.2). Other distortion is generated between the two primary tones and includes F2 + F1 and 2 X (F2 – F1) (Fig. 5.2).

The frequencies that can interact to generate an F2 – F1 in the receptor potential (Fig. 5.3, red circles) are limited by the filter properties of the electrical response of the JO to one tone (Fig. 5.3 and Fig. 5.4, black squares). For Figure 5.3 two tones were delivered onto the flagellum of a male *Cx. quinquefasciatus* to produce a F2 – F1 distortion product at 60 Hz. For Figure 5.3 the difference between the F2 and F1 stimulating frequencies were fixed so that the resulting F2 – F1 distortion product was always produced and encoded at 60 Hz. The particle velocity level needed to elicit a receptor potential

encoding the F2 – F1 distortion product was measured for a range of stimulating frequencies such that F2 was always 60 Hz higher then F1.

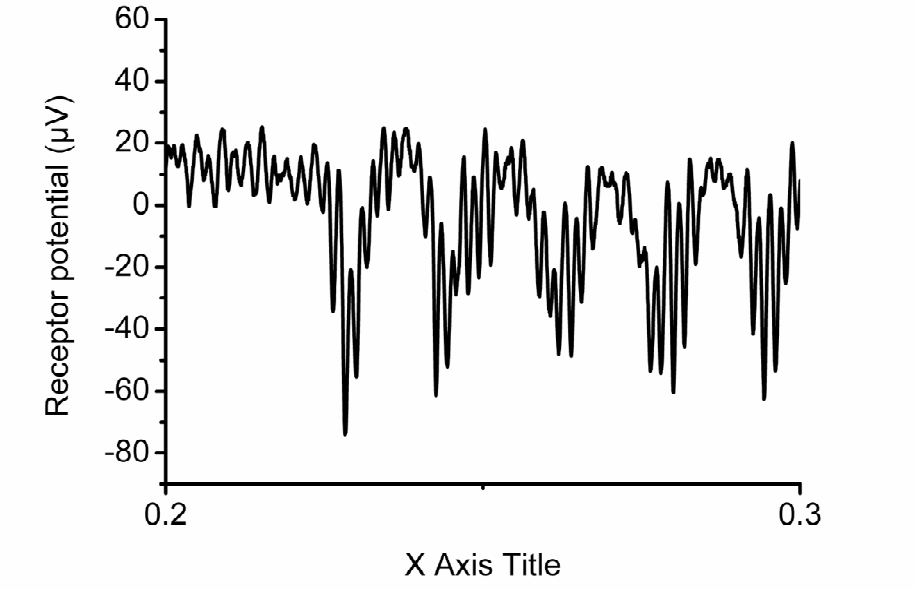

Figure 5.1

Electrical responses recorded from the JO of a male Cx. quinquefasciatus to the simultaneous presentation of two 400 ms duration tones with 14ms rise times at frequencies of 250 and 310 Hz and particle velocities of $2.7X10^{-5}$ m/s. The F2-F1 component is visible as a 60 Hz sinusoid in the response.

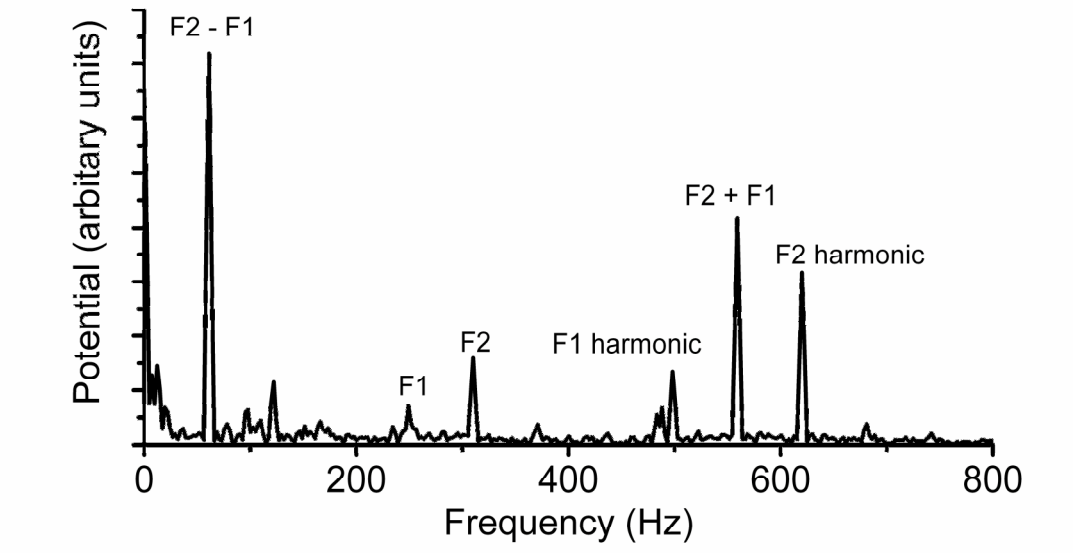

Figure 5.2

A frequency spectrum of the electrical response of the JO of a male *Cx. quinquefasciatus* to a 250 and 310 Hz pure tone at a particle velocity of $2.7X10^{-5}$ m/s (Frequency spectrum of Fig. 6.1). The primaries (F1, F2) their harmonics at twice the frequency of F1 and F2 and the F2 – F1 and F2 + F1 distortion products are indicated.

In Figure 5.3 the most sensitive F2 – F1 distortion product was produced when the two stimulating tones were at 250 and 310 Hz (Fig. 5.3, red trace), either side of the JO's most sensitive frequency response to single tones (Fig. 5.3, black squares). F2 – F1 distortion products were also recorded as potentials in the JO of one male *An. gambiae* in response to two tones, which were fixed with a 250 Hz separation. Thus the F2 – F1 distortion product was always produced at 250 Hz. The frequency of F1 was plotted as a function of the particle velocity level necessary to evoke a F2 – F1 distortion product. In Figure 5.4 the most sensitive F2 – F1 distortion product was produced when the two stimulating tones were at 300 and 550 Hz (Fig. 5.3, red trace). In this case the stimulating tones were above the JO's most sensitive response to single tones, at 200 Hz (Fig. 5.4, black squares), but the F2 – F1 tuning curve (Fig. 5.4, red circles) followed the same shape as the tuning curve derived from a single tone (Fig. 5.4, black squares). Thus the ability to generate a F2 – F1 distortion product depends on the response of the JO to the two primary tones (Fig. 5.3, Fig. 5.4).

To assess the effect, on the sensitivity of the F2 – F1 distortion product, of varying the frequency separation between the two stimulating tones the F1 tone was held at 100 Hz whilst the F2 tone was increased in frequency above 100 Hz (Fig. 5.5).

The lowest particle velocity needed in order to elicit an isoresponse receptor potential encoding the F2 – F1 distortion product was when F2 was 80-220 Hz above F1 (i.e. for pairs of tones between 100, 180 Hz and 100, 320 Hz) (Fig. 5.5). The sensitivity of the receptor potential encoding a F2 – F1 distortion component decreased rapidly when the separation between the primaries was lower then 30Hz or higher then 300Hz (Fig. 5.5). The particle velocity level needed to elicit a receptor potential encoding the F2 – F1 component depends on the frequency separation between F1 and F2. This may be due to the frequency specific tuning properties of the JO when responding to either F1 or F2. For instance the particle velocity required to elicit a F2 – F1 receptor potential rapidly increases when F2 is above 320 Hz (Fig. 5.5) but the

mechanical response of the flagellum and the electrical response of the JO also decrease above 320 Hz (Fig. 4.1 and Fig. 4.8).

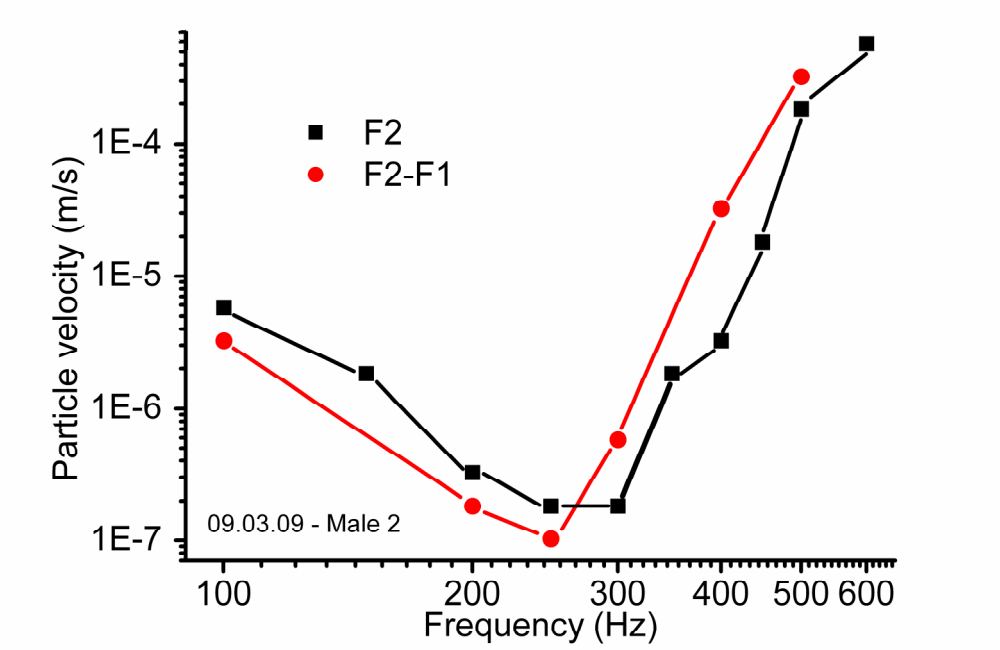

Figure 5.3

Electrical isoresponse tuning curve based on the F2 component of the receptor potential to one tone (black) and electrical isoresponse distortion product tuning curve based on the F2 – F1 component of the receptor potential to two tones presented simultaneously (red) for one male *Cx. quinquefasciatus*. For the distortion product tuning curve the frequency of F1 is plotted (the frequency of F2 is always 60 Hz above F1) against the particle velocity level sufficient to evoke an isoresponse level of the F2 – F1 distortion product. The isoresponse or 'threshold' criterion for the distortion product tuning curve was when F2-F1 was 10 dB above noise floor (Average noise floor 0.1µV).

In order to establish if the frequency separation between the two primary tones has an effect on the sensitivity of the resulting F2 – F1 distortion product, independently of the frequency tuning properties of the JO, two primary tones were presented at frequencies far from the resonant frequency (i.e. above 1000 Hz) (Fig. 5.6). At these high frequencies the particle velocity needed to generate a receptor potential (Fig. 4.9, black trace) or an isoresponse displacement of the flagellum (Fig. 4.1, black trace) does not significantly change over 300 Hz for which F2 was varied in Figure 5.5. The lowest particle velocity required to elicit a receptor potential encoding the F2 – F1 distortion product was when the F1 and F2 frequencies were ~80 Hz apart (when F1=1001 and F2=1081) (Fig 5.6).

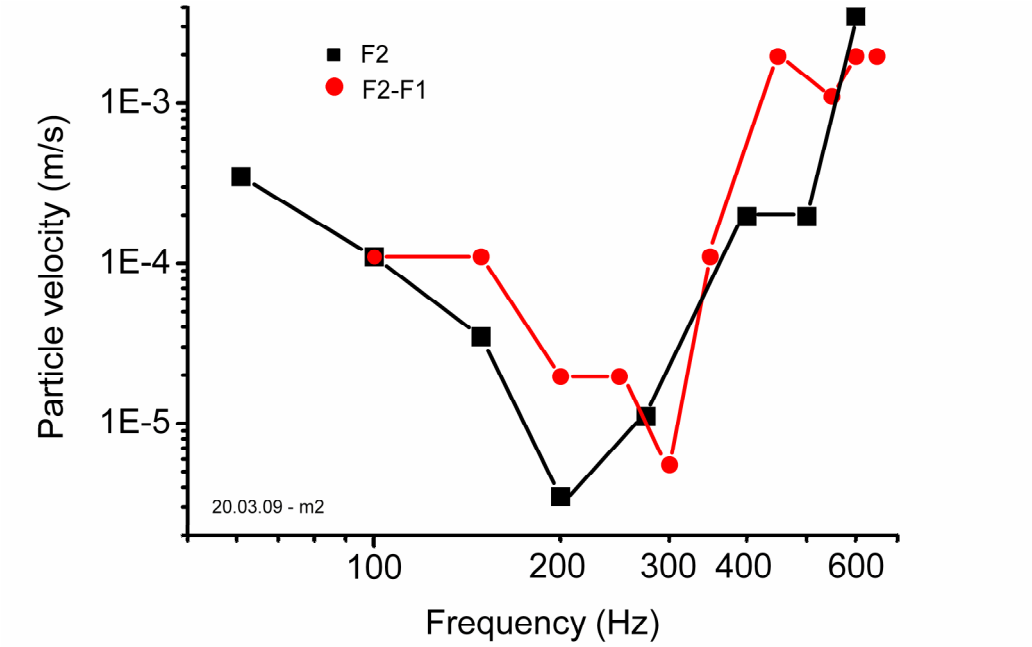

Figure 5.4

Electrical isoresponse tuning curve based on the F2 component of the receptor potential to one tone (black) and electrical isoresponse distortion product tuning curve based on the F2 – F1 component of the receptor potential to two tones presented simultaneously (red) for one male *An. gambiae*. For the distortion product tuning curve the frequency of F1 is plotted (the frequency of F2 is always 250 Hz above F1) against the particle velocity level sufficient to evoke an isoresponse level of the F2 – F1 distortion product. The isoresponse or 'threshold' criterion for the distortion product tuning curve was when F2-F1 was 10 dB above noise floor (Average noise floor 0.1µV).

The generation of mechanical distortion products in the flagellum of the antenna

The flagellum responds mechanically to acoustical stimulation well above the high frequency limit of mechano-electrical transduction by the JO (Chapter V). In *An. gambiae* the flagellum mechanically responds, not only, to two tones at 1399 and 1499 Hz but also at the frequency of the F2 – F1 component generated between them at 100 Hz (Fig. 5.7). Further mechanical distortion is generated between the stimulating tones and spontaneous oscillations (SOs) of the flagellum (Fig, 5.7). The same stimulus tones, which mechanically displaced the flagellum, failed to elicit receptor potentials at 1399 and 1499 Hz. (Figure 5.8, arrows). However, the F2 – F1 distortion product generated between 1499 and 1399 at 100 Hz was recorded in the receptor potential from the JO (Fig. 5.8).

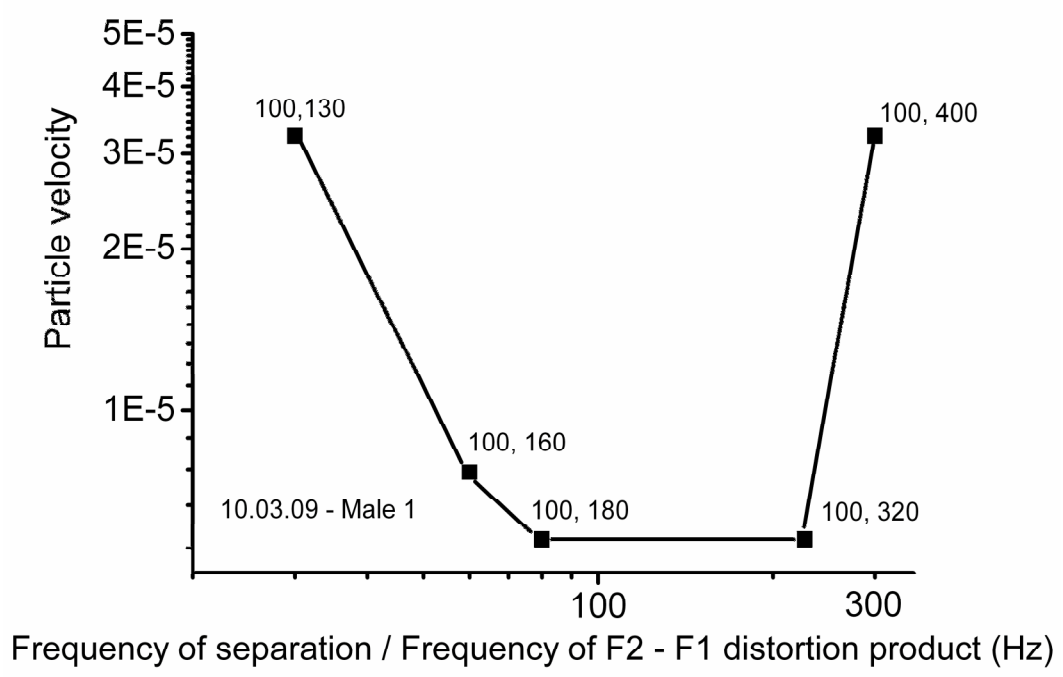

Figure 5.5

Electrical isoresponse distortion product tuning curve based on the F2 – F1 component of the receptor potential to two tones presented simultaneously for one male *Cx. quinquefasciatus*. The frequency of F1 was held constant at 100 Hz, whilst the frequency of F2 was increased above 100 Hz. The frequencies of F1 and F2 are shown for each presentation. The frequency separation between F1 and F2 (i.e. F2 – F1) is plotted against the particle level sufficient to evoke an isoresponse level of the F2 – F1 distortion product. The isoresponse or 'threshold' criterion for the distortion product tuning curve was when F2-F1 was 10 dB above noise floor (Average noise floor 0.1µV).

Temperature dependence of mechanical distortion products in the flagellum of the antenna

To assess the physiological nature of distortion of the antennae, mechanical distortion of the flagellum was measured at 21.0℃ and at 5.5℃. At 5.5℃ spontaneous oscillations of the JO fell below the recording noise floor and metabolic processes of the JO were significantly reduced (Chapter VI). The dominating F2 – F1 distortion product was used as a measure of mechanical distortion of the flagellum, of 7 male *Cx. quinquefasciatus*. The F2 – F1 distortion product was generated and measured at 60 Hz by stimulating the

flagellum with two tones (both with a particle velocity of 8.57X10^{-5} m/s), which were always held 60 Hz apart. If mechanical distortion was dependant on metabolic processes in the JO, originating from the sensory cells, it should be affected by a decrease in the temperature to 5.5℃. To assess the reversibility of cooling the mosquito on the generation of mechanical distortion, isolevel mechanical tuning curves measuring the displacement of the flagellum at the F2 – F1 frequency were made at 21.0℃, 5.5℃ then at 21.0℃ again (Fig. 5.9). The maximum displacement of the flagellum at F2 – F1 in response to two tones was largest when F1 was 400 and 350 Hz (± 50 Hz) at room temperature, before and after cooling, whereas during cooling it shifted down to 250 Hz.

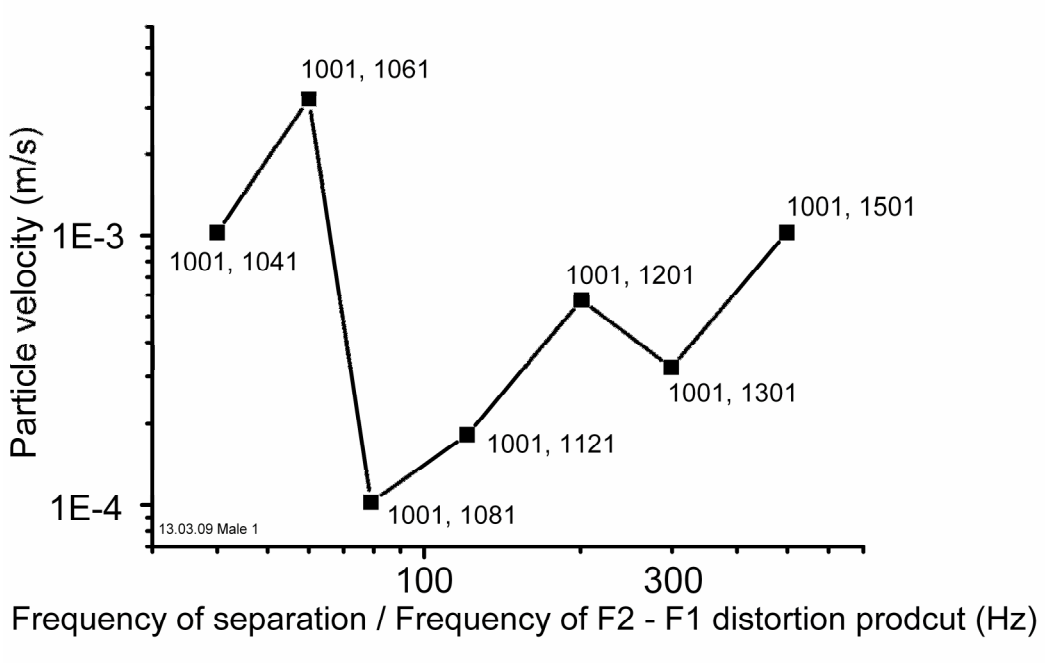

Figure 5.6

Electrical isoresponse distortion product tuning curve based on the F2 – F1 component of the receptor potential to two tones presented simultaneously for one male *Cx. quinquefasciatus*. An average of three recordings for each point was taken. The frequency of F1 was held constant at 1001 Hz, whilst the frequency of F2 was increased above 1001 Hz. The frequencies of F1 and F2 are shown for each presentation. The frequency separation between F1 and F2 (i.e. F2 – F1) is plotted against the particle level sufficient to evoke an isoresponse level of the F2 – F1 distortion product. The isoresponse or 'threshold' criterion for the distortion product tuning curve was when F2-F1 was 10 dB above noise floor (Average noise floor 0.1µV).

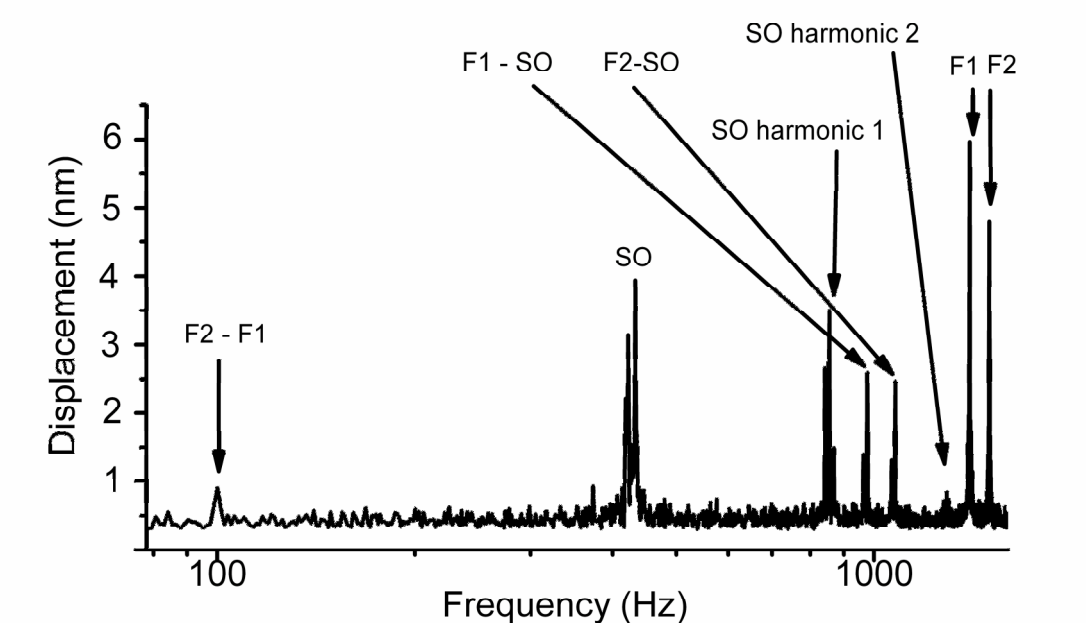

Figure 5.7

Amplitude spectrum of the displacement of the flagellum to two tones at 1399 and 1499 Hz at 0.001 m/s for a male *An. gambiae.* Various (F2 – F1) distortion products are generated between the two stimulating tones and between the SOs and the stimulating tones.

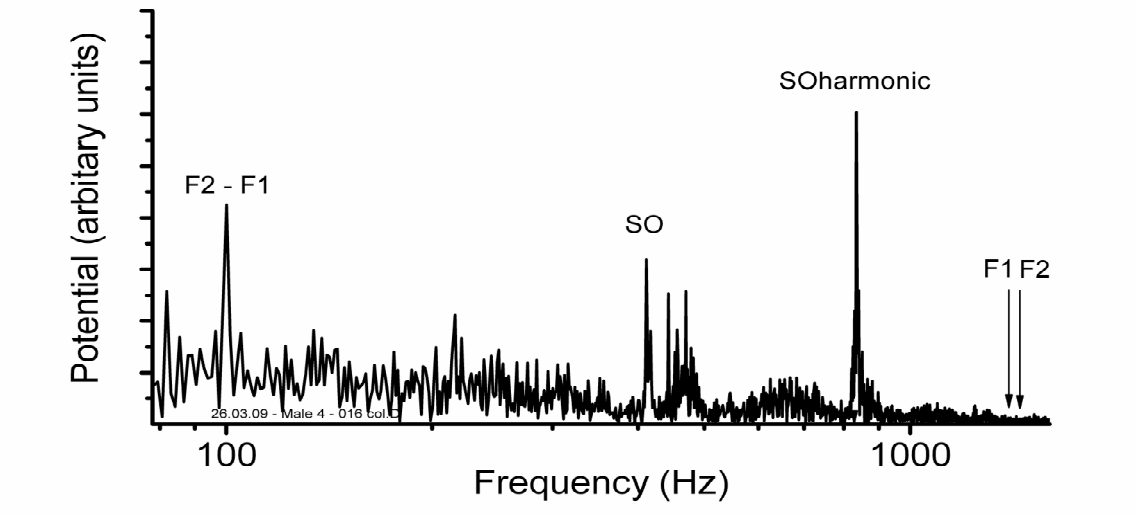

Figure 5.8

Amplitude spectrum of the electrical potential of the JO to two tones at 1399 and 1499 Hz at a particle velocity level of 0.001 m/s for a male *An. gambiae.* A large F2 – F1 component is visible at 100 Hz.

There is no statistically significant difference in the frequencies of F1 and F2, which gave the largest F2 – F1 distortion product before and after cooling (Tukey's paried test $p>0.05$, 7 individuals) but during cooling the frequencies of F1 and F2, which gave the largest displacement at F2 – F1 were significantly reduced (Tukey's paired test $p<0.05$, 7 individuals). Therefore, the affect of cooling was reversible. The largest amplitude of the F2 – F1 distortion product also significantly increased upon cooling (Tukey's paried test $p<0.05$, 7 individuals) but returned to pre-cooling levels after cooling (Tukey's paired test, $p<0.05$, 7 individuals). At the intensity used for the isolevel tuning curves the F2 – F1 components fall into the noise floor at about 600 Hz.

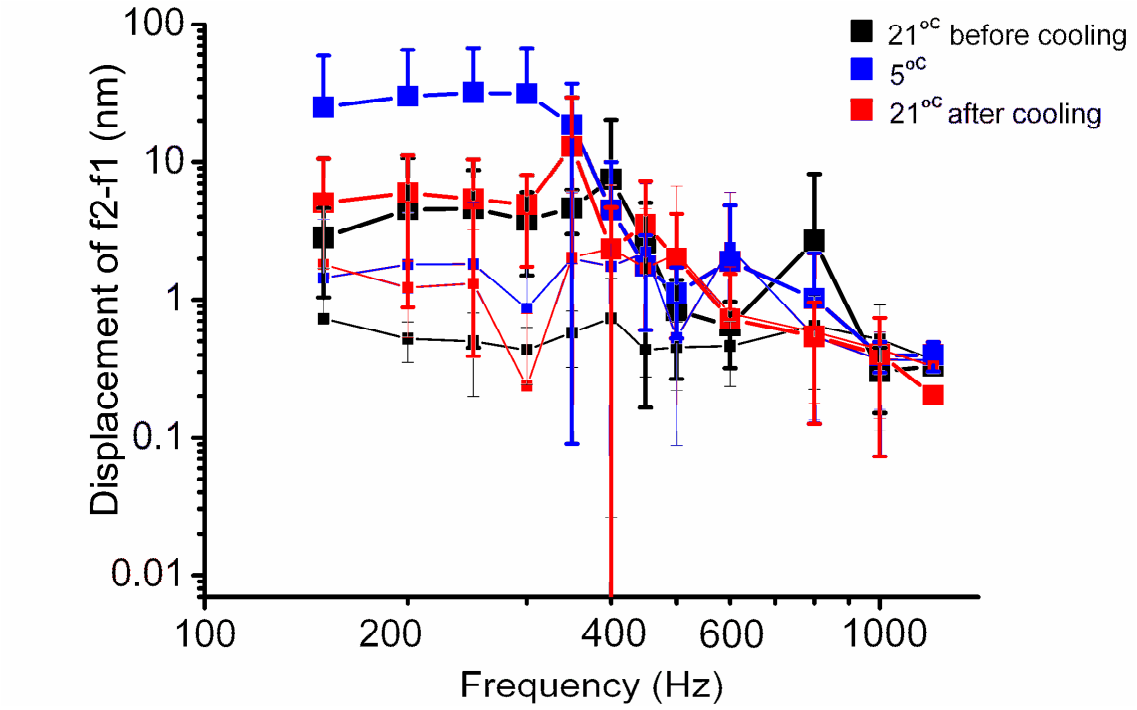

Figure 5.9

Distortion product Isolevel tuning curves derived from the displacement of the flagellum at F2 – F1 (thick traces) of 7 male *Cx. quinquefasciatus* (error bars indicate ± 1 standard deviation.) to two tones, presented simultaneously, at a particle velocity of $8.6X10^{-5}$ m/s. The temperature was varied from 21.0 ℃ (black), 5.5 ℃ (blue) then at 21.0 ℃ again (red) (all measurements ± 0.3 ℃ standard deviation). Noise floor plotted as thin lines for each temperature. Frequency of F1 is plotted on graph; F2 is always 60 Hz above.

DISCUSSION

It might be expected that the generation of strong even order distortion products in the receptor potential of the JO, in response to the presentation of pairs of stimulating tones is due to a quadratic, stiffening nonlinearity. Indeed the largest distortion product in the receptor potential of the mosquito JO is F2 – F1 (Fig. 5.2). The F2 – F1 distortion product, which is encoded into receptor potentials by the JO often, has a larger magnitude then the receptor potential encoding the F1 and F2 tones (Fig. 5.1 and Fig. 5.2). The magnitude of the receptor potential depends on, not only, the particle velocity level delivered onto the flagellum but also the nature of nonlinear mechanoelectrical transduction carried out by the JO. For male *Cx. quinquefasciatus* most of the energy contained within the primary frequencies (F1 and F2) are dissipated into the F2 – F1 distortion product. Indeed if the input-output function of the JO could be described as a perfect quadratic transfer function, such as INPUT = OUTPUT^2 there would be no primaries in the receptor potential. Even though the JO is unable to transduce two high frequency tones, outside its auditory range, the JO can still transduce the F2 – F1 component generated at a lower frequency, within its auditory range (Fig. 5.7) This property of the JO gives a plausible mechanism by which frequency matching, between the higher harmonics produced by the WBFs, otherwise, outside of the auditory range of the JO could be mediated. Frequency matching between two frequency matching harmonics (i.e. the 3rd harmonic of the female and the 2nd harmonic of the male), can be mediated by the detection and concurrent reduction of the F2 – F1 distortion component through changing the WBF (Fig. D.1).

Distortion products recorded as pressure differences in the ear canal of mammals have been attributed to the active nonlinear processing of sound (Dallos, 1992). The generation of distortion product does not require energy input into a system and can arise passively. Therefore, although the distortion products disappear post mortem and appear to be metabolically vulnerable this does not offer definitive proof that they are due to an active as opposed to a passive nonlinear process. In the bush-cricket distortion was shown to be

reversibly decreased in response to carbon dioxide hypoxia (Kössl and Boyan, 1998). Assuming that there is negligible change in the structural properties of the cuticle comprising the tympanum during CO_2 hypoxia, the nonlinearity can be attributed to the only active metabolically vulnerable attachments to the tympanum; the mechanosensitive cilia. The hypoxic-dependant distortion products of the bush-cricket could also be explained by the active properties of the mechanosensitive cilia holding the tympanum in a mechanical state where distortion is created. In this scenario acoustic distortion is not directly produced by the active energy-contributing properties of the mechanosensitive cilia. Male *Cx. quinquefasciatus* were cooled in an effort to decrease the metabolic input of the sensory cilia of the JO and therefore decrease any metabolically active processes. If distortion is dependant on active properties of the sensory cilia then distortion would be expected to decrease upon cooling. As a measure of mechanical distortion the magnitude of displacements of the flagellum, in response to two tones, at the F2 - F1 frequency was measured. Surprisingly, the displacement of the flagellum, at the F2 – F1 frequency or the amount of mechanical distortion of the flagellum increased upon cooling to 5.5℃ (Fig. 5.9) (Tukey's paired test $p<0.05$, 7 individuals).

The increase in amplitude and decrease in resonant frequency of the generated F2 – F1 distortion product upon cooling can be explained as a decrease in stiffness of the flagellum (Fig. 5.10). Mechanical properties of the flagellum, such as stiffness, are underpinned by input, from the metabolically sensitive sensory cell cilia of the JO in *drosophila* (Albert *et al*., 2007a). Assuming that this is the case for mosquitoes, compromising the metabolic processes of the sensory cells, through cooling, leads to a decrease in their stiffness and therefore a decrease in the stiffness of the flagellum. A decrease in stiffness of a resonant system leads to a decrease in the resonant frequency and an increase of the amplitude of forced oscillations, below the resonant frequency (Fig. 5.10).

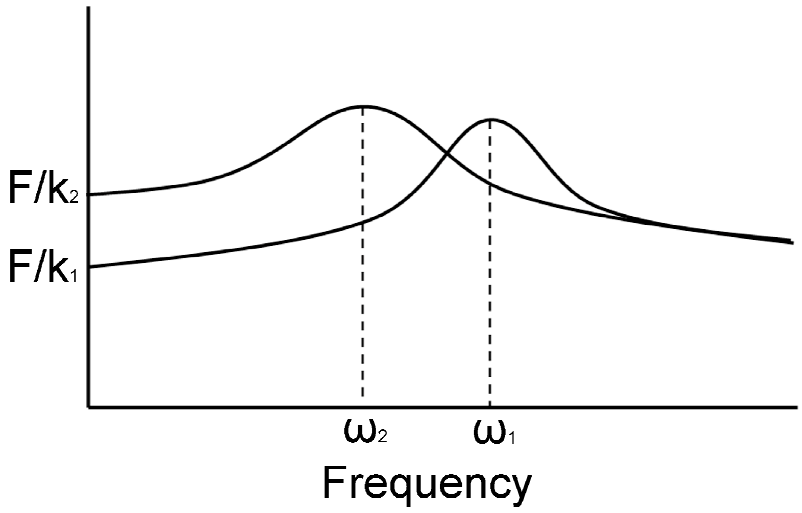

Figure 5.10

Response of a harmonic oscillator to the same force (F) across a range of frequencies. When the stiffness (k) is decreased ($k_1>k_2$) the resonant frequency decreases (from ω_1 to ω_2) and the amplitude below the resonant frequency increases.

Below the resonant frequency stiffness determines the amplitude of a harmonic oscillator. Assuming that the largest F2 – F1 distortion product is produced around the resonant frequency of the flagellum then a stiffness change will lead to the observed increase in the amplitude of the F2 – F1 distortion created. The change in the nonlinear stiffness of the mosquito flagellum leads to a change in the displacement of the flagellum at each of the primary frequencies but could also change the transfer function (such as INPUT = OUTPUT^2) which defines the amount of distortion. It is not strictly known what the decrease in stiffness affects the most; the transfer function leading to the F2 – F1 distortion product or the amplitude of the primaries recorded as movements of the flagellum. Further experiments would need to be conducted to establish, which of these is most affected by a decrease in the stiffness. If it is found that the transfer function underpinning distortion in the antennae of mosquitoes is not affected by cooling then it can be concluded that, distortion is generated through the passive nonlinear mechanics of the flagellum and not through the metabolically sensitive active energy contributing properties of the sensory cells as is proposed to be the case for other acoustical organs (Fettiplace, 2006; Kössl and Boyan, 1998; Manley, 2001; Mockel *et al*., 2007).

Mechanical changes in the stiffness of the sensory cell cilia, due to MET channel closing, quantitatively explain stiffness changes in the *drosophila* antennae (Nadrowski *et al*., 2008). Thus a decrease in the stiffness of the flagellum of mosquitoes could be due to MET opening or closing. How cooling could lead to a change in the open probability of MET channel is not strictly known. One probable cause is a decrease in the receptor lymph potential, which could be brought about by the decreased kinetics of ion pumps in the basal membrane of the sensory cells and in the supporting cells which enclose the receptor lymph space in the scolopidia. A change in the endocochlear potential of the cochlea fluid has been shown to change the operating point of the cochlear transducer, which presumably is brought about by a change in the operating point of the MET channel (Van Emst *et al*., 1997). The probability of MET channels being open depends on the operating point of the transfer function (Nadrowski *et al*., 2008). For instance, in drosophila about 50% of the MET channels are thought to be open at rest at any one time (Albert *et al*., 2007a; Nadrowski *et al*., 2008). Therefore, the change in the receptor lymph potential could therefore regulate the amount of open MET channels and therefore the stiffness of the sensory cells and the attached flagellum. Indeed the dynamic properties of the MET channel can account for the active mechanical properties of the *Drosophila* antenna.

The generation of mechanical F2 – F1 distortion products at the flagellum is heavily bounded by the mechanical response of the flagellum. For instance the largest F2 – F1 distortion product is generated when the two stimulating tones are close in frequency to the mechanical resonance of the flagellum (Fig. 5.9) As such, a shift in the frequency of the stimulus tones at which a maximal F2 – F1 distortion product is mechanically generated, for instance by a change in the temperature, is due to a change in the mechanical properties of the flagellum (Fig. 5.9). A change in the resonant frequency of the flagellum is due to either a change in the mass or stiffness of the antennae. In the *Drosophila* JO the mechanical properties of the flagellum are shown to be dominated by the stiffness of the sensory cilia and not the mass of the sound receiver (Göpfert *et al*., 2005). Assuming that this is the case for the similar antenna of mosquitoes

and that mass remains constant a decrease in the resonant frequency upon cooling would indicate a reduction in stiffness of the ciliary connections to the extended flagellum. When cooling *Cx. quinquefasiatus*, a decrease in stiffness of the ciliary connections results in the frequencies which generate the largest mechanical distortion shifting to lower frequencies (Fig. 5.9).

CHAPTER VI SPONTANEOUS OSCILLATIONS OF THE ANTENNA

ABSTRACT

It has been demonstrated previously in *Tx. brevipalpis* and *Drosophila* that the auditory sensitivity of the Johnston's organ is enhanced through non-linear power amplification of the responses. Spontaneous autonomous oscillations of the flagella in *Tx. brevipalpis* and *Drosophila* which have been observed, especially when the physiological state of the animals was compromised have also been attributed to the same active process that powers active amplification. In this chapter it is shown that the flagellum of the mosquito *Cx. quinquefasciatus* actively oscillates when animals are in normal physiological conditions. To identify the molecular machinery underlying the active oscillations, we studied the temperature dependence of the oscillation frequency and amplitude. It was found that: (1) activation energy of the reaction responsible for the active oscillations was similar to the activation energy of the dynein ATPases and (2) that compromising the microtubule cytoskeleton, to which dynein binds, impairs spontaneous oscillations without abolishing transduction and (3) the application of a transduction channel blocker can eliminate transduction whilst maintaining spontaneous oscillations of the JO. These results suggest that the dynein-tubulin motor, which is the ancestral mechanism that powers the motile cilia of eukaryotes, is responsible for the active oscillations and power amplification in the mosquito hearing organ but could operate independently of mechanoelectrical transduction. This chapter is largely based on Warren *et al.* (2010).

INTRODUCTION

Responses of the JO are thought to be powered by an active feedback mechanism which selectively amplifies low-level responses of the antennal receptor to sound (Göpfert and Robert, 2001; Göpfert *et al*., 2005; Jackson and Robert, 2006). In the vertebrate inner ear, a functionally similar amplification mechanism associated with strong feedback leads, occasionally, to loss of system stability and generation of self-sustained oscillations. These autonomous oscillations manifest themselves as spontaneous acoustic emissions which can be recorded in the ear canal (Kemp, 1979) or, *in vitro*, as oscillations of the stereociliary bundles of the inner ear receptor hair cells (Crawford and Fettiplace, 1985). These oscillations have been demonstrated to enhance frequency selective gain and sensitivity of the system in noisy environments (Martin and Hudspeth, 2001; Nadrowski *et al*., 2004), although they have also been considered as signatures of system instability caused by excessive gain (Camalet *et al*., 2000). Motility of the hair bundles within the cochlea, due to two opposing, feedback controlled, forces, is proposed to create a bifurcation, where only the correct amount of force will create an optimally sensitive system (Nadrowski *et al*., 2004). If the opposing forces are too great, due to excessive feedback, then the system is set into an oscillatory state (Fig. I.11). Spontaneous oscillations (SO) of the antennal flagellum have also been documented for some Dipteran species when their physiological state was compromised (Göpfert and Robert, 2001; Göpfert and Robert, 2003). They have also been recorded after prolonged repetitive stimulation (Göpfert and Robert, 2001) and are thought to be powered by the sensory neurons through the same mechanism that provides power amplification of the response of the flagellum to sound (Göpfert and Robert, 2001). Therefore, through identifying the origin of the spontaneous oscillations, the mechanism of the power amplification of responses in the insect hearing organ might also be revealed.

Two mechanisms have been suggested to amplify the mechanical response of the flagellum to sound. The first mechanism is associated with the mechanosensitive channels responsible for mechanoelectrical transduction and

is essentially the same as that described for the vertebrate, hair bundle-based, amplifier (Fettiplace *et al*., 2001; Hudspeth, 1997). In the hair bundle model, active forces and spontaneous oscillations are produced by the hair bundle through the interplay between the gating kinetics of the transducer channels and their adaptation machinery (Hudspeth, 1997). Because the transducer machinery contributes significantly towards the mechanical properties of the *Drosophila* acoustic receiver (Albert *et al*., 2007a; Nadrowski *et al*., 2008), a similar mechanism may be responsible for active force production and active oscillations in the mosquito flagellum. An alternative idea is that this motility is conferred by motor molecules separate from the transduction machinery. This suggestion was first proposed by Gray and Thurm (Gray and Pumphrey, 1958; Thurm, 1965) based on the morphology of the cilia of the sensory cell, where transduction takes place. The cytoskeletal components of the dendritic cilia, namely the dynein-tubulin system, match the functional components known to power motile cilia and flagella. Thus, previously, it has been proposed that the cilia of insect sensory cells can produce a form of ciliary beating using a mechanism similar to that conserved in all eukaryotic branches (Mitchell, 2007; Wiederhold, 1976). Hence, through synchronizing their beats, through mechanical coupling (Jackson *et al*., 2009), the ~15,000 cilia of the sensory cells in the JO could produce oscillations of the flagellum.

RESULTS

Spontaneous oscillations of the flagellum

SOs of the flagellum were observed in both male and female mosquitoes in normal physiological condition (Fig. 6.1). Normal physiological conditions of the mosquito, before and after altering the temperature, were confirmed by checking a response to tarsal stimulation and the presence of abdominal contractions. The amplitude of the SOs at room temperature remained at almost constant amplitude and frequency throughout the experiment. In this study we present data collected only from male mosquitoes because the SO amplitude was much larger in males. SOs were observed in 31 out of 35 male mosquitoes that were thought to be in normal physiological conditions. Normal physiological conditions were confirmed through observing abdominal contractions and elicited motor activity of the legs. The inset in Fig. 6.1 shows a typical example of SOs of the flagellum recorded in the time domain. The SO frequency in this case was about 290 Hz with a maximum, peak to peak, amplitude of 15 nm recorded at a point 200 μm distal to the pivot of the flagellum which corresponded to $4.3X10^{-3}$ degrees of angular displacement. The SOs appear usually as a single peak in the amplitude spectra of the mechanical responses. It was not uncommon, however, to observe two peaks corresponding to different frequencies (for example 289 Hz and 312 Hz in Fig. 6.1) clustered together. Similar peak splitting has been observed for isolated axonemes (Kamimura and Kamiya, 1989) and its origin is not clear. A shift of the SO frequency during the sampling period may be responsible for the peak splitting in the mechanical recordings. The SOs of the flagellum were metabolically sensitive and disappeared post mortem and when the physiological conditions of animals were compromised through cooling to 5°C (Fig. 6.1, red trace). Similar metabolic sensitivity of the SOs has been demonstrated in other mosquito genera and *Drosophila* by injection of dimethyl sulfoxide, which slowly eliminated the SOs upon death (Göpfert and Robert, 2001; Göpfert and Robert, 2003).

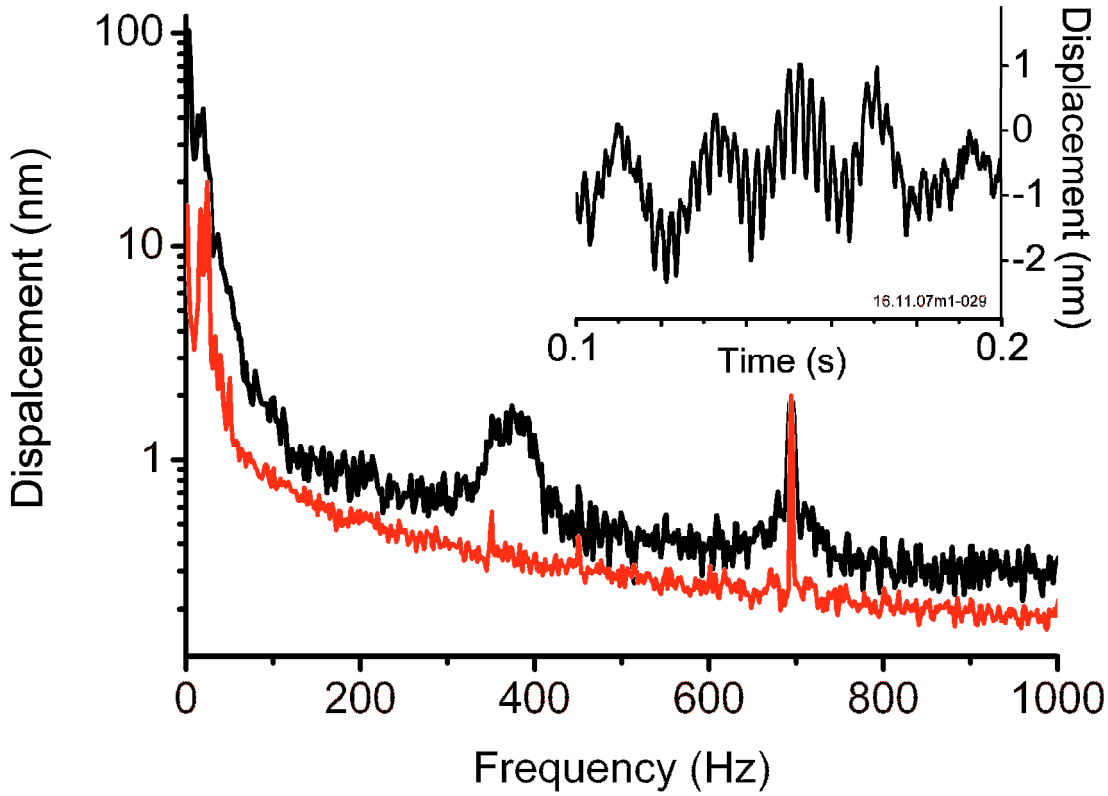

Figure 6.1

Mechanical SOs of the flagellum. Amplitude spectrum of the displacement of the flagellum without stimulation showing the frequency specific SOs (black). The red trace shows a recording from the same mosquito upon colchicine injection and loss of SOs. The sharp peak at 800 Hz is a 2nm movement of a piezoelectric crystal used to calibrate displacements recorded by the laser. Inset the waveform of the SOs in the time domain. Copied from Warren *et al.* (2010).

To assess the mechanical nature of the SOs displacements of the flagellum were recorded in response to mechanical stimulation (Fig. 6.2). Although SOs are thought to be underpinned by the same mechanism that supplies power amplification to the JO, SOs do not match their frequency to that of the external stimulus when an evoked tone is presented close in frequency at high levels (Fig. 6.2).

Temperature dependence of the oscillation frequency

The frequency of the SOs of the flagellum depends on temperature. Measurements of this dependence were confined to between 5 and 35℃

because outside of this range the amplitudes of the SOs fall below the noise floor of our recording system. SO frequency vs. temperature when plotted in Arrhenius coordinates (Fig. 6.3) is not linear and has a break point at about 15°C.

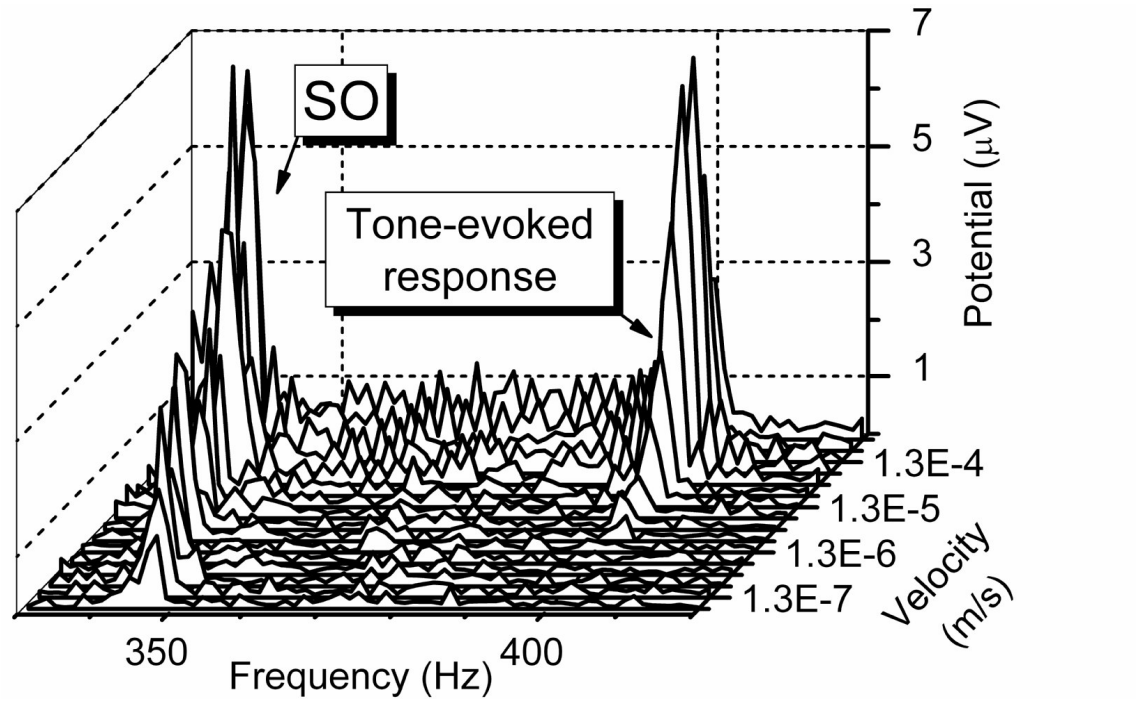

Figure 6.2

Amplitude spectrum showing the electrical response of the JO to a 400 Hz pure tone increasing in intensity. Copied from Warren *et al.* (2010).

To calculate where the approximate break point lays, a polynomial line was fitted to the data and the largest value of the second derivative was used to assess the approximate break point. A straight line was then fitted for all data points 2° C below and 2° C above the approximated break point, thus excluding data around the approximated break point. The intercept of the two linear fits was used as the exact break point of 15° C. A break point in the temperature dependence of the beat frequency has been documented for different types of motile cilia and flagella (Coakley *et al.*, 1974; Grove *et al.*, 2005). A break point in temperature dependence has been shown for the activity of several motor molecules (Bohm *et al.*, 2000; Millar *et al.*, 1983; Stein *et al.*, 1982) and is likely to be associated with conformational changes or/and phosphorylation in the motor ATPases or/and in associated molecules (Coakley and Holwill, 1974;

Grove *et al*., 2005; Salathe, 2007). The dependence shown in Fig. 6.3 is fitted well by two linear regression lines above and below the breakpoint. Let us assume that the SO frequency is proportional to the rate constant of the reaction responsible for the SO. Then the regression lines correspond to the natural logarithms of a modified Arrhenius equation

$$\ln(\omega(T)) = \frac{-E}{R}\frac{1}{T}\ln(K) \qquad [1]$$

which gives the dependence of the SO frequency $\omega(T) = 2\pi f$ on the absolute temperature T and activation energy E of a single rate limited reaction responsible for the SOs. In this equation K is the pre-exponential factor and R is the gas constant. Corresponding activation energies derived from the slopes of the regression lines are 30 kJ/mol for temperatures above 15° C and 43 kJ/mol for temperatures below that. These energies are within the range found for the dynein and kinesin ATPase family (~31 kJ/mol) and are significantly lower than the activation energy measured for myosin ATPases (~66 kJ/mol) for in vivo systems (see Table 6.4 and references within).

Temperature dependence of the oscillation amplitude

Pooled data for the dependence of the normalized amplitude $A_N(\omega(T)) = A(\omega(T))/A_{MAX}$ of SOs on temperature T are shown in Fig. 6.5 Here $A(\omega(T))$ and A_{MAX} are the frequency dependent amplitude and maximal amplitude of SOs respectively. The normalized amplitude was plotted to avoid variations in the amplitude measurements associated with slightly different positions of the recording location along different flagella. The dependence $A_N(\omega(T))$ is bell-shaped and falls below the noise floor of the recording system beyond the temperature range 5-35° C, which matches the maximum range of

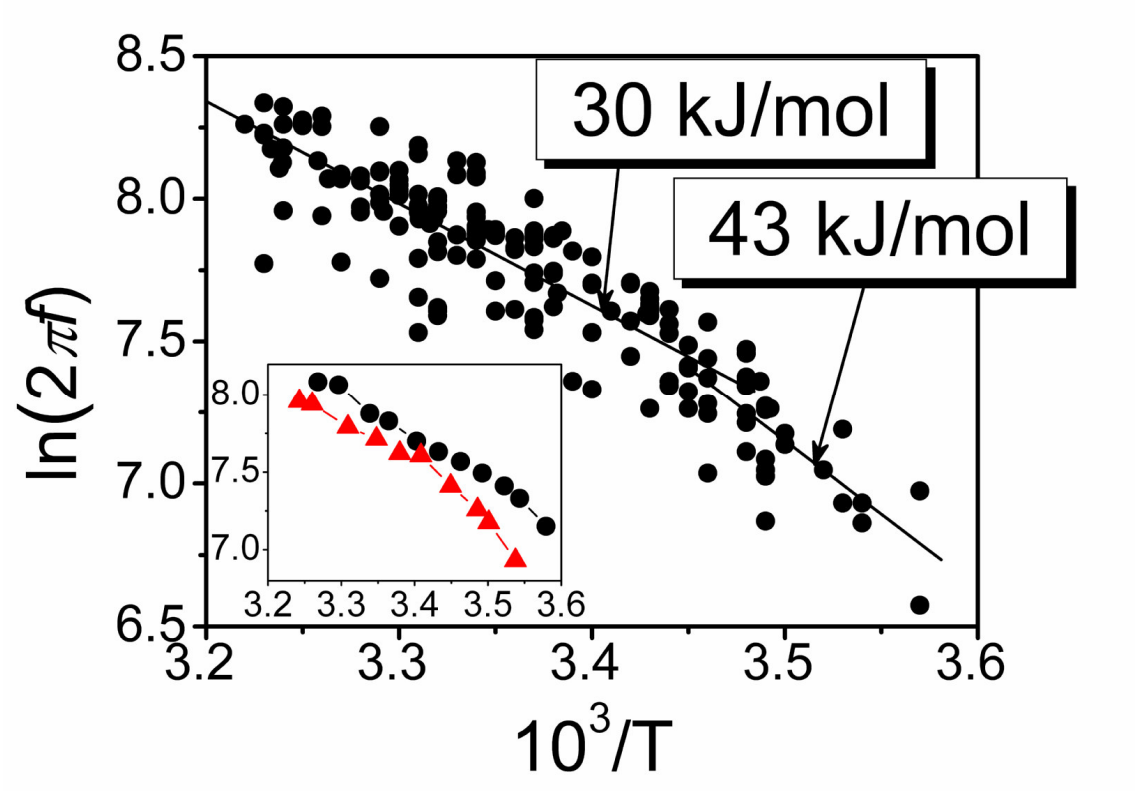

Figure 6.3

Temperature dependence of the SO frequency. Arrhenius plot of the natural logarithm of SO frequency against the inverse absolute temperature for 12 male *Cx. quinquefasciatus*. Two linear regression plots are fitted with a break at about 15 ℃. The activation energy values are plotted for both the linear regression plots. Inset Arrhenius plots of two individual mosquitoes. Copied from Warren *et al.* (2010).

temperatures in the habitat of *Cx. quinquefasciatus* mosquitoes. Within this range the observed maximum of the amplitude is scattered between 20-28° C (mean is 23.6 ± 2.7℃, *N*=9) which, according to the regression line in Fig. 6.3, corresponds to changes in the frequency between 311-431 Hz (the value corresponding to the mean temperature of 23.6 $^{\circ C}$ is 361 Hz). Normalized amplitude data in Fig. 6.5 are fitted by the equation for the amplitude of vibrations of a harmonic oscillator

$$A_N(\omega(T)) = \frac{C}{([\omega_0{}^2 - \omega(T)^2]^2 + [\gamma\omega(T)]^2)^{1/2}} \qquad [2]$$

with temperature dependant changes in the angular frequency $\omega(T)$ defined by Eq. 1. ω_0 in Eq. 2 is the natural angular frequency of the flagellum. $C = F/mA_{MAX}$ and $\gamma = b/m$ are constants, with *m* and *b* being the effective mass

Activation energy (kJ/mol)	Reference
Dynein	
57	Calculated from Gray, (1923)
31	Holwill and Silvester, (1967)
44	Holwill, (1968)
40	Stephens and Levine, (1970)
51	Calculated from Machemer, (1972)
29	Coakley and Holwill, (1974)
25	Holwill and Wais (1979)
20	Calculated from Auger *et al.*, (1990)
12	Calculated from Clary-Meinesz *et al.*, (1992)
Median 31	
Myosin	
66	Stein *et al.*, (1982)
53	Barany, (1967)
84	Ranatunga, (1984)
50	Anson, (1992)
94	Grove *et al.*, (2005)
Median 66	

Table 6.4

Activation energy values for *in vivo* systems operating in their natural temperature range. Copied from Warren *et al.* (2010).

of the flagellum and damping coefficient respectively. *F* is the effective force acting on the flagellum. The fitted curve in Fig. 6.5 reveals the pooled natural frequency of the flagellum $f_0 = \omega_0 / 2\pi = 353 \pm 8$ Hz (n=12) and its pooled damping coefficient $b = m\gamma = (1.915 \pm 0.532) \times 10^{-4}$ Ns/m, taking into account that the flagella mass measured independently is $m = 276 \pm 58 \times 10^{-9}$ g (for 11 males). Then the quality factor for pooled data is $Q = \omega_0 / \gamma = 3.2 \pm 0.6$. When Eq. 2 is used to fit data obtained from individual flagella (Fig. 6.6, inset), the damping coefficient is almost two times smaller being $b = (1.054 \pm 0.350) \times 10^{-4}$ Ns/m, which corresponds to sharper tuning with $Q = 6.1 \pm 1.3$ (n=7). The averaged natural frequency of the individual fits $f_0 = 354 \pm 45$ Hz (n=7) is not however significantly different from the pooled natural frequency. Table 6.6 systematizes the parameters that

characterise the mechanical properties of the flagellum, including its stiffness-coefficient $K = m\omega_0^2$, obtained from the pooled data and individual fits.

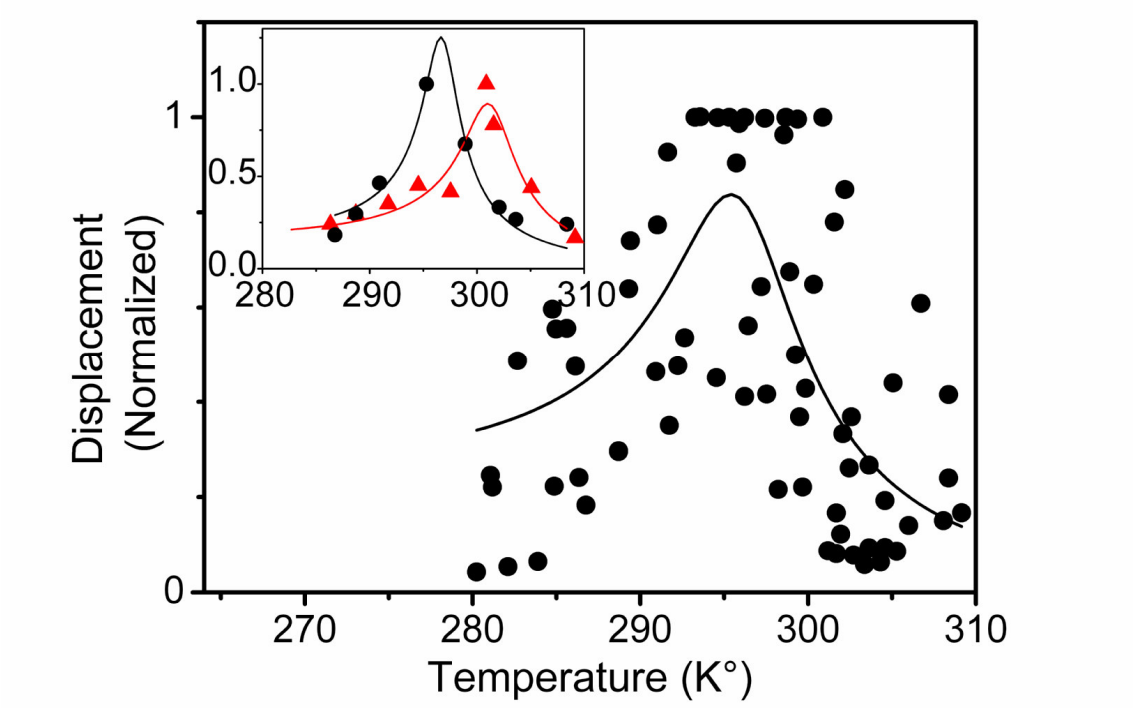

Figure 6.5

Temperature dependence of the amplitude of mechanical SOs. A simple harmonic oscillator model was fitted to the dependence of the normalised amplitude of the SOs with respect to temperature for 9 male *Cx. quinquefasciatus*. Inset illustrates the same model fitted to the temperature dependences from two individual mosquitoes. Copied from Warren *et al.* (2010).

	Fit to pooled data		Individual fit	
	mechanical (n=9)	Electrical (n=11)	mechanical (n=7)	electrical (n=11)
f_0, Hz	353 ± 8	419 ± 7	354 ± 45	413 ± 54
γ, 1/ s	694 ± 126	643 ± 98	382 ± 98	312 ± 88
b, $\times 10^{-4}$ Ns/m	1.915 ± 0.532	1.775 ± 0.461	1.054 ± 0.350	0.861 ± 0.303
Q	3.2 ± 0.6	4.1 ± 0.6	6.1 ± 1.3	8.8 ± 2.0
K, N/m	1.36 ± 0.29	1.91 ± 0.41	1.37 ± 0.38	1.86 ± 0.52
m, $\times 10^{-9}$ g	276 ± 58 (n = 11)			

Table 6.6

Parameters characterising the mechanical properties of the flagellum. Copied from Warren *et al.* (2010).

Temperature dependence of the JO neural responses

Oscillations of the compound electrical responses could be recorded from inside the JO at the frequency of the SOs of the flagellum (Fig. 6.7). The similarity in frequency of the mechanical and electrical endogenous SOs indicates the close association between these two types of activity and, probably, that they share the same origin. We commonly recorded a component of the electrical response at twice the frequency of the SOs (Fig. 6.7). Frequency doubling of the electrical responses of the JO to a pure-tone acoustic stimulus is a well documented phenomenon for mosquitoes (Wishart *et al*., 1962). The magnitude of the electrical oscillations followed the same bell-shaped temperature dependence (Fig. 6.8) as the amplitude of the mechanical displacement of the flagellum (Fig. 6.5). Assuming that the magnitude of the electrical oscillations is governed by properties of the same harmonic oscillator as the mechanical SOs and fitting this dependence with combination of Eqs. 1 and 2, we find slightly different values for the natural frequency (Table 6.6). To investigate the difference in natural frequency calculated from mechanical and electrical measurements of the SOs simultaneous measurements were conducted on two mosquitoes (Fig. 6.9). Figure 6.9 shows that the simple harmonic oscillator model, when fitted to temperature dependant changes of the electrical SOs, gives a higher resonant frequency and more sharply tuned oscillator, compared to values derived from mechanical recordings. The sharper tuning of the harmonic oscillator model fitted to the electrical oscillations, as compared with the mechanical oscillations, could be explained through a more limited frequency response of the JO neural responses. The other characteristics of the harmonic oscillator however are not significantly different from parameters obtained from the temperature dependence of the mechanical SOs (Table 6.6). This suggests that electrical and mechanical oscillations are tightly coupled. It is worth noting that, for the temperature dependence of the electrical SOs (Fig. 6.8), the fitting of equations to data obtained from individual JOs (Fig. 6.8, inset) also reveals significantly sharper tuning (compare the two columns of parameters for electrical responses in Table 6.6). As for the mechanical SOs, this difference in parameters between

pooled and individual data reflects the scatter of the maximum amplitude of mechanical responses obtained from different mosquitoes (Fig. 6.5).

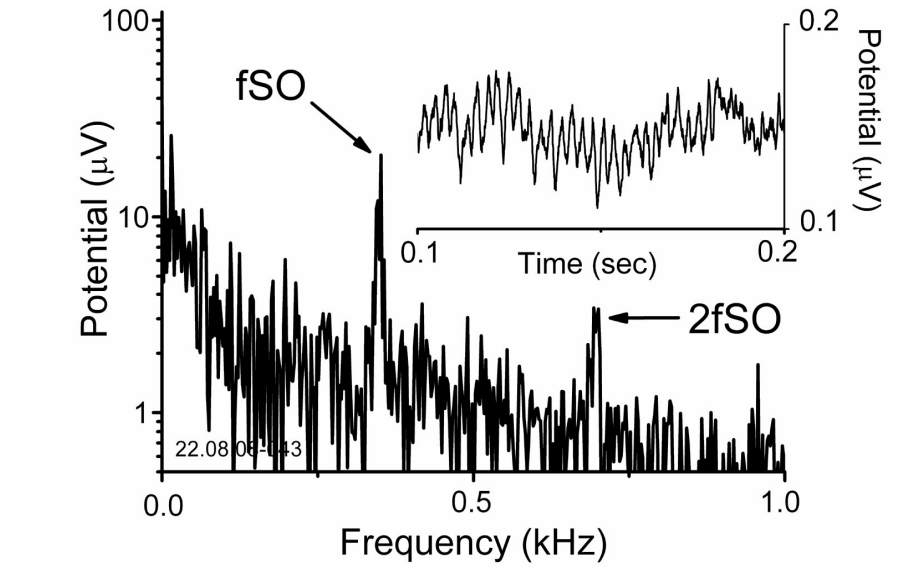

Figure 6.7

Amplitude spectrum of the electrical potential of a JO without stimulation. Inset the waveform of the SOs in the time domain. Copied from Warren *et al.* (2010).

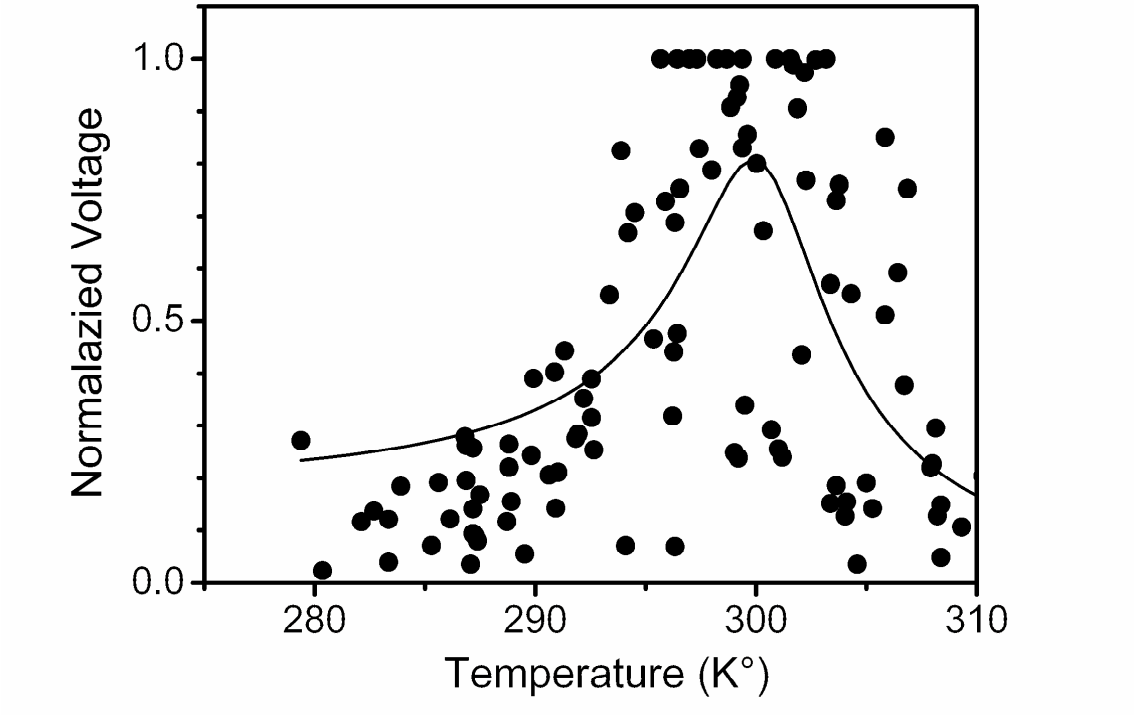

Figure 6.8

Temperature dependence of the amplitude of electrical SOs. A simple harmonic oscillator model fitted to the normalised amplitude of the electrical SOs of the JO with respect to temperature for 11 male *Cx. quinquefasciatus*.

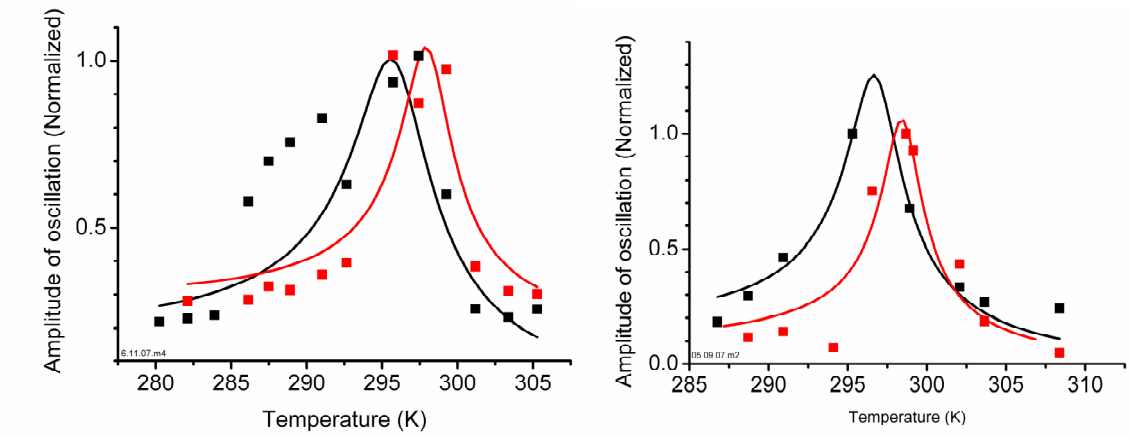

Figure 6.9

Simultaneous recordings showing the temperature dependence of the amplitude of mechanical (black) and electrical (red) SOs for two individual mosquitoes.

Colchicine blocks the SOs

Extracellular application of the alkaloid colchicine causes disruption of microtubules in the dendritic cilia of Arthropoda mechanoreceptors (Moran *et al.*, 1971). To examine the involvement of the microtubular system in SO generation we injected insect saline containing 10 mM of colchicine and 9 mM of methylene blue into the JO. Methlylene blue was used as a marker to ensure that solutions filled the JO (Fig. 6.10). Staining of the JO with methylene blue was confirmed by inspection of cryosections of the injected JO after the experiment. Injections of colchicine containing solution blocks SOs within 10 minutes (Fig. 6.10 A,B). SOs did not re-appear during further observations (up to 2 hours). The oscillations remained after injection of a control, colchicine-free physiological solution, which contained methylene blue only (Fig. 6.11 C,D). Although the injection of all 3 solutions also affected the mechanical SOs recorded as movements of the flagellum (Table 6.12).

Sound evoked electrical responses composed of receptor potentials, could still be elicited in the JO by its acoustical stimulation after the colchicine associated block of the SOs (Fig. 6.11 E). This observation confirms the integrity of the

transduction apparatus after the colchicine application advocating that the mechanism responsible for the SOs oscillations is not part of the transduction apparatus.

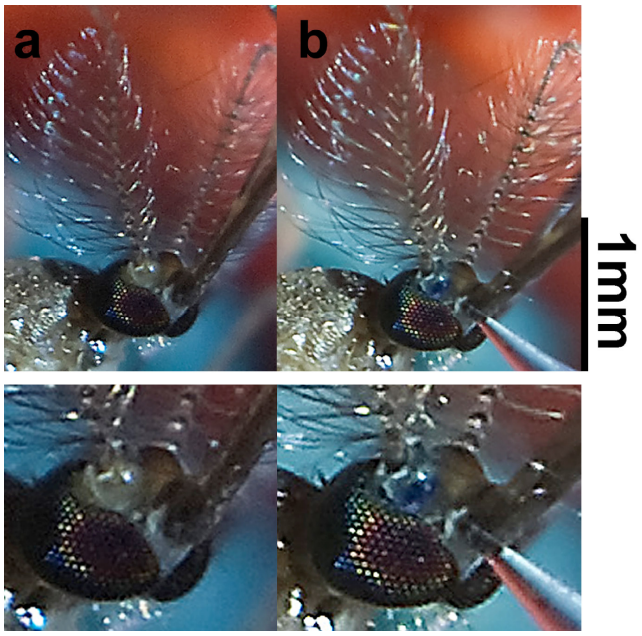

Figure 6.10

JO before (left column) and after (right column) injection of *Drosophila* saline containing methylene blue.

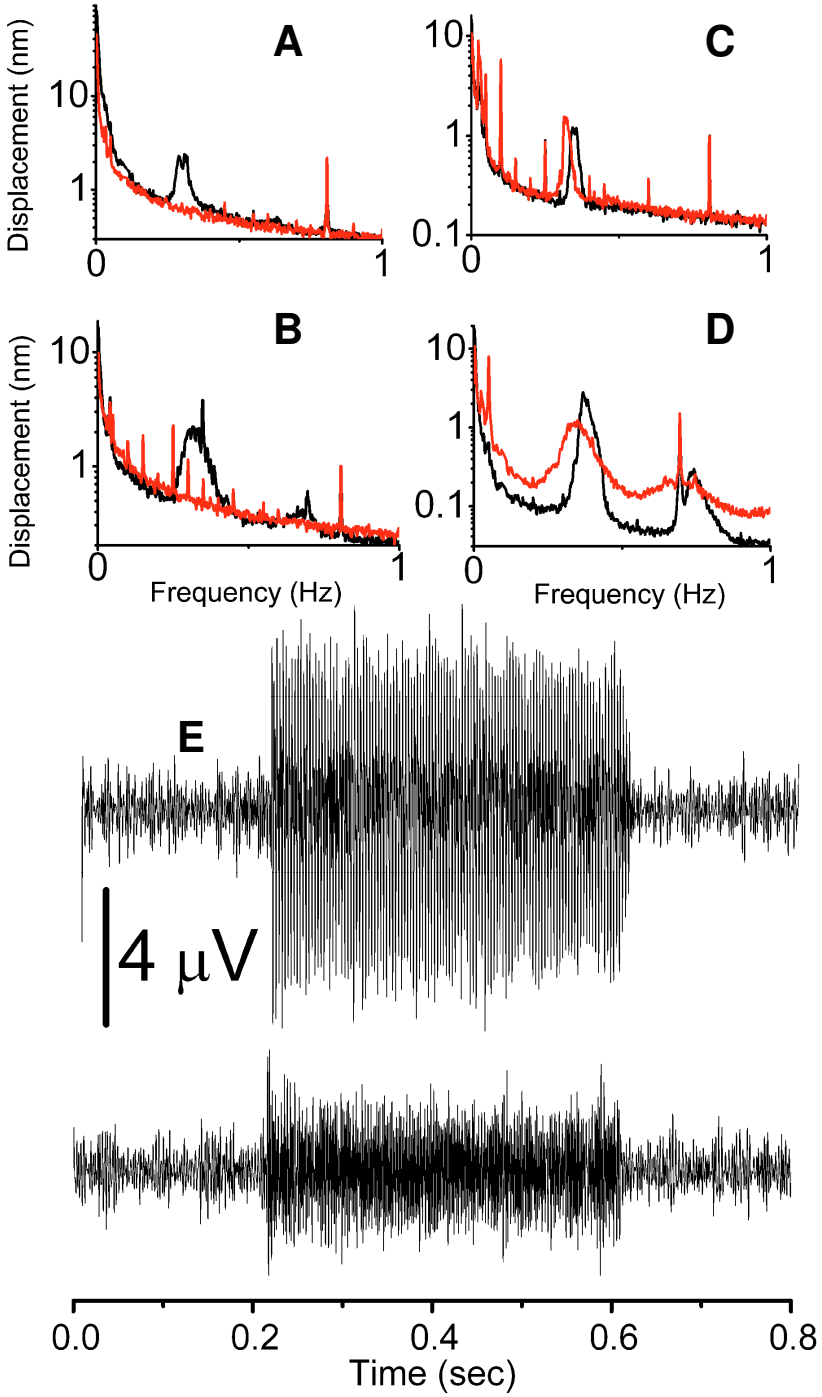

Figure 6.11

Effect of colchicine on SOs and mechanoelectrical transduction.
SOs before and after injection of colchicine. Amplitude spectrum of the displacement of the flagellum before (black) and 10 minutes after (red) injection of colchicine solution (a,b) and colchicine-free solution (c,d). (e) Electrical potential of the JO to a pure tone presented between 0.2 and 0.6 seconds at an intensity of $1X10^{-4}$ m/s at 300 Hz before (above) and after (bottom) injection of colchicine. The sharp peak at 700 Hz is a 1-2nm movement of a piezoelectric crystal used to calibrate displacements recorded by the laser.

Dihydrostreptomycin blocks electrical transduction in the JO

Solutions based on *Drosophila* saline containing dihydrostreptomycin (DSM) a transduction channel blocker, colchicine a microtubule depolymerising agent and a control solution were injected into the pedicel of mosquitoes to assess the role of the MET channel and microtubules in the JO's response to sound. The decrease in amplitude of electrical responses following the injection, of all 3 solutions, could be owing to changes in the electrical properties of the JO or to local damage of the sensory cells in the vicinity of the pipette tip caused by the injection.

	Ratio of 2F component of receptor potential after/before injection ± standard deviation	Ratio of SOs after/before injection ± standard deviation	n
Electrical			
DSM	0.26 ± 0.29	0.32 ± 0.27	7
Colchicine	0.24 ± 0.17 (n=3)	0.52 ± 0.53 (n=5)	
Control	0.4 ± 0.28	0.11 ± 0.16	3
Mechanical			
DSM	N/A	1.2 ± 1.6	6
Colchicine	N/A	SOs gone after injection	7
Control	N/A	0.54 ± 0.76	6

Table 6.12

Characterisation of the effect of a solution (DSM, colchicine, methylene blue control) on electrical and mechanical oscillations and transduction. Ratios were calculated by dividing the amplitude of oscillations before injection by amplitudes after injection. Transduction was measured using the 2F component of the receptor potential in response to a 300 Hz pure tone at $5X10^{-4}$ m/s.

Fortunately transduction was completely blocked in one mosquito after injection of DSM (Figure 6.13). Electrical spontaneous oscillations and their harmonics were still recorded in this mosquito after loss of all transduction (Figure 6.14).

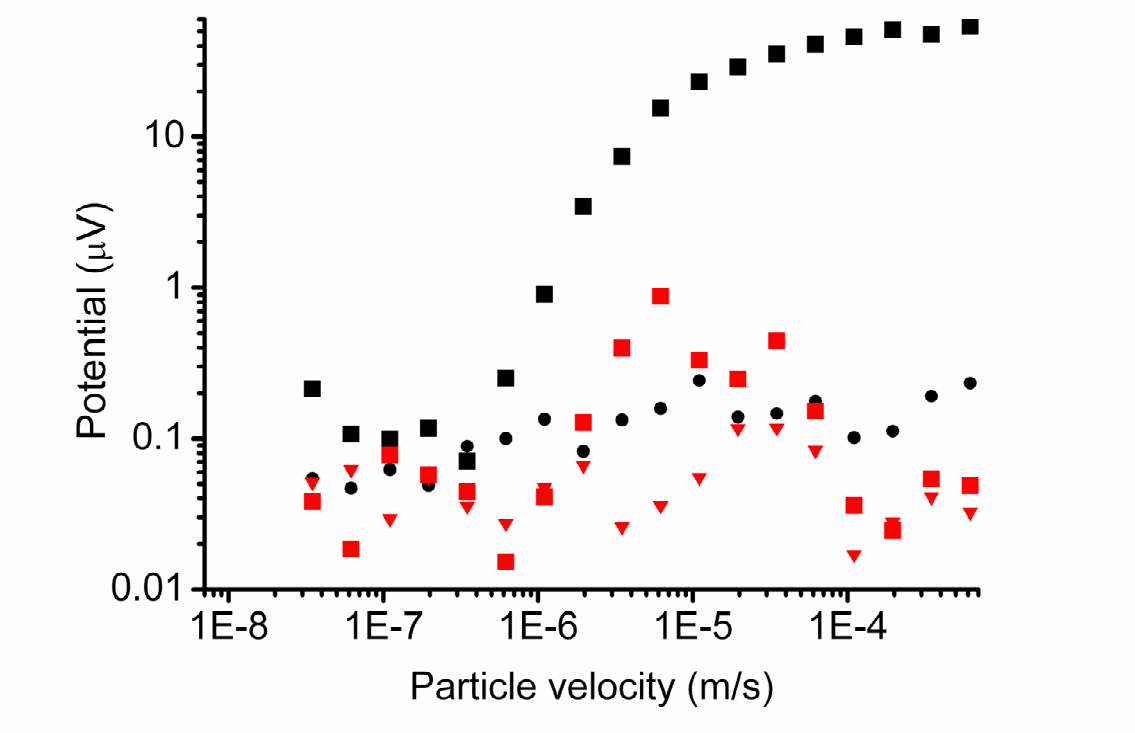

Figure 6.13

The amplitude of the transduction current to a 300 Hz pure tone increasing in amplitude before (black) and after (red) DSM injection (noise floor before black circles, after red triangles).

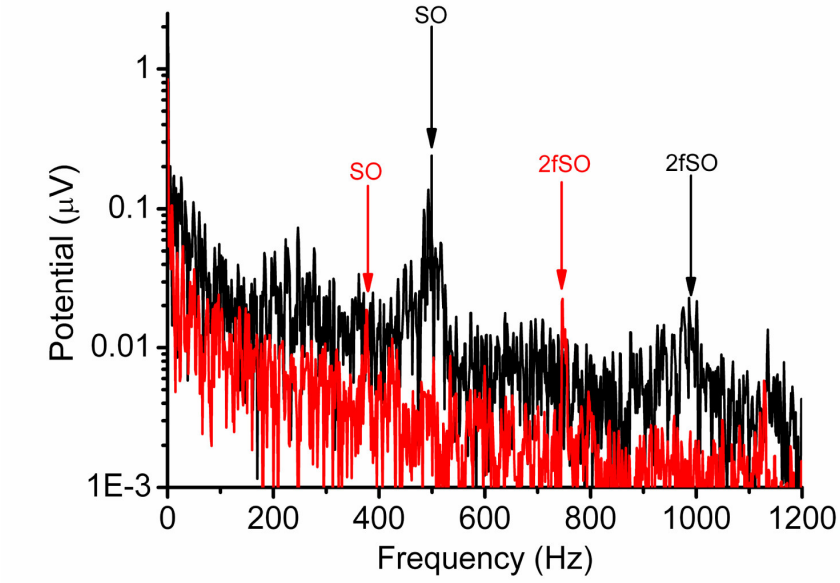

Figure 6.14

Electrical spectrum of the JO before (black) and after (red) DSM injection (2fSO is the 2nd harmonic component at twice the frequency of the SO).

DISCUSSION

Dendritic cilia of the sensory neurones of the JO are the only non-cuticular attachments to the prongs of the mosquito flagellum and are assumed to underlie its SOs (Göpfert and Robert, 2001). Most of the evidence in support of this hypothesis came from studies of the *Drosophila* antennal receiver which has an organization and function similar to that of the mosquito JO. It has been demonstrated that generation of SOs by the *Drosophila* antennal receiver is due to an active non-linear process associated with cilia of the auditory neurones (Göpfert and Robert, 2003; Göpfert *et al*., 2005). Mechanical responses of the antennal receiver become linear and passive and SOs are never observed in *Drosophila* mutants with ciliary defects (Göpfert and Robert, 2003). It has been suggested (Göpfert *et al*., 2005) that the molecular motor driving the active amplification of responses, and hence likely to drive the SOs of the antennal receiver works in an identical way to the molecular machinery responsible for the SOs that have been measured in the hair bundles of vertebrate hair cell cells where oscillations are generated due to interaction between the mechanoelectrical transducer gating kinetics and a myosin based adaptation mechanism (Martin *et al*., 2000). While the transducer apparatus contributes significantly towards the mechanical properties of the antennal receiver (Albert *et al*., 2007a; Nadrowski *et al*., 2008), the presence of a myosin-actin motor associated with transducer channels of the JO sensory neurones has not been demonstrated. In fact, data presented in this report show that the rate limiting reaction associate with the SOs of the mosquito antennal organ is unlikely to be due to a myosin-based motor.

SO frequency closely matches the WBF of conspecific female mosquitoes. It is possible, therefore, that SOs are involved in the detection of the female fundamental WBF perhaps amplifying at that frequency.

The dynein-tubulin system powers the SOs

Our estimates of the activation energy of the rate limiting molecular processes powering the SOs for temperatures above 15°C, which is well within the usual temperature range of *Cx. quinquefasciatus*, gives a value of 30 kJ/mol (Fig. 6.3). This activation energy, and in fact the activation energy of 43 kJ/mol for temperatures below 15°C, is lower than for *in vivo* systems based on the myosin ATPase but matches that of *in vivo* systems powered by dynein and kinesin (see Table 6.4 and references within). Dynein, however, is the only motor molecule distributed throughout the length of the sensory cilium (Thurm *et al*., 1983). This strongly suggests that the dynein-tubulin system powers the SOs.

Independence of SOs and transduction

SOs are thought to share the same molecular machinery as the transduction apparatus (Göpfert *et al*., 2005). However, the frequency and amplitude stability of SOs during sound stimulation strongly indicates that SOs do not change their frequency to match and amplify an evoked tone. Indeed the frequency of the SOs changes little upon exposure to a pure tone, close in frequency, and remains distinct (Fig. 6.2). Although SOs do not interact directly this does still not preclude them from enhancing signal detection (Martin *et al*., 2001; Nadrowski *et al*., 2004). The injection of DSM and the knockout of transduction (Fig. 6.12) revealed that electrical SOs still persisted (Fig. 6.13). If the mechanoelectrical transduction channels were blocked or compromised then the electrical SOs must be underpinned by another mechanism.

Molecular mechanisms of SOs

Based on the morphology of the sensory cilia (Boo, 1981) and mechanical responses of the antennal receptor (Nadrowski *et al*., 2008) the dynein-tubulin system may be involved in the generation of the SOs through two fundamentally different mechanisms.

Firstly, the SOs may be generated using the same ancestral mechanism that powers motile cilia. This idea is based on similar morphology of the dendritic cilia of insect scolopidial neurones to motile cilia (Wiederhold, 1976). In fact, dendritic cilia of the JO having 9x2+0 axonemal organization lack the central pair of microtubules, which, however, does not generally prevent cilia from being motile (Göpfert and Robert, 2008). Sensitivity of motile cilia to mechanical stimulation is well documented (Wiederhold, 1976 and references within). Hence, it is logical to suggest that cilia with a primary sensory function can also be motile (Wiederhold, 1976), utilizing this motility for active amplification of responses to weak stimulation. So far active bending of cilia in scolopidial organs has been demonstrated in morphological studies only (Moran *et al*., 1977). The idea of an independent motile cilium operating concurrently within a mechanosensory system is supported by observations of Göpfert and Robert (2001) who recorded flagellar oscillations in mosquitoes, which failed to elicit electrical responses in the JO.

Involvement of dynein-tubulin motor in SO generation does not, however, exclude involvement of the transducer machinery. In this second scheme, the dynein-tubulin system plays the role of an adaptation motor, analogous to the tip-link associated myosin adaptation motor of hair cells of lower vertebrates (Kernan and Zuker, 1995). Here SOs are generated due to interplay between the gating kinetics of the transducer channels and the dynein-tubulin based adaptation motor. It is worth noting however that cyclic movement is natural to the dynein-tubulin complex as demonstrated by *in vitro* experiments when the presence of microtubules was sufficient to activate oscillatory movement of the dynein ATPase (Kamimura and Kamiya, 1989; Shingyoji *et al*., 1998).

Physiological significance of SO

It has been demonstrated that autonomous oscillations can significantly improve system sensitivity and gain in noisy environment (Martin and Hudspeth, 2001; Nadrowski *et al*., 2004). The SOs of male mosquitoes are observed within the

frequency range of the female WBF and, hence, may be functionally significant in detecting flying females when mating in swarms (Gibson and Russell, 2006). It is worth noting that both frequency of SOs at any given temperature (Fig. 6.3) and calculated natural frequencies of oscillations of the antennal receivers demonstrate a significant scatter which may be important for covering the range of the female mosquito flying tones.

Conclusion

The results presented here provide the first *in vivo* evidence for the involvement of the dynein-tubulin system in the generation of SOs and, hence, power amplification in mosquito antennal receivers. The auditory receptor of mosquitoes has recruited a mechanism already engineered for generating motility in cilia and flagella. This mechanism is molecularly distinct from the mechanoelectrical transduction channels in the cilia membrane and, therefore, different from that in vertebrate auditory and vestibular receptors where motility and transduction have been attributed to the transduction apparatus.

GENERAL DISCUSSION

FREQUENCY-MATCHING

Frequency-matching is reported here for *Cx. quinquefasciatus* and *An. gambiae* and, from separate studies (Cator *et al*., 2009; Gibson and Russell, 2006), for *Tx. brevipalpis* and *Ae. aegypti.* Thus frequency-matching appears to be a generic feature across a wide range of mosquito genera in separate geographical locations and habitats with unique lifecycles. For instance *Tx. brevipalpis* do not swarm or seek blood meals instead these nectar feeding mosquitoes mate by pursuing a flying female normally from a stationary position on plant matter (Bonnet and Stephen, 1951). All the other mosquitoes however form mating swarms with the females taking blood meals. The occurrence of frequency-matching in mosquitoes, which have speciated 200-250 million years ago (Krzywinski *et al*., 2006), indicates that frequency-matching behaviour is functionally important in mosquito behaviour. Sexual recognition in *Tx. brevipalpis* and *Cx. quinquefasciatus* appears to be underpinned by frequency-matching behaviour, with same sex and opposite sex conspecifics avoiding and frequency-matching respectively. Findings presented in chapter III suggest that frequency-matching, in *An. gambiae,* is important in subspecies recognition. Same-form pairs frequency-match significantly more then mixed-form pairs. Indeed this is the first robust phenotype that has been identified in the M and S forms of *An. gambiae*, which is linked to reproduction and therefore, could explain reproductive isolation in mixed swarms. Previous studies have failed to find any difference in the wing-beat frequencies of M and S form *An. gambiae* (Tripet *et al*., 2004). Tripet *et al*. (2004) measured differences in the amplitude of the higher harmonics using a tachometer, which optically sensed minute changes in the intensity of light due to the flapping of the mosquitoes wings. The capability of optical recordings to measure the higher harmonics produced by flapping of the mosquitoes wings is not known. The behavioural significance of frequency-matching cannot be firmly determined until free flight recordings have been performed. However frequency-matching may allow the male to

synchronise with the potentially turbulent air stream of larger female and approach and grasp her during free flight (Roth, 1948).

The JO of *Tx. brevipalpis* is most sensitive to frequencies produced by the flight-tone of both sexes. Therefore frequency matching by *Tx. brevipalpis* can be achieved through a simple algorithm, possibly in the Johnston's organ centre, that calculates the difference in WBF between its own WBF and that of its acoustically interacting partner. However, for blood feeding mosquitoes, where the fundamental WBF is vastly different between the sexes, frequency matching occurs between the higher harmonics at frequencies up to 2 kHz, well above the most sensitive frequency of the JO. As shown in Chapter V, although the bandwidth of the receptor potential, as determined by the F2 component, it limited to ~800 Hz (also see findings from Clements, 1999; Wishart *et al*., 1962), the frequency range of the F1 component of the receptor potential encompasses those associated with matching by blood feeding mosquitoes, but only at high particle velocities (equivalent to those encountered by two mosquitoes flying ≤ 1cm apart. Frequency-matching, through detection of the F1 component of the receptor potential, does not, however, account for the frequency matching documented here where mosquitoes were flown at least 3 cm apart. Nonlinearities created by the flagellum in response to two tones impinging upon it induce a receptor potential at the frequency difference between the tones, which is generated through the F2 – F1 distortion product and may be used as an 'error' signal to mediate frequency matching in haemophilic mosquitoes between frequencies beyond their auditory range.

The mechanical properties of the mosquito antenna are characteristically nonlinear and thought to have a large quadratic nonlinearity based on our findings of a level dependant increase in the resonant frequency of the flagellum and the production of large even order distortion products such as F2 ± F1. For mosquitoes interacting acoustically during flight, distortion generated at the antennae could be utilised to aid frequency-matching. For instance, the flight tone of a male and a female, interacting acoustically in free flight, would cause large F2 – F1 components in the mechanical vibrations of the flagellum. In

Chapter V we have shown that such mechanical distortion products are transduced into receptor potentials, even though the higher harmonics, which generate the distortion, are not transduced. By minimising the frequency of the F2 – F1 component through changes in the mosquitoes own WBF the mosquitoes can mediate frequency-matching. Upon first detection of a low frequency distortion component generated between the flight-tone of two mosquitoes the mosquito would have to discover if an increase or a decrease in WBF leads to an increase of the wavelength of the 'error signal' and therefore a decrease in F2 – F1. As the flight-tone harmonics change to converge onto the same frequency, the F2 – F1 component will tend to decrease to zero, thereby making the F2 – F1 component hard to detect in the inherent low frequency electrical noise of the JO. This could lead to less-than-perfect frequency-matching, which is apparent in the spectrogram recordings in Chapter II. Only through an interactive feedback between the motor commands sent to the wing muscles and the F2 – F1 distortion detected can precise frequency-matching be facilitated (Figure D.1). Interestingly, direct connections between the JO and wing muscles have been postulated based on anatomical studies (Ignell *et al*., 2005). Action potentials can be measured near and wing and leg areas in the thorax of male *Cx. quinquefasciatus,* within ~6 ms, in response to an acoustic stimulus. Assuming that these action potentials could be motor potentials governing frequency matching behaviour, the neural circuit mediating frequency matching, from acoustic detection at the JO, through to changes in motor output at the wing areas, may only have up to 3 synapses and involve up to four neurons.

Through evolution from the Jurassic era, the JO of mosquitoes has emerged as the most sensitive arthropod detector known. Although the male JO is most sensitivity tuned to the female fundamental flight-tone, further anatomical adaptations (investigated in Chapter V), in both sexes, may aid the mechanical detection of higher harmonics used for frequency-matching. For instance the fibrillae contribute to the mechanical tuning of the flagellum and create high frequency maxima in the mechanical respones of the flagellum (Göpfert *et al*., 1999). The frequency of such high frequency maxima encompass the male's 2nd

harmonic and female's 3rd harmonic where most frequency-matching occurs for *Cx. quinquefasciatus*.

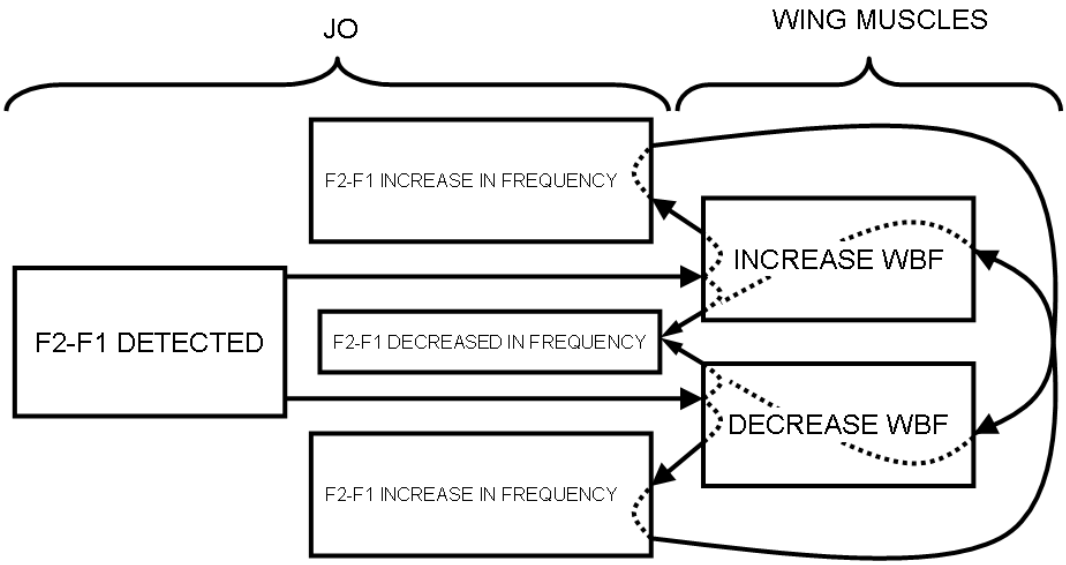

Figure D.1

Hypothetical circuit, which leads to frequency-matching.

MECHANOTRANSDUCTION IN MOSQUITOES

In *Drosophila* compound action potentials are thought to dominate extracellular electrical recordings of the JO (Albert *et al*., 2007a). This proposal is based on predictions about the open probability of the mechanically gated cation channels in the JO of *Drosophila,* derived from mechanical measurements of the sound receiver to stimulation (Albert *et al*., 2007a). At rest the open probability of the MET channels is 0.5, which is also when the channels are in their most sensitive state as predicted by the steepest part of a Boltzmann function fitted to the data (Fig. D.2). The open probability of the channels due to forcing steps can be modelled by a Boltzmann function reflected in the x axis for any external force imposed on the sound receiver (Fig. D.2). This is due to the arrangement of the mechanosensitive cells, opposite populations of which, can be stimulated when moving the sound receiver in a positive or negative direction (Fig. D.2). Any decrease or increase in external force applied to the

sound receiver x from the resting conditions (when x=0) will lead to the same increase in channel open probability y (Fig. D.2). Any receptor potential produced by the depolarisation of sensory cells will be balanced by an equal and opposite hyperpolarisation of the cells and therefore a summed potential change of zero. Thus compound action potentials are thought to dominate the electrical responses of the JO in *Drosophila* (Albert *et al.,* 2007a). This model may not be appropriate for extracellular responses measured from the JO of mosquitoes, where the extracellularly recorded electrical responses have been shown to be dominated by the receptor potentials (Pennetier *et al*., 2009), and see Chapter V)). A more likely basis, for the origin of the frequency doubling of the extracellular responses recorded from the mosquito JO, is that the receptor potentials are not symmetrical, but asymmetrical. The frequency doubling is most probably due to the summation of the receptor potentials from two oppositely polarised populations of receptors that generate asymmetrical receptor potentials, as first proposed by Flock (1965) for the lateral line system of fishes.

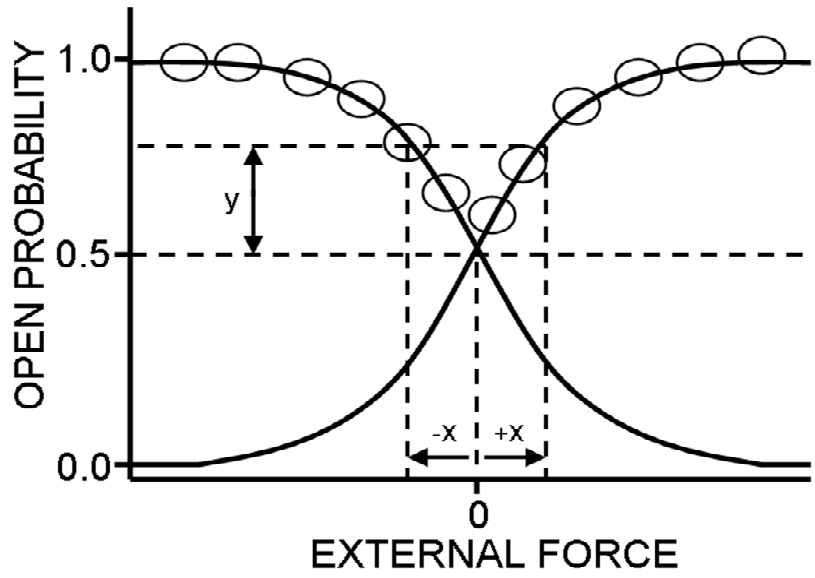

Figure D.2

MET open probability based on *Drosophila* antennal mechanics. Circles represent data points, which only follow the Boltzmann function above an open probability of 0.5. Any positive or negative external force x applied to the sound receiver from resting conditions will lead to the same change in the open probability of the MET channels y (Copied and adapted from (Albert *et al*., 2007a)).

A MODEL OF THE TRANSDUCTION APPARATUS IN THE SENSORY CILIA OF THE MOSQUITO JO

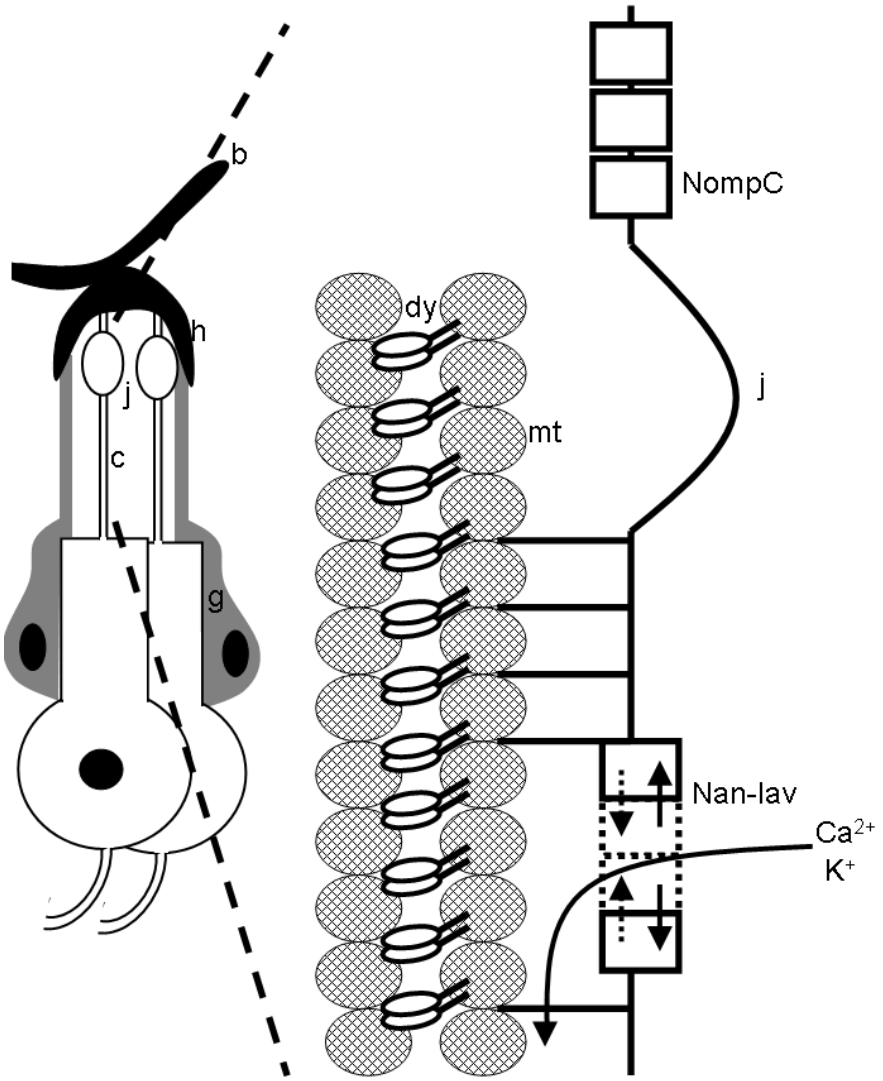

Figure D.3

Model of transducer function in the sensory cilium of the JO. b, prongs; h, cuticular cap; j, ciliary dilation; c, sensory cilium; g, supporting cell; mt, microtubule filament; dy, dynein. Solid lines indicate position of transducer components when under tension; when stimulated. Dashed line indicates position of membrane and channels under reduced tension. The NompC protein is a vital membrane component allowing tension to be transmitted effectively along the membrane. Nan-Iav acts as the primary MET mediating the inflow of cations under tension.

The involvement of dynein in the transduction apparatus (Chapter VI) and the roles of the two MET channel candidates NompC and Nan-Iav in transduction (Albert *et al*., 2007b; Gong *et al*., 2004; Göpfert *et al*., 2006; Kim, 2003; Walker

et al., 2000) and the localisation of Nan-Iav to the proximal sensory cilium (Gong *et al*., 2004) can be consolidated in a new model of transducer functioning in the JO (Fig D.3). This model explains mechanical amplification of the flagellum of mosquitoes (Jackson *et al*., 2006) as being due to the adaptation motor of the MET complex (Nadrowski *et al*., 2008). This model takes into account the localisation of the Nan-Iav channel to the proximal cilia (Gong *et al*., 2004).

In this model NompC, which has been shown not to form an ion channel (Liang *et al*. 2010), is simply a membrane bound structure, without ion conducting properties, which acts to stiffen the membrane allowing tension to be transmitted optimally from the distal cilium to the proximal cilium. Tension is transmitted to the Nan-Iav MET channel which opens to allow the influx of cations, which are responsible for the MET current. Mechanical amplification is mediated through the mechanical interaction of the Nan-Iav channel and dynein motor. In the absence of NompC the MET current is reduced by about half (Eberl *et al*., 2000) and mechanical amplification is abolished. The MET current is reduced but not eliminated in NompC mutants because the distal membrane, without the presence of NompC, is less stiff, and tensioning forces are not transmitted optimally to the proximal cilium where Nan-Iav resides. Thus the Nan-Iav still transduces a smaller mechanical signal. Amplification is abolished in NompC knockout mutants because, without NompC in the membrane, the distal membrane is not stiff enough to allow mechanical forces to be transmitted from the proximal to distal end of the cilium. The MET current is abolished in Nan-Iav mutants (Gong *et al*., 2004; Kim, 2003) because it is the only cation permeable channel. Mechanical amplification is increased in Nan-Iav mutants (Göpfert *et al*., 2006), often to the point where SOs are produced due to lack of cations through the Nan-Iav channel. Cations act to regulate the amount of amplification provided for by dynein.

INVOLVEMENT OF SOs IN MECHANOTRANSDUCTION

The identity of the active force producing process, enhancing detection of faint signals has been proposed to be due to components and manifestations of the MET complex (Göpfert *et al*., 2005). Two opposing forces of the MET complex pull and push the extended flagellum in phase with a sinusoidal signal, therefore amplifying movements of the flagellum, like pushing a child on a swing (Jackson *et al*., 2009). These two forces are the gating compliance of the transduction channels, where calcium binds near an open transduction channel and somehow mediates its closure, and forces imposed by the adaptation apparatus which tend to keep the transduction channels at their optimal sensitivity (Martin *et al*., 2000). SOs are hypothesised to be due to cyclic interplay between these two forces, when they are closely matched, which results in the system becoming unstable (Camalet *et al*., 2000) (Fig. I.11). It is not known what is the force producing molecule mediating the calcium induced channel closure. The motor molecule mediating channel opening is hypothesised to be myosin in the hair cell model which has been well fitted to the mechanics of *Drosophila* antennae. Others have hypothesized that dynein plays the part of the adaptation apparatus of the MET channel (Kernan, 2007; Mitchell, 2007). This seems more plausible as the cytoskeleton in the sensory cells consists of a prominent microtubule structure. Although actin filaments exist in the supporting cells they are not present in the cilia of the sensory cells. Previous to this thesis, no functional evidence supporting the involvement of dynein in transduction has been gathered.

In Chapter VI, it has been shown that the rate limiting reaction responsible for the SOs matches that of other *in vivo* systems powered by dynein but falls below that of other such systems powered by actin. Our study provides the first evidence that dynein powers mechanical activity in the JO. However further experiments failed to show a close involvement between the SOs and the transduction apparatus but implied that they were separate processes.

In an effort to disrupt dynein function, I injected colchicine into the pedicel containing the JO to depolymerise the microtubule cytoskeleton, to which dynein is attached. Although this resulted in abolition of SOs it did not however eliminate or heavily affect transduction as measured through receptor potentials of the JO. Thus SOs but not transduction necessitates the need for dynein. It can be argued that injection of colchicine interferes with the integrity of the microtubule cytoskeleton, needed in order to maintain optimal tension of the MET complex, which shifts the operating point of the MET channels away from their most sensitive point. The MET channels are most sensitive, at the steepest part of the Boltzmann function (Fig. D.2), here when two forces; calcium mediated MET closure and MET channel opening through the adaptation complex is closely matched SOs are produced through their interplay (Nadrowski *et al*., 2004) (Fig. I.11). However, when I injected DSM to block the MET channels, this resulted in a complete block of transduction, even for a high intensity stimulus, although electrical SOs were still recorded. Further to this, spontaneous electrical oscillations were recorded, at the same time and close in frequency, to a receptor potential produced in response to acoustic stimulation (Fig. 6.2). This suggests that there are two distinct electrical operations in the cilia which are producing electrical activity; one to transduce mechanical stimulus into a receptor potential and the other which is either due to electrical resonating properties of the sensory cell or a consequence of reverse mechanotransduction originating from the mechanical oscillations of the dynein molecules. To date SOs of the flagellum have been observed only in mosquitoes and flies upon lethal injection of dimethyl sulfoxide after repetitive stimulation but has not been advocated as a natural feature of the antennae of Diptera (Göpfert and Robert, 2001; Göpfert and Robert, 2003). However I observed SOs in 31 out of 35 *Culex* mosquitoes (Chapter VI) and the vast majority of *An. gambiae* mosquitoes which all had positive signs of life (abdominal contractions elicited motor responses; see Chapter I). SOs only decreased and disappeared as the mosquito's physiological state deteriorated. Therefore, in contradiction to previous findings, SOs appear to be a feature of healthy wild type mosquitoes. Interestingly the frequency of the SOs, of male mosquitoes as measured in Chapter VI, were closer in frequency then the most

sensitive frequency of either, the mechanics of the flagellum or transduction by the JO, to the average females fundamental WBF. Indeed the SOs, at room temperature, were about 100-150 Hz above the most sensitive frequency of the flagellum or JO.

The close association of the SO frequency of male *Cx. quinquefasciatus* with that of the fundamental flight-tone of female would suggest that the SOs help to tune the flagellum to higher frequencies to aid in the detection of female WBFs. This would be similar to the mechanics of the *Drosophila* JO. Here an active process adds mechanical energy, at low frequencies, to the sound receiver, which tunes it more sensitively to lower frequencies, whereas in its passive state it is tuned to considerably higher frequencies (Göpfert *et al*., 2005). The dominant frequency of the *Drosophila* love song occupies low frequencies, thus tuning of the receiver to lower frequencies aids detection. We have shown that in mosquitoes, however, no amplification or increase in sensitivity close to the SO frequency was observed. Further to this, the frequency and amplitude of the SO remained constant throughout stimulation by sound. Even though the SOs do not appear to be directly involved in amplifying acoustic stimuli they may still aid in acoustic detection. It has been demonstrated that autonomous oscillations can significantly improve system sensitivity and gain in noisy environments (Martin and Hudspeth., 2001; Nadrowski *et al*., 2004).

Findings presented in this thesis indicate that SOs are incredibly robust and can themselves interact with acoustically evoked oscillations of the antennae to create distortion products. If they do not play a role in increasing mechanosensitivity, their stubborn nature suggests they could act as a reference signal. In male mosquitoes the SOs are usually close in frequency to the female WBF. Thus male mosquitoes could act to decrease an F2 – F1 component generated between the SO frequency and the female fundamental flight-tone when detected by the JO. If, in males, the SOs maintain a harmonic ratio to their own WBF (i.e. SO frequency is 350 Hz, WBF is 700 Hz of the same mosquito), the SOs could provide a reference for frequency-matching between opposite sex pairs. Such an inherent reference signal may increase the

sensitivity of the JO to distortion between its own WBFs and those of a conspecific, even though the F2 – F1 component is generated between SOs and a conspecific flight tone. This proposal is supported by our finding (Chapter V) that that the particle velocity necessary to elicit a receptor potential encoding the F2 – F1 in the JO is similar to that required to elicit a pure tone electrical response at the F2 – F1 frequency.

The outcomes of this present study reformulate the high frequency limits of audition in mosquitoes. They also present the first evidence of distortion products being used to elicit behaviour. We have also revealed that acoustic-motor interaction between flying, tethered, mosquitoes can provide a role in, and an assay for, sex and subspecies recognition. This work provides the first physiological evidence that the dynein motor provides the driving force for SOs in insect mechanoreceptors. SOs of the antennae, although suggested to be due to manifestations of the same mechanism that provides power amplification (Göpfert and Robert, 2001), appear to be due to a molecular mechanism that is distinct from that of the transduction apparatus, where amplification is proposed to occur (Göpfert *et al*., 2005).

FURTHER EXPERIMENTS

Free flight experiments need to be conducted in order to establish the significance of frequency-matching; it is still not known if this phenomenon occurs in free flight when a male approaches a female. For how long do mosquitoes interact in flight before leaving the swarm and mating? *An. gambiae* are able to detect the sub species of the other mosquito and therefore avoid leaving the swarm *in copula.* When exactly does this occur, does frequency-matching underpin subspecies recognition and are any other sensory modalities used such as contact chemoreception?

Results in this thesis strongly suggest that the origin of the SOs are dynein motor molecules. Dynein moves microtubule doublets relative to each other in

the sensory cilia. How is this mechanical movement faithfully conveyed into an electrical potential measured from the JO? One theory is that the MET channels open in response cilia bending caused by dynein powered deformation of the cilium membrane. However when the MET channels were blocked using DSM the electrical SOs persisted. This suggests that they maybe more than one MET channel as has been postulated previously (Göpfert *et al*., 2006). Injection of solutions into the JO appeared to significantly affect the ionic environment and/or electrical function. Therefore further experiments using MET channel blockers and agents to interfere with dynein's function need to be introduced an alternative way. It is possible to induce heat activated transcription in *Drosophila*. This would be an ideal non-intrusive way to introduce proteins to interfere with specific processes in the sensory cells of the JO.

Although SOs have been used as a hallmark of amplification (Göpfert *et al*., 2001) we were unable to show that SOs increased the sensitivity of the JO's response to acoustic stimulation. Experiments where dynein is absent from the sensory cilia, as in *tilB Drosophila* mutants (Göpfert *et al.,* 2005), show that nonlinear amplification of antennal displacements is abolished. However, dynein may have a structural as well as functional role in the sensory cell cilia. Measuring quantitatively temperature dependence of mechanical amplification in the flagellum may give us a good idea of contribution of dynein in amplification. Further to this, measuring the temperature dependence of adaptation of the JO to a constant sound source and then comparing this with the temperature dependence of the SOs of the mosquito flagellum (already calculated in Chapter VI), the involvement of dynein, as part of the adaptation motor of the MET complex can be investigated.

REFERENCES

Albert, J.T., Göpfert, M.C. 2006. A *Drosophila* gating-spring channel for hearing. J. Neurogenet. 20, 69-69.

Albert, J.T., Nadrowski, B., Göpfert, M.C. 2007a. Mechanical signatures of transducer gating in the Drosophila ear. Curr. Biol. 17, 1000-1006.

Albert, J.T., Nadrowksi, B., Göpfert, M.C. 2007b. Drosophila mechanotransduction - Linking proteins and functions. Fly 1, 238-241.

Andersen, S.O. 1979. Biochemistry of insect cuticle. Annu. Rev. Entomol. 24, 29-61.

Anson, M. 1992. Temperature-Dependence and Arrhenius activation-energy of F-actin velocity generated *in vitro* by skeletal myosin. J. Mol. Biol. 224, 1029-1038.

Arthur, B.J., Wyttenbach, R.A., Harrington, L.C., Hoy, R.R. 2010. Neural responses to one- and two-tone stimuli in the hearing organ of the dengue vector mosquito. J. Exp. Biol.213, 1376-85.

Auger, J., Serres, C., Feneux, D. 1990. Motion of individual human spermatozoa, both normal and lacking the outer dynein arms, during a continuous temperature rise. Cell Motil. Cytoskelton 16, 22-32.

Bailey, W.J. 2003. Insect duets: underlying mechanisms and their evolution. Physiol. Entomol. 28, 157-174.

Barany, M. 1967. Atpase activity of myosin correlated with speed of muscle shortening. J. Gen. Physiol. 50, 197-&.

Bartlett Healy, K., Crans, W., Gaugler, R. 2008. Phonotaxis to amphiban vocalisation in Culex territans waler (Diptera: Culicdae). Ann. Entomol. Soc. Am. 101, 95-103.

Belton, P. 1974. An analysis of direction finding in male mosquitoes. In Experimental Analysis of Insect Behaviour (Ed. L. Barton Browne), Springer-Verlag, Berlin, Heidelberg and New York, pp. 139-148.

Belton, P. 1989. The structure and probable function of the internal cuticular parts of Johnston's organ in mosquitoes (*Aedes aegypti*). Can. J. Zool. 67, 2625-2632.

Bisgrove, B.W., Yost, H.J. 2006. The roles of cilia in developmental disorders and disease. Development 133, 4131-4143.

Bohm, K.J., Stracke, R., Baum, M., Zieren, M., Unger, E. 2000. Effect of temperature on kinesin-driven microtubule gliding and kinesin ATPase activity. FEBS lett. 466, 59-62.

Bonnet, D.D., Stephen, M.K.H. 1951. The introduction of *Toxorhynchites brevipalpis* Theobald into the territory of Hawaii. Proc. Hawaiian Entomol. Soc. 14, 237-242.

Boo, K.S. 1980. Antennal sensory receptors of the male mosquito, *Anopheles-Stephensi.* Zeitschrift Fur Parasitenkunde-Parasitology Research 61, 249-264.

Boo, K.S. 1981. Discontinuity between ciliary root processes and triple microtubules of distal basal body in mosquito sensory cilia. Korean J. Entomol. 11, 5-18.

Boo, K.S., Richards, A.G. 1975. Fine structure of scolopidia in Johnston's organ of female *Aedes aegypti* compared with that of the male. J. Insect physiol. 21, 1129-1139.

Brodgon, W.C. 1998. Measurement of the flight tone differences among members of the *Anopheles gambiae* species complex (Diptera: Culicidae). J. Med. Entomol. 35, 681-684.

Camalet, S., Duke, T., Julicher, F., Prost, J. 2000. Auditory sensitivity provided by self-tuned critical oscillations of hair cells. Proc. Natl. Acad. Sci. U.S.A. 97, 3183-3188.

Cator, L.J., Arthur, B.J., Harrington, L.C., Hoy, R.R. 2009. Harmonic convergence in the love songs of the dengue vector mosquito. Science. 323, 1077-9.

Chapman, K.M., Mosinger, J.L., Duckrow, R.B. 1979. Role of distributed viscoelastic coupling in sensory adaptation in an insect mechanoreceptor. J. Comp. Physiol. 131, 1-12.

Cheatham, M.A., Naik, K., Dallos, P. 2010. Using the cochlear microphonic as a tool to evaluate cochlear function in mouse models of hearing. J. Assoc. Res. Otolaryngol. 12, 113-125.

Clary-Meinesz, C.F., Cosson, J., Huitorel, P., Blaive, B. 1992. Temperature effect on the ciliary beat frequency of human nasal and tracheal ciliated cells. Biol. Cell 76, 335-8.

Clements, A.N. 1956. The antennal pulsating organs of mosquitoes and other diptera. Q. J. Microsc. Sci. 97, 429-433.

Clements, A.N. 1999. The biology of mosquitoes Vol. 2 Sensory Reception and Behaviour (New York: CABI Publishing).

Clements, A.N., Bennett, F.D. 1969. Structure and biology of a new species of *Mallophora* Macq (Diptera Asilidae) from Trinidad W.I. Bull. Entomol. Res. 58, 455-&.

Coakley, C.J., Holwill, M.E.J. 1974. Effects of pressure and temperature-changes on flagellar movement of *Crithidia oncopelti*. J. Exp. Biol. 60, 605-&.

Cooper, N.P., Kemp, D.T. 2008. concepts and challenges in The Biophysics of Hearing, 437-438.

Coro, F., Kössl, M. 1998. Distortion-product otoacoustic emissions from the tympannic organ in two noctuoid moths. J. comp. physiol. 183, 525-531.

Crawford, A.C., Fettiplace, R. 1985. The mechanical-properties of ciliary bundles of turtle cochlear hair-cells. J. Physiol. (Lond.) 364, 359-&.

Dallos, P. 1992. The active cochlea. J. Neurosci. 12, 4575-4585.

Diabate, A., Dao, A., Yaro, A.S., Adamou, A., Gonzalez, R., Manoukis, N.C., Traore, S.F., Gwadz, R.W., Lehmann, T. 2009. Spatial swarm segregation and reproductive isolation between the molecular forms of *Anopheles gambiae*. Proc. Roy. Soc. Lond. Series B Biol. Sci. 276, 4215-4222.

Downes, J.A. 1969. Swarming and mating flight of Diptera. Ann. Rev. Entomol. 14, 271-&.

Duhrkopf, R.E., Hartberg, W.K. 1992. Differences in male mating response and female flight Sounds in *Aedes Aegypti* and *Aedes Albopictus* (Diptera, Culicidae). J. ed.Entomol.29, 796-801.

Eberl, D.F., Hardy, R.W., Kernan, M.J. 2000. Genetically similar transduction mechanisms for touch and hearing in Drosophila. J. Neurosci.20, 5981-5988.

Erler, G. 1983. Sensitivity of an insect mechanoreceptor after destruction of dendritic microtubules by means of vinblastine. Cell Tiss. Res. 229, 673-684.

Fettiplace, R. 2006. Active hair bundle movements in auditory hair cells. J. Physiol. 576, 29-36.

Fettiplace, R., Ricci, A.J., Hackney, C.M. 2001. Clues to the cochlear amplifier from the turtle ear. Trends Neurosci. 24, 169-175.

Fletcher, N.H. 1978. Acoustical response of hair receptors in insects. J. Comp. Physiol. 127, 185-189.

Flock, A. 1965. Transducing mechanisms in lateral line canal organ receptors. Cold Spring Harb. Symp. Quant. Biol. 30, 133-145.

French, A.S. 1988. Transduction mechanisms of mechanosensila. Ann. Rev. Entomol. 33, 39-58.

French, A.S., Sanders, E.J. 1981. The mechanosensory apparatus of the femoral tactile spine of the cochroach, Periplaneta-americana. Cell Tiss. Res. 219, 53-68.

French, A.S., Kuster, J.E. 1982. The effects of temperature on mechanotransduction in the cockroach tactile spine. J. Comp. Physiol. 147, 251-258.

Gibson, G. 1985. Swarming behaviour of the mosquito *Culex pipiens quinquefasciatus* - a Quantitative-Analysis. Physiol. Entomol. 10, 283-296.

Gibson, G., Russell, I.J. 2006. Flying in tune: Sexual recognition in mosquitoes. Curr. Biol. 16, 1311-1316.

Gillespie, P.G., Walker, R.G. 2001. Molecular basis of mechanosensory transduction. Nature 413, 194-202.

Gillespie, P.G., Cyr, J.L. 2004. Myosin-1c, the hair cell's adaptation motor. Ann. Rev. Physiol. 66, 521-545.

Gong, Z., Son, W., Chung, Y.D., Kim, J., Shin, D.W., McClung, C.A., Lee, Y., Lee, H.W., Chang, D.J., Kaang, B.K., Cho, H., Oh, U., Hirsh, J., Kernan, M.J., Kim, C. 2004. Two interdependant TRPV channel subunits, Inactive and Nanchung, mediate hearing in Drosophila. J. Neurosci. 24, 9059-9066.

Göpfert, M., Robert, D. 2002. The mechanical basis of Drosophila audition. J. Exp. Biol. 205, 1199-1208.

Göpfert, M., Briegel, H., Robert, D. 1999. Mosquito hearing: sound-induced antennal vibrations in male and female Aedes aegypti. J. Exp. Biol. 202, 2727-2738.

Gopfert M., R.D., Briegel H. 1999. Mosquito hearing: sound-induced antennal vibrations in male and female Aedes aegypti. J. exp. Boil. 202, 2727-2738.

Göpfert, M.C., Robert, D. 2000. Nanometre-range acoustic sensitivity in male and female mosquitoes. Proc. Roy. Soc. Lond. Series B Biol. Sci. 267, 453-457.

Göpfert, M.C., Robert, D. 2001. Active auditory mechanics in mosquitoes. Proc. Roy. Soc. Lond. Series B Biol. Sci. 268, 333-339.

Göpfert, M.C., Robert, D. 2003. Motion generation by Drosophila mechanosensory neurons. Proc. Natl. Acad. Sci. U.S.A. 100, 5514-5519.

Göpfert, M.C., Robert, D. 2008. in *Active Processes and Otoacoustic emissions*, eds Manley G A, Fay R R, Popper A N (Springer), 191-209.

Göpfert, M.C., Albert, J.T., Nadrowski, B., Kamikouchi, A. 2006. Specification of auditory sensitivity by Drosophila TRP channels. Nat. Neurosci. 9, 999-1000.

Göpfert, M.C., Humphris, A.D.L., Albert, J.T., Robert, D., Hendrich, O. 2005. Power gain exhibited by motile mechanosensory neurons in drosophila ears. Proc. Natl. Acad. Sci. U.S.A. 102, 325-330.

Gray, E.G., Pumphrey, R.J. 1958. Ultra-structure of the insect ear. Nature 181, 618-618.

Gray, J. 1923. The mechanism of ciliary movement. III. The effect of temperature. Proc. Roy. Soc. Lond. Series B Biol. Sci. 95, 6-15.

Grove, T.J., McFadden, L.A., Chase, P.B., Moerland, T.S. 2005. Effects of temperature, ionic strength and pH on the function of skeletal muscle myosin from a eurythermal fish, *Fundulus heteroclitus*. J. Muscle Res. Cell Motil. 26, 191-7.

Holwill, M.E.J. 1968. Kinetic studies of the flagellar movement of sea-urchin spermatozoa. J. Exp. Biol. 50, 203-222.

Holwill, M.E.J., Silvester, N.R. 1967. Thermodynamic aspects of flagellar activity. J. Exp. Biol. 47, 249-&.

Holwill, M.E.J., Wais, J. 1979. Thermodynamic and hydrodynamic studies relating to the mechanochemical cycle in the flagellum of *Crithidia oncopelti*. J. Exp. Biol. 82, 177-195.

Horridge, G.A. 1969. Statocysts of Medusae and evolution of stereocilia. Tiss. Cell 1, 341-353.

Howard, J., Hudspeth, A.J. 1987. Mechanical relaxation of the hair bundle mediates adaptation in mechanoelectrical transduction by the bullfrogs saccular hair cell. Proc. Natl. Acad. Sci. U.S.A. 84, 3064-3068.

Hudspeth, A.J. 1997. Mechanical amplification of stimuli by hair cells. Curr. Opin. Neurobiol. 7, 480-486.

Ignell, R., Dekker, T., Ghaninia, M., Hansson, B.S. 2005. Neuronal architecture of the mosquito deutocerebrum. J. Comp. Neurol. 493, 207-240.

Jackson, J., Robert, D. 2006. Nonlinear auditory mechanism enhances female sounds for male mosquitoes. Proc. Natl. Acad. Sci. U.S.A. 103, 16734-16739.

Jackson, J.C., Windmill, J.F., Pook, V.G., Robert, D. 2009. Synchrony through twice-frequency forcing for sensitive and selective auditory processing. Proc. Natl. Acad. Sci. U.S.A. 106, 10177-82. Epub 2009 Jun 11.

Johnston, C. 1855. Auditory apparatus of the Culex mosquito. Q. J. Microscopical Sci. 3, 97-102.

Kamikouchi, A., Shimada, T., Ito, K. 2006. Comprehensive classification of the auditory sensory projections in the brain of the fruit fly *Drosophila melanogaster*. J Comp. Neurol. 499, 317-356.

Kamikouchi, A., Albert, J.T., C, G.M. 2010. Mechanical feedback amplification in *Drosophila* hearing is independent of synaptic transmission. Eur. J. Neurosci. 31, 697-703.

Kamikouchi, A., Inagaki, K.H., Effertz, T., Hendrich, O., Fiala, A., Göpfert, G. C., Itl, K. 2009. The neural basis of *Drosophila* gravity sensing and hearing. Nature 458, 165-171.

Kamimura, S., Kamiya, R. 1989. High-frequency nanometer-scale vibration in quiescent flagellar axonemes. Nature 340, 476-478.

Kamimura, S., Yano, M., Shimizu, H. 1985. ATP hydrolysis coupled to microtubule sliding in sea-urchin sperm flagella. J. Biochem. 97, 1509-1515.

Keil, T.A. 1997. Functional morphology of insect mechanoreceptors. Microsc. Res. Tech. 39, 506-531.

Kemp, D.T. 1978. Stimulated acoustic emissions from within human auditory-system. J Acoust. Soc. Am. 64, 1386-1391.

Kemp, D.T. 1979. Evidence of mechanical nonlinearity and frequency selective wave amplication in the cochlea. Arch. Otorhinolaryngol. 224, 37-45.

Keppler, E. 1958. Über Das Richtungshoren Von Stechmücken. Zeitschrift Fur Naturforschung Part B-Chemie Biochemie Biophysik Biologie Und Verwandten Gebiete 13, 280-284.

Kernan, M., Zuker, C. 1995. Genetic approaches to mechanosensory transduction. Curr. Opin. Neurobiol. 5, 443-448.

Kernan, M., Cowan, D., Zuker, C. 1994. Genetic dissection of mechanosensory transduction: mechanoreception-defective mutants of drosophila. Neuron 12, 1195-1206.

Kernan, M.J. 2007. Mechanotransduction and auditory transduction in *Drosophila*. Pflügers Archiv – Eur. J. Physiol. 454, 703-720.

Kim, J. 2003. A TRPV family ion channel required for hearing in drosophila. Nature 424, 81-84.

Kössl, M., Boyan, G.S. 1998. Otoacoustic emissions from a nonvertebrate ear. Naturwissenschaften 85, 124-127.

Kössl, M., Coro, F., Seyfarth, E.A., Nassig, W.A. 2007. Otoacoustic emissions from insect ears having just one auditory neuron. J. Comp. Physiol. A Neuroethol. Sens. Neural Behav. Physiol. 193, 909-915.

Kössl, M., Mockel, D., Weber, M., Seyfarth, E.A. 2008. Otoacoustic emissions from insect ears: evidence of active hearing? J. Comp. Physiol. A Neuroethol. Sens. Neural Behav. Physiol. 194, 597-609.

Krzywinski, J., Grushko, O.G., Besansky, N.J. 2006. Analysis of the complete mitochondrial DNA from *Anopheles funestus*: An improved dipteran mitochondrial genome annotation and a temporal dimension of mosquito evolution. Mol. Phylogenet. Evol. 39, 417-423.

Kuppers, J. 1974. Measurements on the ionic milieu of the receptor terminal in mechanoreceptive sensilla of insects. Journal Schwartzkopf, 387-394.

Lee, J., Moon, S., Cha, Y., Chung, Y.D. 2010. Drosophila TRPN(=NOMPC) channel localizes to the distal end of mechanosensory cilia. PLoS 5, e11012.

Liang, X., Madrid, J., Saleh, H.S., Howard, J. 2010. NOMPC, a member of the TRP channel family, localizes to the tubular body and distal cilium of *Drosophila* campaniform and chordotonal receptor cells. Cytoskeleton 68, 1-7.

Lukashkin, A.N., Bashtanov, M.E., Russell, I.J. 2005. A self-mixing laser-diode interferometer for measuring basilar membrane vibrations without opening the cochlea. J. Neurosci. 148, 122-129.

Machemer, H. 1972. Temperature influences on ciliary beat and metachronal coordination in *Paramecium*. J. Mechanochem. Cell Motil. 1, 57-66.

Manley, G.A. 2001. Evidence for an active process and a cochlear amplifier in nonmammals. J Neurophysiol. 86, 541-9.

Marcotti, W., van Netten, S.M., Kros, C.J. 2005. The aminoglycoside antibiotic dihydrostreptomycin rapidly enters mouse outer hair cells through the mechano-electrical transducer channels. J Physiol. 567, 505-521.

Martin, P., Hudspeth, A.J. 1999. Active hair-bundle movements can amplify a hair cell's response to oscillatory mechanical stimuli. Proc. Natl. Acad. Sci. U.S.A. 96, 14306-14311.

Martin, P., Hudspeth, A.J. 2001. Compressive nonlinearity in the hair bundle's active response to mechanical stimulation. Proc. Natl. Acad. Sci. U.S.A. 98, 14386-14391.

Martin, P., Mehta, A.D., Hudspeth, A.J. 2000. Negative hair-bundle stiffness betrays a mechanism for mechanical amplification by the hair cell. Proc. Natl. Acad. Sci. U.S.A. 97, 12026-12031.

Mayer, A.N. 1874. Experiments on the supposed auditory apparatus of the mosquito. Am. Nat. 8, 577-592.

McIver, S. 1971. Comparative studies on sense organs on antennae and maxillary palps of selected male Culicine mosquitoes. Can. J. Zool. 49, 235-&.

McIver, S.B. 1980. Sensory aspects of mate-finding behaviour in male Mosquitoes (Diptera, Culicidae). J Med. Entomol. 17, 54-57.

McIver, S.B. 1982. Sensilla of mosquitos (Diptera, Culicidae). J Med. Entomol. 19, 489-535.

Millar, N.C., Geeves, M.A. 1983. The limiting rate of the ATP-mediated dissociation of actin from rabbit skeletal-muscle myosin subfragment-1. FEBS Lett. 160, 141-148.

Mitchell, D.R. 2007. The evolution of eukaryotic cilia and flagella as motile and sensory organelles, Eukaryotic Membranes and Cytoskeleton: Origins and Evolution, Vol. 607. pp. 130-140.

Mockel, D., Seyfarth, E.A., Kossl, M. 2007. The generation of DPOAEs in the locust ear is contingent upon the sensory neurons. J. Comp. Physiol. A Neuroethol. Sens. Neural Behav. Physiol. 193, 871-879.

Moran, D.T., Varela, F.G. 1971. Microtubules and sensory transduction. Proc. Natl. Acad. Sci. U.S.A. 68, 757-&.

Moran, D.T., Rowley, J.C. 1975. The fine-structure of cockroach subgenual organ. Tiss. Cell 7, 91-105.

Moran, D.T., Varela, F.J., Rowley, J.C. 1977. Evidence for active-role of cilia in sensory transduction. Proc. Natl. Acad. Sci. U.S.A. 74, 793-797.

Nadrowski, B., Martin, P., Julicher, F. 2004. Active hair-bundle motility harnesses noise to operate near an optimum of mechanosensitivity. Proc. Natl. Acad. Sci. U.S.A. 101, 12195-12200.

Nadrowski, B., Albert, J.T., Gopfert, M.C. 2008. Transducer-based force generation explains active process in *Drosophila* hearing. Curr. Biol. 18, 1365-1372.

Narahashi, T., Deguchi, T., Urakawa, N., Ohkubo, Y. 1960. Stabilization and rectification of muscle fiber membrane by tetrodotoxin. Am. J. Physiol. 198, 934-8.

Narins, P.M. 1995. Frog communication. Sci. Am. 273, 78-83.

Nijhout, H.F. 1977. Control of antennal hair erection in male mosquitoes. Biol. Bull. 153, 591-603.

Nijhout, H.F., Sheffield, H.G. 1979. Antennal hair erection in male mosquitoes - new mechanical effector in insects. Science 206, 595-596.

Pedersen, S.F., Owsianik, G., Nilius, B. 2005. TRP channels: An overview. Cell Calcium 38, 233-252.

Pennetier, C., Warren, B., Dabire, K.R., Russell, I.J., Gibson, G. 2009. "Singing on the wing" as a mechanism for species recognition in the malarial mosquito *Anopheles gambiae*. Curr. Biol. 30, 131-136.

Ranatunga, K.W. 1984. The force-velocity relation of rat fast-twitch and slow-twitch muscles examined at different temperatures. J Physiol. 351, 517-529.

Risler, H. 1955. Das Gehororgan der Mannchen von *Culex pipiens* L., *Aedes aegypti* L. und *Anopheles stephensi* Liston (Culicidae), eine vergleichend morphologische Untersuchung. . Zool. Jahrb. Abt. Anat. Ontog. Tiere. 74, 478-490.

Rosowski, J.J., Peake, W.T., White, J.R. 1984. Cochlear nonlinearities inferred from 2-tone distortion products in the ear canal of the alligator lizard. Hear. Res. 13, 141-158.

Roth, L.M. 1948. An experimental laboratory study of the sexual behaviour of *Aedes aegypti* (Linnaeus). Am. Midl. Nat. 40, 265-352.

Ruiz-Sanchez, E., O'Donnell, M.J. 2007. Characterization of transepithelial transport of salicylate by the Malpighian tubules of *Drosophila melanogaster* and the effects of changes in fluid secretion rate. Physiol. Entomol. 32, 157-166.

Salathe, M. 2007. Regulation of mammalian ciliary beating. Ann. Rev. Physiol. 69, 401-422.

Satir, P., Mitchell, D.R., Jekely, G. 2008. How did the cilium evolve? Curr. Top. Dev. Biol. 85, 63-82.

Schmidt, K. 1967. Die Entwicklung der Scolopidien im JohnstonschenOrgan von Aedes aegypti wahrend der puppenpase. Verh. Deutsch. Zool. Ges. 31, 750-762.

Schneider, D. 1964. Insect antennae. Ann. Rev. Entomol. 9, 103-122.

Shingyoji, C., Higuchi, H., Yoshimura, M., Katayama, E., Yanagida, T. 1998. Dynein arms are oscillating force generators. Nature 393, 711-714.

Slifer, E.H., Sekhon, S.S. 1962. Fine structure of sense organs on antennal flagellum of yellow fever mosquito *Aedes Aegypti* (Linnaeds). J. Morphol. 111, 49-&.

Sotomayor, M., Corey, D.P., Schulten, K. 2005. In search of the hair-cell gating spring: Elastic properties of ankyrin and cadherin repeats. Structure 13, 669-682.

Stein, R.B., Gordon, T., Shriver, J. 1982. Temperature-dependence of mammalian muscle contractions and ATPase activities. Biophys. J. 40, 97-107.

Stephens, R.E. 1974. in *Cilia and flagella*, eds Sleigh M A (Academic Press. New York). pp39-76.

Stephens, R.E., Levine, E.E. 1970. Some enzymatic properties of axonemes from cilia of *Pectin irradians*. J. Cell Biol. 46, 416-421.

Taylor, G.K., Nudds, R.L., Thomas, A.L. 2003. Flying and swimming animals cruise at a Strouhal number tuned for high power efficiency. Nature. 425, 707-11.

Thorpe, W.H. 1975. The biological significance of duetting and antiphonal song. Acta. Neurobiol. Exp. 35, 517-28.

Thurm, U. 1965. .I. Fine structure and adequate stimulus. Cold Spring Harb. Symp. Quant. Biol. 30, 75-&.

Thurm, U., Kuppers, J. 1980. Epithelial physiology of insect sensilla. Insect biology in the future, p735-758.

Thurm, U., Erler, G., Godde, J., Kastrup, H., Keil, T., Volker, W., Vohwinkel, B. 1983. Cilia Specialized for Mechanoreception. Journal of Submicrosc. Cytol. Pathol. 15, 151-155.

Tischner, H., Schief, A. 1955. Gehorsinn und fluggerausch bei Stechmucken. Umschau. 55, 368-370.

Tripet, F., Dolo, G., Traore, S., Lanzaro, G.C. 2004. The "wingbeat hypothesis" of reproductive isolation between members of the *Anopheles gambiae* complex (Diptera : Culicidae) does not fly. J. Med. Entomol. 41, 375-384.

Van Dijk, P., Meenderink, S.W.F. 2006. Distortion product otoacoustic emissions in the amphibian ear. Auditory Mechanisms: Processes and Models, 332-338.

Van Emst, M.G., Klis, S.F.L., Smoorenburg, G.F. 1997. Identification of the nonlinearity governing even-order distortion products in cochlear potentials. Hear. Res. 114, 93-101.

Walker, R.G., Willingham, A.T., Zuker, C.S. 2000. A *Drosophila* mechanosensory transduction channel. Science 287, 2229-2234.

Warren, B., Gibson, G., Russell, I.J. 2009. Sex recognition through midflight mating duets in Culex mosquitoes is mediated by acoustic distortion. Curr. Biol. 19, 485-491.

Wekesa, J.W., Brogdon, W.G., Hawley, W.A., Besansky, N.J. 1998. Flight tone of field-collected populations of *Anopheles gambiae* and *Anopheles arabiensis* (Diptera : Culicidae). Physiol. Entomol. 23, 289-294.

Wiederhold, M.L. 1976. Mechanosensory transduction in sensory and motile cilia. Ann. Rev. Biophys. and Bioeng. 5, 39-62.

Wishart, G., Sickle, G.R., Riordan, D.F. 1962. Orientation of males of *Aedes aegypti* (Diptera: Culicidae) to sound. Can. Entomol. 94, 613-626.

Wishart, G.R., Riordan, D.F. 1959. Flight responses to various sounds my adult males of *Aedes aegypti* (L.) (Diptera: Culicidae). Can. Entomol. 91, 181-191.

Wolfrum, U. 1990. Actin-filaments - the main components of the scolopale in insect sensilla. Cell Tiss. Res. 261, 85-96.

Wolfrum, U. 1991. Tropomyosin is co-localized with the actin-filaments of the scolopale in insect sensilla. Cell Tiss. Res. 265, 11-17.

Wolfrum, U. 1997. Cytoskeletal elements in insect sensilla. Int. J. Insect Morphol. Embryol. 26, 191-203.

Wondji, C., Simard, F., Fontenille, D. 2002. Evidence for genetic differentiation between the molecular forms M and S within the Forest chromosomal form of *Anopheles gambiae* in an area of sympatry. Insect Mol. Biol. 11, 11-19.